BioMed Research International

Cancer Monitoring Methods

Guest Editors: Aleksandra Nikolic, Oronza Antonietta Botrugno, Jelena Urosevic, and Natasa Tosic

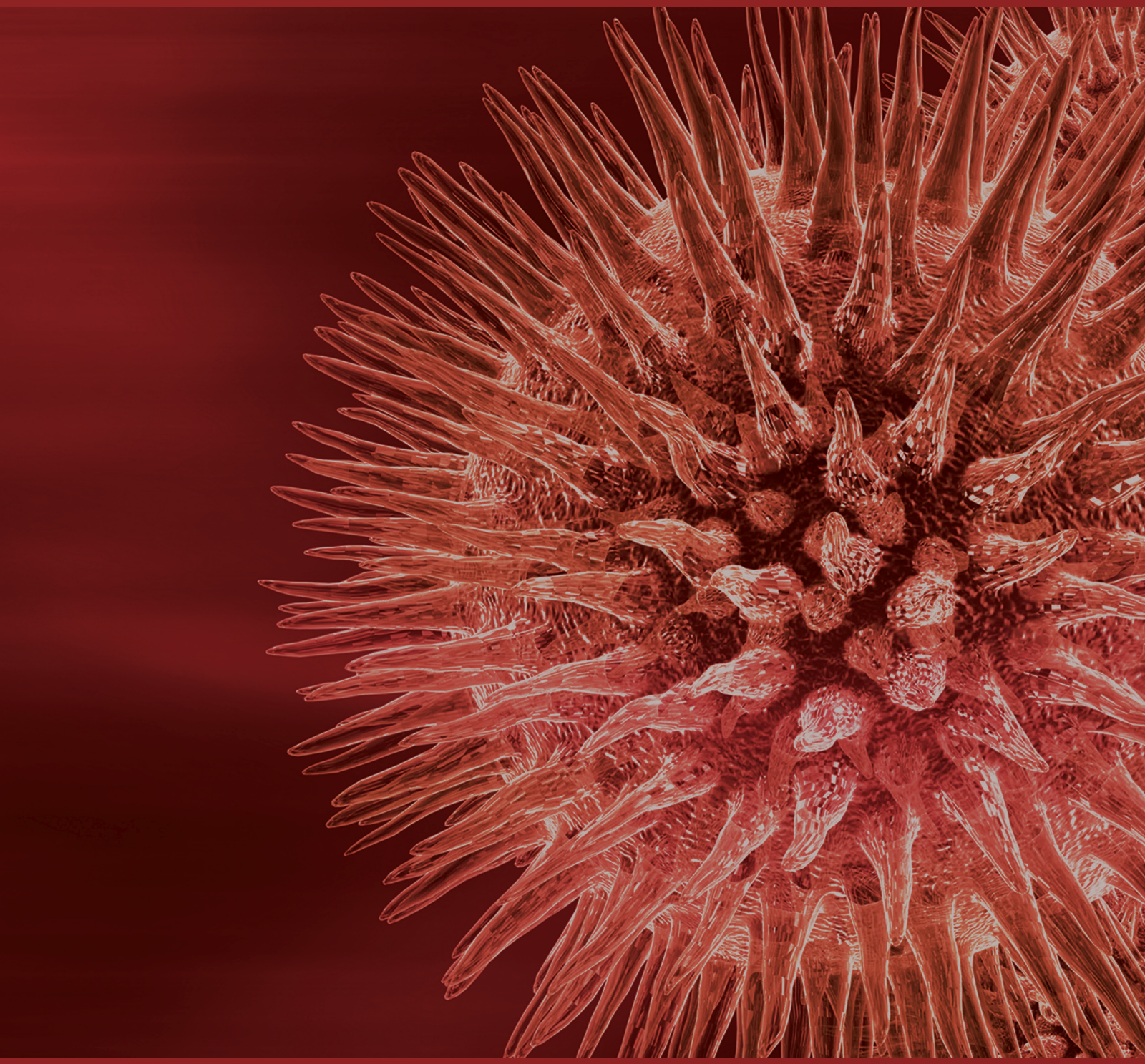

Cancer Monitoring Methods

BioMed Research International

Cancer Monitoring Methods

Guest Editors: Aleksandra Nikolic, Oronza Antonietta Botrugno, Jelena Urosevic, and Natasa Tosic

Contents

Hindawi Publishing Corporation
BioMed Research International
Volume 2014, Article ID 981495, 1 page
http://dx.doi.org/10.1155/2014/981495

Editorial

Cancer Monitoring Methods

Aleksandra Nikolic,[1] Oronza Antonietta Botrugno,[2] Jelena Urosevic,[3] and Natasa Tosic[4]

[1] *Laboratory for Molecular Biology, Institute of Molecular Genetics and Genetic Engineering, University of Belgrade, Vojvode Stepe 444A, 11010 Belgrade, Serbia*
[2] *Drug Discovery Unit, Department of Experimental Oncology, European Institute of Oncology, IFOM-IEO Campus, Via Adamello 16, 20139 Milan, Italy*
[3] *Growth Control and Cancer Metastasis Laboratory, Institute for Research in Biomedicine (IRB Barcelona), Parc Cientific de Barcelona, Carrer de Baldiri Reixac 10, 08028 Barcelona, Spain*
[4] *Laboratory for Molecular Hematology, Institute of Molecular Genetics and Genetic Engineering, University of Belgrade, Vojvode Stepe 444A, 11010 Belgrade, Serbia*

Correspondence should be addressed to Aleksandra Nikolic; aleksni@imgge.bg.ac.rs

Received 12 March 2014; Accepted 12 March 2014; Published 3 April 2014

Methods for cancer monitoring and early detection of the disease are of the utmost importance and represent one of the most active areas of current research. Cancer monitoring is crucial not only for early initial diagnosis of the disease, but also for followup of therapy outcome. Despite being well developed, most methods for cancer monitoring are unsuitable for clinical use because they either are insufficiently accurate, not sensitive enough, or require a lengthy complicated analysis. There is a great necessity for more effective cancer monitoring methods that can improve cancer management in routine clinical setting and increase treatment effectiveness. Advances in this field of research are based on a more detailed understanding of the fundamental biological mechanisms involved in the disease process, as well as on advances in genomic, transcriptomic, proteomic, and metabolomic research.

This special issue encompasses articles on the state of the art, advantages and disadvantages, current limitations, and future perspectives of cancer monitoring methods. Dr. D. Musio with colleagues and Dr. B. Kasper with colleagues present advanced imaging methods in clinical followup of response to therapy. Dr. G. Bertino with colleagues, as well as Dr. P. Mirabelli and Dr. M. Incoronato, offer new insight into the use of some traditional cancer biomarkers in clinical and laboratory practice. The works of Dr. P. Sadlecki with colleagues, Dr. R. Zappacosta with colleagues, and Dr. S. Farivar with colleagues deal with the analysis of protein cancer biomarkers in different types of samples. Of special interest are the articles that report on development, implementation, and validation of novel techniques for cancer monitoring, by Dr. C.-F. Chen with colleagues and Dr. I. Macchia and colleagues.

We would like to thank the authors for their excellent contributions to this special issue. We hope that this issue will be useful to the experts of all profiles dealing with cancer in both clinical and laboratory setting.

Aleksandra Nikolic
Oronza Antonietta Botrugno
Jelena Urosevic
Natasa Tosic

Hindawi Publishing Corporation
BioMed Research International
Volume 2014, Article ID 616850, 11 pages
http://dx.doi.org/10.1155/2014/616850

Research Article

The Role of Hypoxia-Inducible Factor-1α, Glucose Transporter-1, (GLUT-1) and Carbon Anhydrase IX in Endometrial Cancer Patients

Pawel Sadlecki,[1] Magdalena Bodnar,[2] Marek Grabiec,[1] Andrzej Marszalek,[2] Pawel Walentowicz,[1] Alina Sokup,[3] Jolanta Zegarska,[1] and Małgorzata Walentowicz-Sadlecka[1]

[1] *Department of Obstetrics and Gynecology, The Ludwik Rydygier Collegium Medicum in Bydgoszcz, Nicolaus Copernicus University of Torun, Ulica Ujejskiego 75, 85-168 Bydgoszcz, Poland*
[2] *Department of Clinical Pathology, The Ludwik Rydygier Collegium Medicum in Bydgoszcz, Nicolaus Copernicus University of Torun, 87-100 Torun, Poland*
[3] *Department of Gastroenterology, Angiology and Internal Diseases, The Ludwik Rydygier Collegium Medicum in Bydgoszcz, Nicolaus Copernicus University of Torun, 87-100 Torun, Poland*

Correspondence should be addressed to Małgorzata Walentowicz-Sadlecka; walentowiczm@cm.umk.pl

Received 27 October 2013; Accepted 9 February 2014; Published 12 March 2014

Academic Editor: Jelena Urosevic

Hypoxia-inducible factor-1α (HIF-1α), glucose transporter-1 (GLUT-1), and carbon anhydrase IX (CAIX) are important molecules that allow adaptation to hypoxic environments. The aim of our study was to investigate the correlation between HIF-1α, GLUT-1, and CAIX protein level with the clinicopathological features of endometrial cancer patients. *Materials and Methods*. 92 endometrial cancer patients, aged 37–84, were enrolled to our study. In all patients clinical stage, histologic grade, myometrial invasion, lymph node, and distant metastases were determined. Moreover, the survival time was assessed. Immunohistochemical analyses were performed on archive formalin fixed paraffin embedded tissue sections. *Results*. High significant differences ($P = 0.0115$) were reported between HIF-1α expression and the histologic subtype of cancer. Higher HIF-1α expression was associated with the higher risk of recurrence ($P = 0.0434$). The results of GLUT-1 and CAIX expression did not reveal any significant differences between the proteins expression in the primary tumor and the clinicopathological features. *Conclusion*. The important role of HIF-1α in the group of patients with the high risk of recurrence and the negative histologic subtype of the tumor suggest that the expression of this factor might be useful in the panel of accessory pathomorphological tests and could be helpful in establishing more accurate prognosis in endometrial cancer patients.

1. Introduction

Endometrial cancer is the most frequent female genital malignancy in highly developed countries, with a life time risk of its development amounting to 2-3% [1]. The aim of current ongoing studies of endometrial cancer patients is to identify new factors found in tumor tissue or blood serum that could be used in order to predict prognosis, define optimal therapeutic protocol, and estimate the risk of recurrence.

Natural course of endometrial cancer is slow and the disease is characterized by rather good prognosis. Early onset of clinical symptoms enables us to set the diagnosis at the early stage of the disease. The 5-year overall survival (OS) rate of women with endometrial cancer is high, counting more than 80% for all stages and more than 90% for stage I [2]. Endometrial cancer is successfully treated with surgery and/or radiotherapy [3]. However, for patients with advanced or recurrent disease, only limited treatment options are available. There is a group of patients with a poor prognosis, who will benefit from more aggressive treatment. This group will need adjuvant chemo- or radiotherapy. It is of great interest to learn more about the important risk factors predictive of recurrence and/or death.

The recognized so far poor prognostic factors for endometrial cancer are advanced FIGO stage, a nonendometrioid histological subtype, high grade (G3), deep invasion of myometrium (>50%), presence of lymph node metastases, cervical involvement, and lymphovascular space invasion (LVSI) [2]. All risk factors mentioned above are identified after extensive surgical procedure and detailed pathologic report.

Even though our knowledge about tumor cells have improved a lot throughout recent years, the precise mechanisms that rule the process of tumor progression and metastases formation remain unknown. Hypoxia plays a vital role in carcinogenesis. Metabolic reprogramming and changes in gene expression are necessary for adaptation to decreased O2 availability in the tumor microenvironment. Hypoxia-inducible factors (HIFs) are oxygen-sensitive transcription factors that allow adaptation to hypoxic environments. HIFs are important mediators of the cellular response to stress e.g. metabolic, hypoxic, or inflammatory. Metabolic changes occur during tumorigenesis that are, in part, under hypoxia and HIF regulation. Additionally, inflammatory signaling and infiltration secondary to hypoxia is clear drivers of tumor progression [4]. However, despite the well-documented role of hypoxia in tumor microenvironment, its significance in endometrial cancer is not completely understood. HIF-1α is a key regulator of oxygen homeostasis in nearly all nuclear cells of mammals [4, 5]. Immunohistochemical studies revealed that many cancers are characterized by overexpression of HIF-1α as compared to normal tissues [6]. Adaptation to changing levels of cellular oxygen is determined mostly by the alpha subunit of HIF-1 (HIF-1α). Under hypoxemic conditions, the active factor HIF-1α is involved in the regulation of glucose metabolism, pH, angiogenesis, cellular differentiation, migration, and formation of metastases [7–12]. The metabolism of glucose in tumor microenvironment is changed from oxygen mitochondrial process to glycolysis (the Warburg effect) [13]. HIF-1α regulates the activity of glucose transporters (GLUTs), GLUT1 and GLUT3, that are responsible for glucose uptake [14–16]. Expression of GLUT1 increases under hypoxemic conditions what induces a shift in glucose metabolism towards glycolysis. The expression of GLUT-1 was revealed to be regulated by hypoxia in a HIF-1-dependent manner [17]. Carbon anhydrase IX (CAIX) is another factor associated with the activity of HIF-1α [18]. The effect of CAIX on tumor microenvironment is characterized by the regulation of pH. The overexpression of CAIX was observed in many cancer tissues but not in normal tissues [19].

The aim of this study was to verify the usefulness of HIF-1α, GLUT-1, and CAIX, determined immunohistochemically in primary tumor and analyzed together with other clinical parameters, in predicting prognosis and planning tailored treatment of endometrial cancer patients. The detailed objectives included determining expressions of these factors in primary tumor, analysis of their relationships with other clinicopathological characteristics of the tumor, verification of the usefulness of selected immunohistochemically determined proteins as predictors of unfavorable clinicopathological parameters in endometrial cancer patients, and analysis of relationship between expression of the studied proteins and 5-year survival rate.

2. Materials and Methods

2.1. Patients. 92 endometrial cancer patients, aged 37–84 (mean 65.1 ± 9.5), were enrolled to our study between January 2000 and December 2007. After diagnosis of endometrial cancer based on specimens obtained from curettage, all patients underwent total abdominal hysterectomy, with bilateral salpingoophorectomy and pelvic lymph node dissection performed by experienced gynecological oncologists at Department of Oncologic Gynecology of LudwikRydygier Collegium Medicum in Bydgoszcz, Nicolaus Copernicus University. Clinical stage was assessed based on surgical specimens evaluation performed by two independent experienced pathologists according to International Federation of Gynecology and Obstetrics (FIGO) 2009 system. The study group included 27 patients with stage IA, 18 with stage IB, 14 with II, 10 women with stage IIIA, 17 with IIIC, and 6 with IV. Histological grade was assessed according to WHO classification. Histological grade 1 (G1) was noted in 7 patients, G2 in 66, and G3 in 19 women. Deep myometrial invasion (>50%) was observed in 36 patients, lymph node metastases in 23 women, distant metastases in 6, cervical involvement in 38, and adnexal involvement in 11 patients. Baseline characteristics of the study participants are enclosed in Table 1.

According to presently used risk factors, all patients were divided into three groups: low risk: FIGO IA, G1 or G2, and Bokhman type I (endometrioid); intermediate risk: IA G3, IB G1 or G2, and Bokhman type I (endometrioid); high risk: all patients in type II (nonendometrioid), IB G3, FIGO II, and higher. Patients from low risk group did not receive any further treatment after surgery, women from intermediate risk group received brachytherapy (VBT) 5 weeks after surgery, and patients from high risk group underwent teleradiotherapy and VBT. Adjuvant chemotherapy was administered to ten patients with nonendometrioid histopathological subtype (chemotherapy consisted of carboplatin and paclitaxel).

In all cases overall survival was determined (in months). Only cases with proven death related to cancer were analyzed. The follow-up time was 60–80 months.

The Ethical Committee at the Ludwik Rydygier Collegium Medicum, Nicolaus Copernicus University of Torun, approved this study protocol (decision number KB 332/2007). All participants have provided and signed the informed consent.

2.2. Methods. The immunohistochemical staining was performed on archive formalin fixed paraffin embedded tissue sections derived from the Department of Clinical Pathomorphology Collegium Medicum, Nicolaus Copernicus University in Torun. The paraffin blocks were cut on 4 μm thick sections and placed on extra adhesive slides (SuperFrost-Plus, Thermo Scientific). The proper immunohistochemical staining was followed by a series of positive and negative control reactions. The positive control was performed on

Table 1: Baseline characteristics of endometrial cancer patients.

	N (%)
FIGO stage	
IA	27 (29,35%)
IB	18 (19,57%)
II	14 (15,22%)
IIIA	10 (10,87%)
IIIC	17 (18,48%)
IVB	6 (6,52%)
Grading	
G1	7 (7,61%)
G2	66 (71,74%)
G3	19 (20,65%)
Bokhman subtype	
Endometrioid	70 (76,09%)
Nonendometrioid	22 (23,91%)
Lymph node metastases (N)	
Absent N0	69 (75%)
Present N1	23 (25%)
Distant metastases (M)	
Absent M0	86 (93,48%)
Present M1	6 (6,52%)
Myometrial invasion	
<50%	56 (60,87%)
≥50%	36 (39,13%)
Cervical involvement	
Absent	54 (58,70%)
Present	38 (41,30%)
Adnexal Involvement	
Absent	81 (88,04%)
Present	11 (11,96%)

model tissue sections, where from reference sources (The Human Protein Atlas) and from manufactured antibodies datasheet, the presence of the analyzed antigens was indicated. The immunohistochemical studies were performed using, respectively, mouse monoclonal antibody against HIF-1α (clone [H1ALPHA67], ab1, Abcam, Cambridge, UK), rabbit polyclonal antibody against GLUT-1 (07-1401, MILLOPORE), and rabbit polyclonal antibody against CAIX (NB100-417, NOVUS BIOLOGICALS, Cambridge, UK). The immunohistochemical staining of GLUT-1 (dilution 1 : 200) and CAIX (dilution 1 : 1500) were performed automatically in Dako AurostainerLink48 (Dako, Glostrup, Denmark) and against HIF-1α (dilution 1 : 100) was performed manually. Epitopes were unmasked in PT-Link (Dako) using Epitope Retrieval Solution pH-9, subsequently the activity of endogenous peroxidase was blocked by Peroxidase Block (Dako) for 10 minutes, and the nonspecific antibody binding was blocked by 5% BSA (bovine albumin solution) in PBS (Phosphate Buffered Saline). The incubation with primary antibody against GLUT-1 and CAIX was performed for 30 minutes in RT (room temperature) and for HIF-1α overnight at 4°C. Furthermore, tissue sections were incubated with EnVision FLEX-HRP (Dako), and the antigen-antibody complex was localized using DAB (3-3′diaminobenzidine) as a chromogen as the brown reaction product.

2.3. Examination of Protein Expression. The protein expression was evaluated in light microscope ECLIPSE E800 (Nikon Instruments Europe, Amsterdam, The Netherlands) at 20x original objective magnification. The pathologists who were evaluating the immunohistochemical expression of examined antigens worked independently, and they have been blinded for the patients' clinical as well as other data.

The protein expression was estimated using morphometric principles based on Remmele-Stegner scoring scale [20] [IRS: 0–12; SI x PP], as the ratio of the intensity of protein expression [SI][scale (0–3); 0: negative, 1: low staining, 2: moderate staining, and 3: strong staining] and the percentage of positively stained cells or tissue area [PP] [scale (0–4); 0: negative; 1, <10% positive area; 2, 10–50% positive area; 3, 50–80% positive area; 4, ≥80% positive area].

2.4. Statistical Analysis. All statistical analyses were performed using PQStat version 1.4.4.126. The statistical significance of SDF-1, CXCR4, and CXCR7 differences in relation to clinicopathological features was assessed by the use of Kruskal-Wallis and Mann-Whitney *U* test. The overall survival rate was examined for significance using log-rank test and Kaplan-Meier curves. The univariate and multivariate Cox regression were performed. For the analysis, a forward selection with a *P* value of less than 0.05 for entry was applied. The effects of the variables were expressed as hazard ratios per 1 SD change to allow for a better comparability between the effect sizes of the different tested variables. *P* value <0.05 was considered statistically significant.

3. Results

The nuclear expression of HIF-1α was found in 97% cases, the cytoplasmic-membranous expression of GLUT-1 was found in 100% cases, and the cytoplasmic-membranous expression of CAIX was found in 89% cases of endometrial cancer (Figure 1).

The results of expression of analyzed proteins according to patients' histological features are shown in Tables 2–4.

Statistical analyses revealed significant differences between the HIF-1α expression and Bokhman subtypes of endometrial cancer ($P = 0.0115$).

Moreover, higher HIF-1α expression was found for nonendometrial compared to endometrial cancer. High significant difference ($P = 0.0434$) was found between the HIF-1α expression and the risk of the recurrence. And higher HIF-1α, expression was associated with the higher risk of recurrence (Table 2). However, no statistically significant differences were obtained between the HIF-1α expression and the FIGO clinical stage, grading, lymph node, and distant metastases (Table 2). Nevertheless, statistical analyses did not reveal any significant differences between HIF-1α expression and deep myometrial invasion (≥50%), cervical involvement, and adnexa involvement (Table 2).

Table 2: The HIF1-α expression according to clinicopathological features.

	Average	Standard deviation	Minimum	Lower quartile	Median	Upper quartile	Maximum	P
FIGO stage								
IA	6.31	3.30	0	4	6	9	12	
IB	6.82	2.74	3	4	6	9	12	
II	5.14	1.46	3	4	6	6	8	NS
IIIA	7.20	2.35	4	6	8	8	12	
IIIC	5.65	3.10	0	4	6	8	12	
IVB	4.33	2.34	0	4	5	6	6	
Grading								
1	5.86	3.48	2	4	4	9	12	
2	6.25	2.77	0	4	6	8	12	NS
3	5.50	2.83	0	4	6	8	9	
Bokhman subtype								
1	5.56	2.29	0	4	6	6	12	0.0115
2	7.64	3.67	0	6	7	12	12	
Lymph node metastases								
0	6.30	2.77	0	4	6	8	12	NS
1	5.39	2.92	0	4	6	6	12	
Distant metastases								
0	6.19	2.82	0	4	6	8	12	NS
1	4.33	2.34	0	4	5	6	6	
Myometrial invasion >50%								
0	6.38	3.07	0	4	6	9	12	NS
1	5.57	2.33	0	4	6	6	12	
Cervical infiltration								
0	6.21	3.07	0	4	6	9	12	NS
1	5.87	2.46	0	4	6	8	12	
Infiltration of adnexa								
0	6.05	2.81	0	4	6	8	12	NS
1	6.18	3.03	0	4	6	8	12	
Risk of recurrence								
Low	4.90	2.15	0	4	5	6	9	0.0434
Intermediate and high	6.40	2.91	0	4	6	8	12	

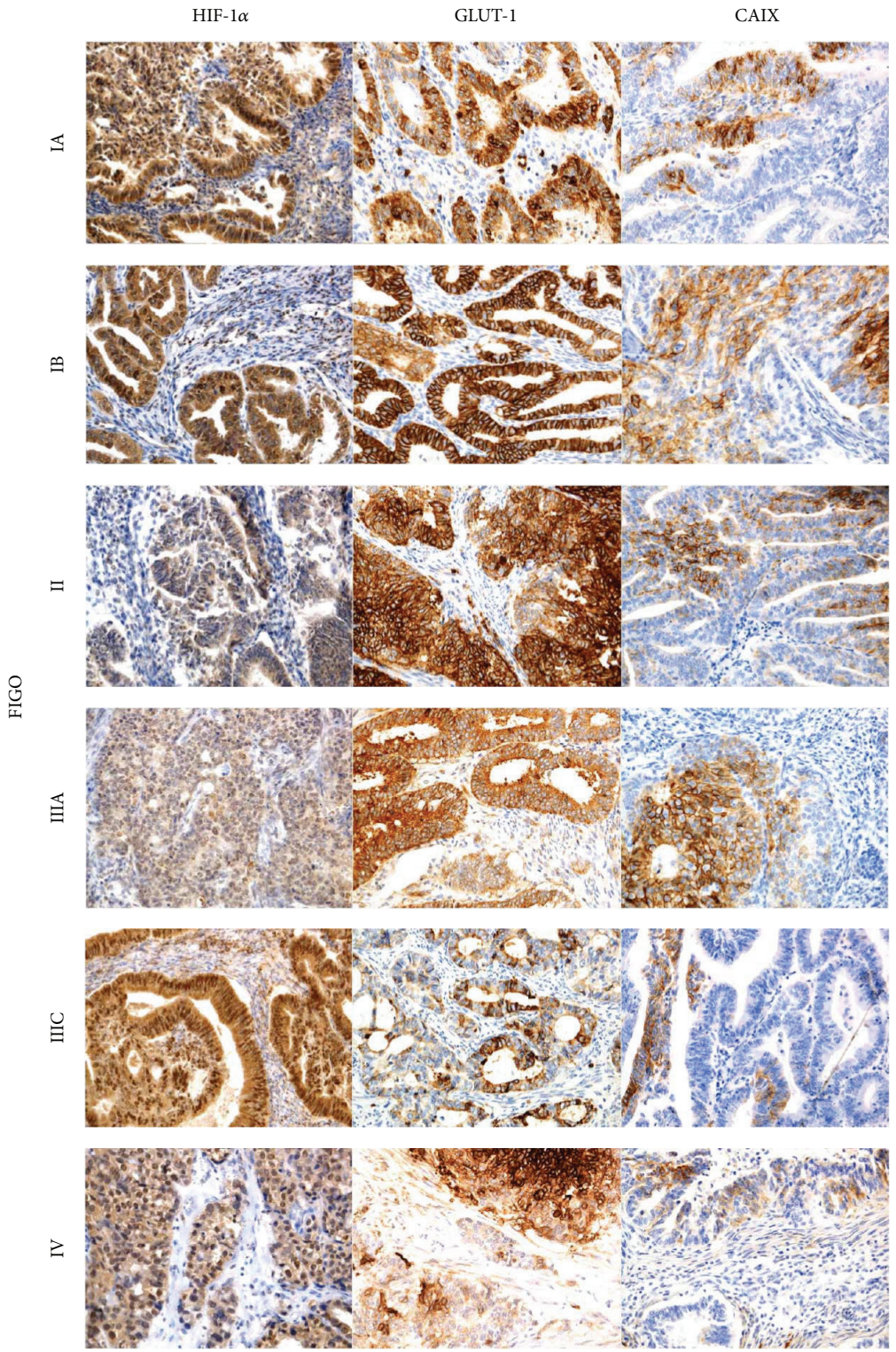

Figure 1: Immunohistochemical representative microphotographs representing the HIF-1α, GLUT-1, and CAIX expression in endometrial cancer according to FIGO classification (IA, IB, II, IIIA, IIIC, and IV). Primary objective magnification 20x.

According to GLUT-1 and CAIX expression, the statistical analyses did not reveal any significant differences in these proteins expression and FIGO clinical stage, histological grade (G), the Bokhman subtypes of endometrial cancer, lymph node involvement (N), distant metastases (M), deep myometrial invasion (≥50%), cervical involvement, involvement of adnexa, and recurrence (Tables 3-4).

Moreover, the associations between HIF-1α, GLUT-1, and CAIX expression and survival rate was also performed according to univariable and multivariable Cox regression analysis (including variables such as advanced FIGO stage (III + IV), high grade (G3), nonendometrioid subtype (Bokhman II), lymph node metastases, and deep myometrial infiltration (≥50%) (Tables 5-6). Advanced FIGO stage, high grade, lymph node infiltration, and deep myometrial invasion were statistically important prognostic factors in univariate analysis for 5-year survival.

HIF-1α expression was conditionally important. Neither nonendometrioid subtype nor GLUT-1 and CAIX expression were important in univariate analysis (Table 5). In multivariate analysis only deep myometrial invasion was statistically important (Table 6).

4. Discussion

Hypoxia plays an important role in carcinogenesis. However, despite the well-documented role of hypoxia in tumor microenvironment, its importance in endometrial cancer is not well explained. The growth of tumor requires constant increasing supply of oxygen and nutrients, which enhance development of new vasculature. Frequently, the growth of tumor precedes the development of its blood vessels which is reflected by the presence of hypoxemic areas. These areas are located both in the tumor periphery, as a consequence of enhanced proliferation, and in its central part, where the penetration of blood vessels is insufficient [21]. The hypoxia-induced synthesis of HIF-1α causes modification of tumor microenvironment. Moreover, with tumor progression cancer cells become independent of external regulatory factors and can migrate towards body regions which are better supplied in oxygen. It is postulated that the expression of HIF-1α is associated with the resistance to chemo- and radiotherapy. Such assumption stimulated research for novel agents that could overcome the therapeutic resistance associated with HIF-1α overexpression [22]. It is currently postulated that HIF-1α plays a vital role during cellular response to hypoxia. Furthermore, it was revealed that apart from hypoxia, high levels of HIF-1α can also result from stimulation with viral oncogenes [23].

It also should be mentioned that HIF-1α is involved in endometrial repair during menstrual cycle. Increased expression of HIF-1α is associated mostly with the secretory phase, with the peak expression documented during its late stages [24]. Recent studies confirmed the HIF-1α-dependent effect of decreased progesterone level and hypoxia on the induction of endometrial secretion of angiogenic factors, interleukin-8 (IL-8), and VEGF [25]. Moreover, HIF-1α was revealed to be a coactivator of estrogen-dependent VEGF synthesis [26].

HIF-1α modulates angiogenesis not only in normal endometrium but also in endometrial cancer. It was revealed that HIF-1α-positive myofibroblasts release VEGF during myometrial invasion [26]. Moreover, hypoxia acts synergistically with prostaglandin E receptor, promoting proliferation of endometrial cancer cells and growth of this tumor in an animal model [27].

HIF-1α is involved in the progression of endometrial cancer through the regulation of p27kip cell cycle inhibitor [28]. Moreover, the presence of polymorphism in HIF-1α gene is associated with greater stability of HIF-1α and its constant activation. The presence of such polymorphism was documented in endometrial cancer cells as a de novo mutation (proline serine 582). This defect was associated with higher vascular density and greater growth potential of the tumor. However, it is unclear if the presence of this polymorphism is associated with increased risk of endometrial cancer as the available data are inconclusive [28, 29].

Moreover, the stabilization of HIF-1α can result from activation of PTEN/mTOR signaling pathway. Mutations of the PTEN encoding gene enhance proliferation, increasing expression of cell cycle proteins and DNA replication. In the case of normal endometrial cells this is reflected by their self-regeneration. In contrast, the deactivation of the inhibitory transforming function of PTEN causes malignant transformation of endometrial cells [30]. The protein encoded by the PTEN suppressor gene is a phosphatase responsible for dephosphorylation of cell membrane lipids. Moreover, it acts as an inhibitor of AKT kinase pathway, inhibiting the activity of PI3K. Expression of PTEN protein is documented in approximately 83% of endometrial cancers. Impaired function of PTEN or its lack is reflected by overactivation of PI3K/AKT/mTOR pathway, leading to uncontrolled growth of the tumor. In the case of endometrial cancer cells, the PI3K/AKT/mTOR signal transduction cascade constitutes one of the main activation pathways of tyrosine kinase receptors such as vascular endothelial growth factor receptor 1 (VEGFR-1), platelet-derived growth factor receptor (PDGFR-α), epidermal growth factor receptor 1 (EGFR-1), and c-MET [31]. Due to high prevalence of PTEN mutations and resultant activation of PI3K/AKT pathway, stabilization of HIF-1α and activation of various target genes are frequently observed in endometrial cancer cells.

Currently it is postulated that the expression of HIF-1α increases, from minimal values observed in normal endometrium to intermediate and high levels documented in the case of endometrial hyperplasia and cancer, respectively [28]. The fact that the expression of HIF-1α increases proportionally to the clinical stage of the tumor is equally important. The increase in the expression of HIF-1α is accompanied by an increase in vascular density, a marker of angiogenesis; this points to the relationship between HIF-1α, angiogenesis, and endometrial cancer. Furthermore, the association between the expression of HIF-1α, increasing level of angiopoietin-1/angiopoietin-2, and enhanced synthesis of IL-8 was documented, also confirming the role of HIF-1α in the angiogenesis of endometrial cancer [32].

Our study confirmed the expression of HIF-1α in endometrial cancer. Compared to endometrioid tumors, the exp-

Table 3: The GLUT-1 expression according to clinicopathological features.

	Average	Standard deviation	Minimum	Lower quartile	Median	Upper quartile	Maximum	P
FIGO stage								
IA	6.35	2.24	2	6	6	8	12	
IB	6.65	1.69	4	6	6	9	9	
II	6.64	1.28	6	6	6	6	9	NS
IIIA	6.00	0.00	6	6	6	6	6	
IIIC	5.29	1.21	2	4	6	6	6	
IVB	7.50	1.64	6	6	7.5	9	9	
Grading								
1	6.00	2.52	2	4	6	9	9	
2	6.31	1.62	2	6	6	6	12	NS
3	6.33	1.78	2	6	6	6	9	
Bokhman subtype								
1	6.34	1.75	2	6	6	6	12	NS
2	6.14	1.61	2	6	6	6	9	
Lymph node metastases								
0	6.48	1.75	2	6	6	6	12	NS
1	5.74	1.48	2	6	6	6	9	
Distant metastases								
0	6.20	1.69	2	6	6	6	12	NS
1	7.50	1.64	6	6	7.5	9	9	
Myometrial invasion >50%								
0	6.16	1.90	2	6	6	6	12	NS
1	6.49	1.36	4	6	6	6	9	
Cervical infiltration								
0	6.35	2.07	2	6	6	8.5	12	NS
1	6.21	1.07	4	6	6	6	9	
Infiltration of adnexa								
0	6.25	1.77	2	6	6	6	12	NS
1	6.55	1.21	6	6	6	6	9	
Risk of recurrence								
Low	6.20	2.46	2	5	6	7.5	12	NS
Intermediate and high	6.31	1.45	2	6	6	6	9	

Table 4: The CAIX expression according to clinicopathological features.

	Average	Standard deviation	Minimum	Lower quartile	Median	Upper quartile	Maximum	P
FIGO stage								
IA	3.26	2.61	0	0	3	6	9	
IB	4.53	1.74	2	3	6	6	6	
II	4.07	2.16	0	2	5	6	6	NS
IIIA	4.60	2.55	0	3	5	6	9	
IIIC	4.71	2.52	0	2	6	6	9	
IVB	3.67	2.34	0	2	4	6	6	
Grading								
1	2.86	1.86	0	2	3	4	6	
2	4.38	2.39	0	2	6	6	9	NS
3	3.42	2.29	0	2	3	6	6	
Bokhman subtype								
1	4.19	2.35	0	2	4	6	9	NS
2	3.68	2.46	0	2	4	6	9	
Lymph node metastases								
0	3.96	2.34	0	2	4	6	9	NS
1	4.39	2.48	0	2	4	6	9	
Distant metastases								
0	4.09	2.38	0	2	4	6	9	NS
1	3.67	2.34	0	2	4	6	6	
Myometrial invasion >50%								
0	3.80	2.36	0	2	4	6	9	NS
1	4.49	2.36	0	3	4	6	9	
Cervical infiltration								
0	3.75	2.24	0	2	4	6	9	NS
1	4.50	2.50	0	2	6	6	9	
Infiltration of adnexa								
0	4.04	2.43	0	2	4	6	9	NS
1	4.27	2.00	0	3	4	6	6	
Risk of recurrence								
Low	4.05	2.50	0	2	4	6	9	NS
Intermediate and high	4.07	2.35	0	2	4	6	9	

Table 5: Prognostic factors for overall survival selected by Cox's univariate analysis.

	Parameter evaluation	P value	HR	HR (95% CI)	
				−95% CI	+95% CI
HIF-1α	0.070756	0.092396	0.887741	0.772784	1.019798
GLUT-1	0.112819	0.654167	1.051840	0.843175	1.312143
CAIX	0.079180	0.610033	0.960421	0.822363	1.121656
Figo [III + IV]	0.196299	0.002108	0.299063	0.138543	0.645570
G3	0.204699	0.026614	0.403454	0.180847	0.900066
Bokhman's subtype 2	0.210773	0.606716	0.804931	0.352320	1.838992
N+	0.193138	0.001314	0.289078	0.135586	0.616332
Mm [>50%]	0.200038	0.000652	0.255676	0.116720	0.560059

CI: confidence interval; FIGO: Federation Internationale de Gynecologie et d'Obstetrique; HR: hazard ratio; N+: lymph node involvement.

Table 6: Prognostic factors for overall survival selected by Cox's multivariate analysis.

	Parameter evaluation	P value	HR	HR (95% CI)	
				−95% CI	+95% CI
HIF-1α	0.071684	0.406520	0.942235	0.818732	1.084369
GLUT-1	0.131077	0.642657	1.062705	0.821940	1.373996
CAIX	0.085198	0.545842	0.949842	0.803769	1.122462
Figo [III + IV]	0.400904	0.868605	0.875777	0.181925	4.215931
G3	0.246020	0.448415	0.688668	0.262533	1.806490
Bokhman's subtype 2	0.223343	0.678850	0.831152	0.346307	1.994802
N+	0.336866	0.436507	0.592009	0.158069	2.217227
Mm [>50%]	0.278537	0.043148	0.340540	0.114284	1.014729

CI: confidence interval; FIGO: Federation Internationale de Gynecologie et d'Obstetrique; HR: hazard ratio; N+: lymph node involvement.

ression of anti-HIF-1α antibody was significantly higher in nonendometrioid malignancies ($P = 0.0115$). The level of HIF-1α was significantly associated with the presence of subtype 2 according to Bokhman. Our findings are consistent with the results of the only previous study analyzing the expression of HIF-1α depending on Bokhman's subtype [33]. Pansare et al. revealed that the expression of HIF-1α is higher in nonendometrioid type of endometrial cancer. Moreover, these authors showed that the increased expression of HIF-1α is associated with the presence of unfavorable prognostic factors (histopathological grade, histological subtype, depth of myometrial invasion, involvement of vascular spaces, and/or adnexa) in patients with Bokhman's subtype 1 of endometrial cancer [33].

Furthermore, we observed that the expression of HIF-1α differed significantly depending on the risk of recurrence ($P = 0.0434$). Significantly higher expression of anti-HIF-1α antibody was associated with moderate and high risk of recurrence. Both univariate and multivariate analysis of regression revealed that the expression of HIF-1α protein is a significant predictor of Bokhman's subtype 2 and is associated with moderate or high risk of recurrence. The results of previous studies on the prognostic value of HIF-1α in endometrial cancer are inconclusive and controversial. According to some authors, higher expression of HIF-1α is associated with shorter survival and time to recurrence; in contrast, other researchers postulated that HIF-1α is not associated with prognosis in endometrial cancer patients [34–37]. Noticeably, our study showed that higher expression of this protein is associated with less favorable type of endometrial cancer (subtype 2) and higher risk of recurrence; this seems consistent with the results of Seeber's and Sivridis' studies [34, 35]. Apart from other reasons, the discrepancies between the results of previous studies may result from the lack of unified standards of HIF-1α determination in endometrial cancer patients (solely nuclear versus solely cytoplasmic expression, determination in the whole tumor with or without the necrotic areas) and small size of examined groups. All the facts mentioned above suggest that the role of HIF-1α in endometrial cancer prognosis is still not unambiguously explained and further studies of larger groups of patients are needed in order to solve the problem in question.

The idea behind detailed understanding of molecular mechanisms underlying the development of endometrial cancer is to implement targeted therapies improving the outcome of patients with this malignancy. Confirming the involvement of PTEN/mTOR pathway in endometrial carcinogenesis stimulated research on mTOR inhibitors. In a phase 2 study of rapamycin derivative, temsirolimus, partial response was documented in 14% of endometrial cancer patients without previous chemotherapy and in 4% of women with a history of systemic treatment. Furthermore, 69% of previously untreated women and 48% of the patients after chemotherapy showed stabilization of the disease. However, this study did not reveal a relationship between the expression of PTEN protein or the presence of mutation in PTEN gene

and the outcome of temsirolimus therapy [38]. Currently other mTOR inhibitors are being tested in the therapy of advanced endometrial cancer.

The expression of HIF-1α in a hypoxemic tumor microenvironment changes the metabolism of glucose from aerobic to nonaerobic process. Glucose transporters (GLUTs) and carbonic anhydrases (CAs) are involved in this adaptation to changed aerobic conditions. GLUT-1 is a glucose transporter which is also responsible for the uptake of this sugar. The expression of GLUT-1 increased under nonaerobic conditions, inducing a metabolic shift towards glycolysis. Previous studies failed to document the expression of GLUT-1 in most normal epithelial cells. In contrast, the overexpression of GLUT-1 was confirmed in the case of various neoplasms, for example, in colorectal, esophageal, thyroid, lung, ovarian, and breast cancer [39]. Our study revealed that the expression of GLUT-1 is increased in endometrial cancer as well. However, we did not document significant correlations between the expression of GLUT-1 and clinicopathological characteristics of endometrial cancer. This observation seems consistent with previous reports according to which the presence of GLUT-1 is a marker of neoplastic transformation [40]. The lack of GLUT-1 expression in normal endometrium as well as its weak expression in precancerous lesions and overexpression in endometrial cancer suggests that this molecule can be involved in early stages of endometrial carcinogenesis. According to Xiong et al., the expression of GLUT-1 can be used to distinguish between benign endometrial lesions and endometrial cancer but has no prognostic value in women with this malignancy [39]. This is consistent with the results of our study which did not show significant differences in the expression of GLUT-1 associated with clinical stage or prognosis in endometrial cancer patients.

In order to analyze the hypoxemic tumor microenvironment more comprehensively, we determined its expression of carbonic anhydrase IX (CAIX). This transmembrane HIF-1α-dependent glycoprotein is responsible for the regulation of pH in the tumor microenvironment [18]. CAIX plays an important role in the elimination of acids synthesized during the hypoxia-induced glycolysis. The overexpression of CAIX was observed in many neoplasms but not in normal tissues [19]. Our study confirmed increased expression of CAIX in the microenvironment of endometrial cancer. However, we did not observe significant correlations between the level of this expression and clinicopathological characteristics of the tumor. This finding is in line with the results of two studies published to date [41, 42]. Knapp et al. confirmed that the expression of CAIX in endometrial cancer is higher than in normal endometrium and suggested the involvement of anhydrase IX in the shift of glucose metabolism associated with neoplastic transformation [41]. Also Hynninen et al. claimed on the lack CAIX in normal endometrium and its high expression in endometrial cancer tissue [42]. However, the results of our study suggest that the determination of both GLUT1 and CAIX expression is not useful in establishing prognosis in endometrial cancer patients. The involvement of GLUT1 and CAIX in the early stages of carcinogenesis, that is, in the metabolic "shift," points to their potential application in distinguishing between benign and malignant lesions rather than in prediction of prognosis in endometrial cancer patients.

In conclusion, the important role of HIF-1α in the group of patients with the high risk of recurrence and the negative histologic subtype of the tumor suggests that the expression of this factor might be useful in the panel of accessory pathomorphological tests and could be helpful in establishing more accurate prognosis in endometrial cancer patients.

Conflict of Interests

The authors declare that there is no conflict of interests regarding the publication of this paper.

References

[1] A. Jemal, R. Siegel, J. Xu, and E. Ward, "Cancer statistics, 2010," *CA Cancer Journal for Clinicians*, vol. 60, no. 5, pp. 277–300, 2010.

[2] F. Amant, P. Moerman, P. Neven, D. Timmerman, E. van Limbergen, and I. Vergote, "Endometrial cancer," *The Lancet*, vol. 366, no. 9484, pp. 491–505, 2005.

[3] J. N. Bakkum-Gamez, J. Gonzalez-Bosquet, N. N. Laack, A. Mariani, and S. C. Dowdy, "Current issues in the management of endometrial cancer," *Mayo Clinic Proceedings*, vol. 83, no. 1, pp. 97–112, 2008.

[4] J. E. S. Shay and M. Celeste Simon, "Hypoxia-inducible factors: crosstalk between inflammation and metabolism," *Seminars in Cell and Developmental Biology*, vol. 23, pp. 389–394, 2012.

[5] W. Liu, S.-M. Shen, X.-Y. Zhao, and G.-Q. Chen, "Targeted genes and interacting proteins of hypoxia inducible factor-1," *International Journal of Biochemistry and Molecular Biology*, vol. 3, pp. 165–178, 2012.

[6] H. Zhong, A. M. de Marzo, E. Laughner et al., "Overexpression of hypoxia-inducible factor 1α in common human cancers and their metastases," *Cancer Research*, vol. 59, no. 22, pp. 5830–5835, 1999.

[7] E. A. O'Toole, R. van Koningsveld, M. Chen, and D. T. Woodley, "Hypoxia induces epidermal keratinocyte matrix metalloproteinase-9 secretion via the protein kinase C pathway," *Journal of Cellular Physiology*, vol. 214, no. 1, pp. 47–55, 2008.

[8] T. Ishikawa, K.-I. Nakashiro, S. K. Klosek et al., "Hypoxia enhances CXCR4 expression by activating HIF-1 in oral squamous cell carcinoma," *Oncology Reports*, vol. 21, no. 3, pp. 707–712, 2009.

[9] Y. Li, X. Qiu, S. Zhang, Q. Zhang, and E. Wang, "Hypoxia induced CCR7 expression via HIF-1α and HIF-2α correlates with migration and invasion in lung cancer cells," *Cancer Biology and Therapy*, vol. 8, no. 4, pp. 322–330, 2009.

[10] Q. Sun, H. Zhou, N. O. Binmadi, and J. R. Basile, "Hypoxia-inducible factor-1-mediated regulation of semaphorin 4D affects tumor growth and vascularity," *Journal of Biological Chemistry*, vol. 284, no. 46, pp. 32066–32074, 2009.

[11] Z.-B. Han, H. Ren, H. Zhao et al., "Hypoxia-inducible factor (HIF)-1α directly enhances the transcriptional activity of stem cell factor (SCF) in response to hypoxia and epidermal growth factor (EGF)," *Carcinogenesis*, vol. 29, no. 10, pp. 1853–1861, 2008.

[12] B. D. Kelly, S. F. Hackett, K. Hirota et al., "Cell type-specific regulation of angiogenic growth factor gene expression and

induction of angiogenesis in nonischemic tissue by a constitutively active form of hypoxia-inducible factor 1," *Circulation Research*, vol. 93, no. 11, pp. 1074–1081, 2003.

[13] O. Warburg, "On the origin of cancer cells," *Science*, vol. 123, no. 3191, pp. 309–314, 1956.

[14] M. Hayashi, M. Sakata, T. Takeda et al., "Induction of glucose transporter 1 expression through hypoxia-inducible factor 1α under hypoxic conditions in trophoblast-derived cells," *Journal of Endocrinology*, vol. 183, no. 1, pp. 145–154, 2004.

[15] J. W. Calvert, J. Cahill, M. Yamaguchi-Okada, and J. H. Zhang, "Oxygen treatment after experimental hypoxia-ischemia in neonatal rats alters the expression of HIF-1α and its downstream target genes," *Journal of Applied Physiology*, vol. 101, no. 3, pp. 853–865, 2006.

[16] Y. Liu, Y.-M. Li, R.-F. Tian et al., "The expression and significance of HIF-1α and GLUT-3 in glioma," *Brain Research*, vol. 1304, pp. 149–154, 2009.

[17] C. Chen, N. Pore, A. Behrooz, F. Ismail-Beigi, and A. Maity, "Regulation of glut1 mRNA by hypoxia-inducible factor-1: interaction between H-ras and hypoxia," *Journal of Biological Chemistry*, vol. 276, no. 12, pp. 9519–9525, 2001.

[18] C. Potter and A. L. Harris, "Hypoxia inducible carbonic anhydrase IX, marker of tumor hypoxia, survival pathway and therapy target," *Cell Cycle*, vol. 3, no. 2, pp. 164–167, 2004.

[19] A. Thiry, J.-M. Dogné, B. Masereel, and C. T. Supuran, "Targeting tumor-associated carbonic anhydrase IX in cancer therapy," *Trends in Pharmacological Sciences*, vol. 27, no. 11, pp. 566–573, 2006.

[20] W. Remmele and H. E. Stegner, "Recommendation for uniform definition of an immunoreactive score (IRS) for immunohistochemical estrogen receptor detection (ER-ICA) in breast cancer tissue," *Pathologe*, vol. 8, no. 3, pp. 138–140, 1987.

[21] V. Dousias, T. Vrekoussis, I. Navrozoglou et al., "Hypoxia-induced factor-1a in endometrial carcinoma: a mini-review of current evidence," *Histology and Histopathology*, vol. 27, pp. 1247–1253, 2012.

[22] L. M. S. Seeber, R. P. Zweemer, R. H. M. Verheijen, and P. J. van Diest, "Hypoxia-inducible factor-1 as a therapeutic target in endometrial cancer management," *Obstetrics and Gynecology International*, vol. 2010, Article ID 580971, 8 pages, 2010.

[23] M. Nakamura, J. M. Bodily, M. Beglin, S. Kyo, M. Inoue, and L. A. Laimins, "Hypoxia-specific stabilization of HIF-1alpha by human papillomaviruses," *Virology*, vol. 387, no. 2, pp. 442–448, 2009.

[24] H. O. D. Critchley, J. Osei, T. A. Henderson et al., "Hypoxia-inducible factor-1 expression in human endometrium and its regulation by prostaglandin E-series prostanoid receptor 2 (EP2)," *Endocrinology*, vol. 147, no. 2, pp. 744–753, 2006.

[25] J. A. Maybin, N. Hirani, P. Brown, H. N. Jabbour, and H. O. D. Critchley, "The regulation of vascular endothelial growth factor by hypoxia and prostaglandin F2α during human endometrial repair," *Journal of Clinical Endocrinology and Metabolism*, vol. 96, no. 8, pp. 2475–2483, 2011.

[26] A. Orimo, Y. Tomioka, Y. Shimizu et al., "Cancer-associated myofibroblasts possess various factors to promote endometrial tumor progression," *Clinical Cancer Research*, vol. 7, no. 10, pp. 3097–3105, 2001.

[27] R. D. Catalano, M. R. Wilson, S. C. Boddy, A. T. M. McKinlay, K. J. Sales, and H. N. Jabbour, "Hypoxia and prostaglandin E receptor 4 signalling pathways synergise to promote endometrial adenocarcinoma cell proliferation and tumour growth," *PLoS ONE*, vol. 6, no. 5, Article ID e19209, 2011.

[28] N. Horrée, P. J. van Diest, P. van der Groep, D. M. D. S. Sie-Go, and A. P. M. Heintz, "Hypoxia and angiogenesis in endometrioid endometrial carcinogenesis," *Cellular Oncology*, vol. 29, no. 3, pp. 219–227, 2007.

[29] E. Konac, H. I. Onen, J. Metindir, E. Alp, A. A. Biri, and A. Ekmekci, "An investigation of relationships between hypoxia-inducible factor-1α gene polymorphisms and ovarian, cervical and endometrial cancers," *Cancer Detection and Prevention*, vol. 31, no. 2, pp. 102–109, 2007.

[30] M. P. Myers, I. Pass, I. H. Batty et al., "The lipid phosphatase activity of PTEN is critical for its tumor supressor function," *Proceedings of the National Academy of Sciences of the United States of America*, vol. 95, no. 23, pp. 13513–13518, 1998.

[31] P. J. Wysocki, "MTOR in renal cell cancer: Modulator of tumor biology and therapeutic target," *Expert Review of Molecular Diagnostics*, vol. 9, no. 3, pp. 231–241, 2009.

[32] J. Fujimoto, E. Sato, S. M. Alam et al., "Plausible linkage of hypoxia-inducible factor (HIF) in uterine endometrial cancers," *Oncology*, vol. 71, no. 1-2, pp. 95–101, 2007.

[33] V. Pansare, A. R. Munkarah, V. Schimp et al., "Increased expression of hypoxia-inducible factor 1α in type I and type II endometrial carcinomas," *Modern Pathology*, vol. 20, no. 1, pp. 35–43, 2007.

[34] L. M. S. Seeber, N. Horrée, P. van der Groep, E. van der Wall, R. H. M. Verheijen, and P. J. van Diest, "Necrosis related HIF-1α expression predicts prognosis in patients with endometrioid endometrial carcinoma," *BMC Cancer*, vol. 10, article 307, 2010.

[35] E. Sivridis, A. Giatromanolaki, K. C. Gatter, A. L. Harris, and M. I. Koukourakis, "Association of hypoxia-inducible factors 1α and 2α with activated angiogenic pathways and prognosis in patients with endometrial carcinoma," *Cancer*, vol. 95, no. 5, pp. 1055–1063, 2002.

[36] A. Giatromanolaki, M. I. Koukourakis, K. C. Gatter, A. L. Harris, and E. Sivridis, "BNIP3 expression in endometrial cancer relates to active hypoxia inducible factor 1α pathway and prognosis," *Journal of Clinical Pathology*, vol. 61, no. 2, pp. 217–220, 2008.

[37] G. Acs, X. Xu, C. Chu, P. Acs, and A. Verma, "Prognostic significance of erythropoietin expression in human endometrial carcinoma," *Cancer*, vol. 100, no. 11, pp. 2376–2386, 2004.

[38] A. M. Oza, L. Elit, M.-S. Tsao et al., "Phase II study of temsirolimus in women with recurrent or metastatic endometrial cancer: a trial of the NCIC Clinical Trials Group," *Journal of Clinical Oncology*, vol. 29, no. 24, pp. 3278–3285, 2011.

[39] Y. Xiong, Y. Y. Xiong, and Y. F. Zhou, "Expression and significance of β-catenin, Glut-1 and PTEN in proliferative endometrium, endometrial intraepithelial neoplasia and endometrioid adenocarcinoma," *European Journal of Gynaecological Oncology*, vol. 31, no. 2, pp. 160–164, 2010.

[40] Y. Noguchi, A. Saito, Y. Miyagi et al., "Suppression of facilitative glucose transporter 1 mRNA can suppress tumor growth," *Cancer Letters*, vol. 154, no. 2, pp. 175–182, 2000.

[41] P. Knapp, A. Chabowski, D. Harasiuk, and J. Górski, "Reversed glucose and fatty acids transporter expression in human endometrial cancer," *Hormone and Metabolic Research*, vol. 44, pp. 436–441, 2012.

[42] P. Hynninen, S. Parkkila, H. Huhtala et al., "Carbonic anhydrase isozymes II, IX, and XII in uterine tumors," *APMIS*, vol. 120, no. 2, pp. 117–129, 2012.

Hindawi Publishing Corporation
BioMed Research International
Volume 2013, Article ID 453606, 11 pages
http://dx.doi.org/10.1155/2013/453606

Research Article

Chromogenic In Situ Hybridization and p16/Ki67 Dual Staining on Formalin-Fixed Paraffin-Embedded Cervical Specimens: Correlation with HPV-DNA Test, E6/E7 mRNA Test, and Potential Clinical Applications

Roberta Zappacosta,[1] Antonella Colasante,[2] Patrizia Viola,[2] Tommaso D'Antuono,[2] Giuseppe Lattanzio,[2] Serena Capanna,[2] Daniela Maria Pia Gatta,[1] and Sandra Rosini[1]

[1] *Cytopathology Unit, Experimental and Clinical Sciences Department, "G. d'Annunzio" University of Chieti-Pescara, Via dei Vestini, 66100 Chieti, Italy*
[2] *Surgical Pathology Unit, "SS Annunziata" Hospital, ASL2 Abruzzo, Chieti, Italy*

Correspondence should be addressed to Roberta Zappacosta; zappacosta2@hotmail.com

Received 16 July 2013; Revised 20 September 2013; Accepted 30 September 2013

Academic Editor: Oronza Antonietta Botrugno

Although HPV-DNA test and E6/E7 mRNA analyses remain the current standard for the confirmation of human papillomavirus (HPV) infections in cytological specimens, no universally adopted techniques exist for the detection of HPV in formalin-fixed paraffin-embedded samples. Particularly, in routine laboratories, molecular assays are still time-consuming and would require a high level of expertise. In this study, we investigated the possible use of a novel HPV tyramide-based chromogenic in situ hybridization (CISH) technology to locate HPV on tissue specimens. Then, we evaluate the potential usefulness of $p16^{INK4a}$/Ki-67 double stain on histological samples, to identify cervical cells expressing HPV E6/E7 oncogenes. In our series, CISH showed a clear signal in 95.2% of the specimens and reached a sensitivity of 86.5%. CISH positivity always matched with HPV-DNA positivity, while 100% of cases with punctated signal joined with cervical intraepithelial neoplasia grade 2 or worse (CIN2+). p16/Ki67 immunohistochemistry gave an interpretable result in 100% of the cases. The use of dual stain significantly increased the agreement between pathologists, which reached 100%. Concordance between dual stain and E6/E7 mRNA test was 89%. In our series, both CISH and $p16^{INK4a}$/Ki67 dual stain demonstrated high grade of performances. In particular, CISH would help to distinguish episomal from integrated HPV, in order to allow conclusions regarding the prognosis of the lesion, while $p16^{INK4a}$/Ki67 dual stain approach would confer a high level of standardization to the diagnostic procedure.

1. Introduction

HPV infection is recognised as the necessary cause of cervical intraepithelial lesions (CIN) and invasive squamous cell carcinoma (SSC). However, only a minority of viral infections ever results in neoplastic lesions. It is well known that the majority of HPV infections may be cleared by the immune system, and that certain high-risk (HR) HPV types (HPV 16, 18, 31, 33, 45, and 54) are significantly more common among high-grade lesions and carcinomas [1].

The most important factor in CIN progression is certainly the integration of HPV sequences into the host genome with the loss of E2 tumor suppressor gene. E2 physiologically regulates the expression of E6 and E7 oncogenes. There is consensus that integration is common in high-grade CIN and cancer, while it is infrequent or is lacking in low-grade CIN. HPV integration, disrupting cell-cycle control and escaping immune system surveillance, would induce stochastic accumulation of genetic aberrations, leading to CIN progression.

Recently, a wide range of molecular techniques has been evaluated on cytological specimens, to improve cervical cancer screening strategies [2, 3]. HPV-DNA test showed a high sensitivity in identifying CIN, but it still lacks clinical

specificity, due to the high prevalence of transient infection [2]. E6/E7 mRNA test, targeting patients at higher risk of CIN progression, demonstrated to be more specific than DNA test in stratifying the risk for cancer development [4].

On tissue specimens, the ideal test for the detection of HPV has not been established yet, although different assays have been analyzed (i.e., PCR, in situ hybridization, ISH). Potential useful marker should target viral genome or related proteins (i.e., DNA, mRNA) or should identify host cell's products whose expression would be stimulated by HPV infection. In this context, immunohistochemical (IHC) localization of $p16^{INK4a}$ (henceforth p16) seems to represent one of the most widely investigated tool.

p16 is a tumor suppressor protein playing a crucial role in cell-cycle regulation. p16 prevents the phosphorylation of the retinoblastoma protein (pRb) by inhibiting cyclin-dependent kinases CDK4 and CDK6. Physiologically, non-phosphorylated pRb binds the transcription factor E2F, thereby preventing E2F stimulation of cell progression into S phase. The functional inactivation of pRb by HPV-E7 oncoprotein induces E2F factor release that becomes subsequently free to drive cell-cycle progression towards S phase.

All the above mentioned markers and technologies are a matter of controversy, each having their advantages and drawbacks.

PCR is considered the most effective method for HPV-DNA detection, but some problems still exist in routinely practice: DNA extraction compromises the preservation of tissue architecture [5]; moreover, it requires a high of expertise and strict laboratory conditions, to avoid contaminations [6]. ISH is cheap and relatively easy to perform. It would permit the detection of HPV-DNA, as well as the preservation of histological pattern. On the other hand, ISH lacks in sensitivity (limit of 10–50 DNA copy/cell) [7, 8]. To by-pass this problem, a tyramide-based signal amplification kit, based on HPV chromogenic in situ (CISH) technology, has been developed [5].

p16 demonstrated to be useful as surrogate biomarker of HPV integration and E7 overexpression. However, pitfalls such as positive staining by nondysplastic cells would limit its clinical accuracy. Recently, a novel concept of biomarker based on the combination of p16 and Ki-67 detection in cervical cytology specimens (p16/Ki-67 double stain) has been proposed. Under physiological conditions, the coexpression of these proteins does not occur, since they typically induce opposite effects [6]. Simultaneous expression of both markers within the same cervical cell would indicate HPV-dependent deregulated cell cycle. Only limited results are available for p16/Ki67 assay [6, 9, 10]; all of these concerning its potential utility on cytological samples. To our knowledge, there are no data regarding the feasibility of p16/Ki67 double stain on histological specimens.

Basing on this background, in the first phase of this study, we aimed to analyze analytical and diagnostic accuracies of the novel CISH technology in detecting viral DNA and in identifying HPV physical status on formalin-fixed and paraffin-embedded tissue. To do that, CISH results were compared with results obtained from HPV-DNA test and HPV-mRNA test.

In the second phase, we assessed the potential usefulness of CINtec PLUS p16/Ki-67 double-stain immunohistochemistry (IHC) on histological samples with different degrees of dysplasia, to detect cervical lesions expressing E6/E7 HPV oncogenes.

2. Materials and Methods

2.1. Cervical Tissue Specimens Selection. This study was performed in agreement with the standards of the ethics review board of "SS Annunziata" Hospital and was approved by the Ethical Committees of "G. d'Annunzio" University, in accordance with the principles outlined in the Declaration of Helsinki of 1975.

From the electronic files of Surgical Pathology Department of "SS Annunziata" Hospital of Chieti, 926 cases of biopsy-proven squamous cervical lesion, obtained from January 2010 to July 2012, were retrospectively retrieved.

Among these casuistries, 154 cases met the following inclusion criteria:

(i) HPV-DNA test result by Hybrid Capture 2 (HC2), performed on liquid-based sample of exfoliated cells, collected from cervix immediately before colposcopy-directed biopsy of the lesion;

(ii) result from mRNA testing, performed on residual cervical liquid-based cytological specimen.

Two pathologists independently reviewed haematoxylin and eosin (H&E) stained slides and reported histological diagnosis according to the World Health Organization nomenclature and criteria as follows:

Cervical Intraepithelial Neoplasia grade 1, CIN1;

CIN grade 2, CIN2;

CIN grade 3, CIN3;

invasive squamous cell carcinoma (SSC).

Only cases reaching consensus in histological diagnosis were finally included in the study (63 formalin-fixed, paraffin-embedded, FFPE).

A written informed consent was obtained from all the participants in the study, and corresponding FFPE specimens were subsequently taken. Identification codes were finally assigned to each case, in accordance with confidentiality standards.

2.2. Laboratory Methods

(i) Cervical Cytology. Cervicovaginal samples were collected from ecto-endocervix immediately before colposcopy-directed biopsy. Cervical specimens were then transferred into PreservCyt cytology medium (Cytyc Corporation, Boxborough, MA) liquid and transported to Cytopathology Departments. Cytological vials were processed using ThinPrep 2000 (Hologic, Marlborough, MA, USA). Slides were next stained with Papanicolaou procedure.

(ii) HPV-DNA Test. After cytological slide preparation, an aliquot (4 mL) of each liquid-based cytological (LBC) sample,

stored at RT, was removed to perform HPV-DNA testing by using the commercially available Hybrid Capture 2 system (HC2, Qiagen, Gaithersburg, MD), in accordance to manufacturer's protocol. HC2 detects oncogenic HPV types (16, 18, 31, 33, 35, 39, 45, 51, 52, 56, 58, 59, and 68). HC2 reactions were read by a luminometer, which provided a relative quantification of each individual sample in comparison to the mean of a series of positive controls containing 1 pg/mL of HPV DNA (corresponding to ~100,000 HPV-16 genomes/mL or 5,000 HPV copies per reaction). The cut-off of 1 relative light unit (RLU) was used to classify a specimen as positive or negative. RLUs value in relation to control (RLU/CO) provided an estimation of the number of HPV-DNA copies of each sample (viral load). The RLU value of each individual sample was then recorded. According to RLU/CO values, HPV-DNA positive cases were arbitrarily categorized into three groups having "low viral load" (RLU/CO from 1.0 to 50.0 RLU/CO), "intermediate viral load" (RLU/CO from 50.1 to 100.00 RLU/CO), and "high viral load" (RLU/CO > 100).

(iii) HPV-mRNA Test. A second aliquot (3 mL) from each residual LBC specimen was transferred into a fresh 10 mL tube for nucleic acids extraction. After centrifugation, the supernatant was removed and the sample was transferred into a tube containing 2 mL Nuclisens Lysis Buffer (BioMèrieux, France). Next, magnetized silica dioxide particles were added to the lysate to initiate the nucleic acids isolation process. Finally, nucleic acids were eluted from the solid phase in 55 μL of elution buffer and stored at −20°C if not further processed immediately after extraction.

15 μL of nucleic acids was used to perform mRNA testing (Nuclisens EasyQ HPV, BioMèrieux, France), in accordance with the manufacturer's instructions.

mRNA testing is based on real-time nucleic acid sequence based amplification (NASBA) procedure, which utilizes molecular beacon probes labelled with 5-carboxyfluorescein (FAM) and Texas Red fluorochromes, at an isothermal temperature of 41°C. The test identifies full-length E6/E7 mRNA from five high-risk carcinogenic HPV types (16, 18, 31, 33, and 45). A fluorescent analyzer measured in real time the emission of the fluorescence from molecular beacon hybridized with amplified mRNA. As performance control, the human U1A mRNA from the small ribonucleoprotein-specific A protein has been used. Negative control reactions, consisting of all reagents except RNA, were performed at each run. mRNA testing was defined as positive if at least one of the five HPV genotypes detected by the test has been found [11].

(iv) Chromogenic In Situ Hybridization. Two serial sections were cut to a thickness of 4 μm, one for CISH investigation and one for p16/Ki67 dual-stain IHC. The extra sections cut before and after each tissue section were stained with H&E and used to evaluate the adequacy of each FFPE for the subsequent investigations.

Bond ready-to-use DNA CISH HPV protocol (Bond ready-to-use DNA ISH HPV Probe by Leica Biosystems, Newcastle Ltd, Newcastle, UK) able to detect 5 oncogenic HPV types (types 16, 18, 31, 33, and 54) was optimized for reproducible sensitive and background free usage. Slides were then processed using the Bond-Max automated slide-staining system (Leica Biosystems, Newcastle Ltd, Newcastle, UK). Finally, CISH sections were counterstained with haematoxylin. HPV-positive controls consisted of FFPE sections containing two sets of cells: CaSki cervical cancer cell line (containing 200 to 400 copies of HPV-DNA types 16 per cell) and HeLa cervical cancer cell line (containing 10 to 50 copies of HPV-DNA types 18 per cell). Thyroid tissue has been used as negative control, since in the literature we could not find any evidence for the presence of HPV.

Two pathologists independently evaluated CISH slides. CISH signals were determined for at least 10 high power fields. Nuclear peroxidase staining was considered a positive result for HPV-DNA. Positive CISH signal patterns were classified as follows: (1) diffuse (D), when nuclei were completely stained (indicative of episomal HPV); (2) punctated, when distinct dot-like intranuclear signals were noted (indicative of integrated HPV); (3) mixed, diffuses, and punctated (D/P) when both patterns are noted. (Figures 1(a)–1(c)).

(v) p16/Ki67 Dual Stain and p16 Stain. A commercial kit specifically designed for the simultaneous detection of p16 and Ki67 (CINtec PLUS Kit, Roche mtm laboratories, Heidelberg, Germany) was used, accordingly to the supplier's instructions and adapting the protocols for the use on histological samples. One section for each case was stained with p16/Ki67 dual test. A red chromogen marked Ki-67 expression within the nucleus and a brown chromogen marked cytoplasmic/nuclear p16 expression. Sample was scored as positive when the simultaneous expressions of both markers were revealed within the same cells. Cases without any double-immunoreactive cell were called negative.

Another section for each case was prepared for the immunohistochemical evaluation of p16 alone (clone E6/H4) using CINtec Histology Kit (Roche mtm laboratories, Heidelberg, Germany). After antigen retrieval, sections were incubated with mouse monoclonal anti-p16 (Lab Vision/NeoMarkers, Fremont, CA), with EnVision+ System HRP anti-mouse (Dako, Copenhagen, Denmark). Afterwards, diaminobenzidine chromogen (Dako, Copenhagen, Denmark) was applied and counterstaining with haematoxylin was performed. p16 overexpression was visualized as a brown colour precipitate within nucleus and cytoplasm. Expression of p16 in more than 10% of epithelial cells was regarded as a positive result.

For dual stain and p16 immunohistochemistry, positive and negative controls consisted of SCC of uterine cervix, with and without primary antibodies, respectively. All tissue slides plus controls for p16/Ki67 dual test were stained in a single session that was different from that of p16 alone. In both cases, Dako Autostainer (Dako, Copenhagen, Denmark) was used.

Both slide sets were subjected to two pathologists, which evaluated all cases blindly to all study results.

2.3. Statistical Analyses. By standard method authors calculated the prevalence of HPV-DNA, E6/E7 mRNA, p16/Ki67, and CISH positivities. Chi square or Fisher's exact test was used to assess the association between variables. Concordances between histopathological diagnosis and DNA test,

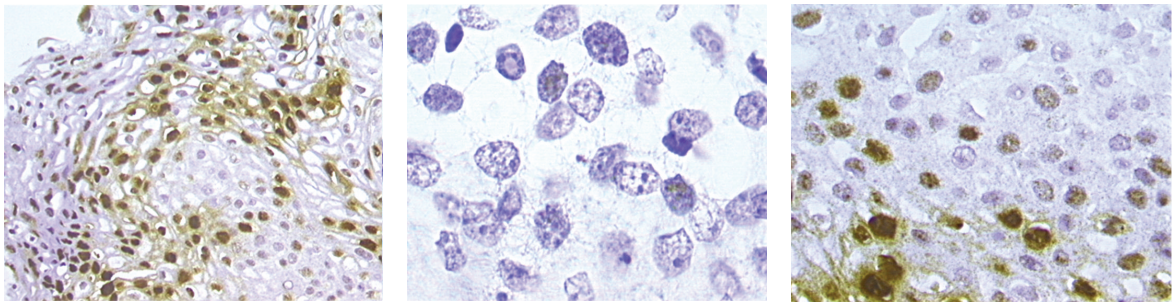

(a) (b) (c)

Figure 1: CISH positive signals. Diffuse pattern, where nuclei are completely stained ((a), 20x magnification). Punctated pattern in invasive squamous cervical cancer: distinct dot-like intranuclear signals were noted within cells infiltrating the stroma ((b), 100x magnification). Mixed patterns, where both diffuse and punctated signals are noted ((c), 40x magnification).

mRNA test, and CISH were calculated by Kappa statistics. According to the criteria of Lands and Koch, the K values were divided into six scales of strength of agreement: poor (<0.00), slight (0.00–0.20), fair (0.21–0.40), moderate (0.41–0.60), substantial (0.61–0.80), or almost perfect (0.81–1.00) [12]. Chi square for trend (Cochran-Armitage test) was calculated to assess the trend of CISH results in relation with the severity of cervical disease.

Accuracy parameters (sensitivity and specificity) of each test separately as well as the comparison of accuracy parameters between tests were assessed by receiver operating characteristic analysis. Histological diagnosis was regarded as the gold standard and CIN2+ lesion was considered as the worse outcome. To do that, histological results were dichotomized into CIN2+ (including CIN2, CIN3, and SCC) and less than CIN2 (CIN2−, including CIN1). Areas under the receiver operating characteristic (ROC) curves and 95% confidence intervals (CI) were estimated to assess differences between test performances [13] and McNemar test was used for statistical significance.

Correlation between CISH signal patterns and HPV viral load categories was evaluated by Cochran-Armitage trend test.

Statistical analyses were performed by using SPSS software (SPSS for Windows, Inc., Chicago, IL), version 15.0. In all analyses, probability values P less than 0.05 were regarded as significant.

2.4. Results. A series of cervical FFPE from sixty-three patients (mean age 34 ± 8 years, median 33 years, range 21–63) were included in the study. Among these cases, 25 were diagnosed as CIN1, 16 as CIN2, 21 as CIN3, and 1 as SCC.

Summary of results from histological diagnosis, HPV-DNA and mRNA tests, HPV viral load, CISH, and p16/Ki67 dual stain from each case included in the study are reported in Table 1.

Molecular Tests. HPV-DNA positivity was detected in 60 of the 63 (95.2%) cytological samples. Among these, 65% (N = 39/60) showed CIN2+ lesions in histological specimens. A positive DNA test result conferred a ≥CIN2+ odds ratio (OR) risk of 3.2 (95% CI: 0.4–26). 4.8% (N = 3/63) of women resulted HPV-DNA negative. Overall percent agreement between DNA testing test and histological diagnosis was 61.9% (Cohen's kappa value: 0.06, $P < 0.05$). E6/E7 mRNA positivity was detected in 71.4% (N = 45/63) of cytological cases; among these, 36 (80%) were CIN2+. Within the 18 mRNA negative cases, 16 (88.9%) were confirmed as CIN2−. mRNA test results were associated to CIN2+ diagnosis with a OR = 32 (95% CI: 7–144). Overall percent agreement between mRNA testing and histological diagnosis was 82.5% (Cohen's kappa value: 0.62, $P < 0.0001$).

Diagnostic performances of both DNA and mRNA tests are represented in Table 2. mRNA test improved specificity of DNA testing. Difference was statistically significant (McNemar test, $P < 0.01$).

CISH Results. CISH showed a clear signal in 95.2% (N = 60/63) of the specimens. Invalid result has been found in 4.8% (N = 3/63) of the cases, due to unclear and weak signal. The rate of positive results was 73% (N = 46/63). Among these, 30.4% (N = 14) were CIN1, 30.4% (N = 14) were CIN2, and 37% (N = 17) were CIN3. The unique case of SCC showed CISH positivity. Negativity has been found in 22.2% (N = 14/63) of the cases. Table 3 shows details of the distribution of CISH signal patterns and their correlation with histological diagnosis. As expected, CISH showed a clear punctated signal pattern in both HPV positive cell lines, whereas no signal was detected in thyroidal tissue. Nonspecific background binding has never been seen among the 60 cases which were considered as valid cases. Notably, about two-thirds of diffuse pattern were associated with CIN1, while the unique case of SCC displayed a punctated pattern. Differences were statistically significant ($P < 0.01$). Dichotomizing histological diagnosis and considering only CISH-positive results, diffuse pattern has been found in 64.3% (N = 9/14) of CIN2− and 3.1% (N = 1/32) of CIN2+. All cases of punctated pattern have been found in CIN2+, as well as 68.8% of mixed patterns. The proportion of punctated pattern increased with the severity of cervical lesion (Cochran-Armitage test for trend $P < 0.0001$) (Figure 2).

Table 1: Summary of results from histological diagnosis, HPV-DNA and mRNA tests, HPV viral load, CISH, and p16/Ki67 dual stain.

Case	Histological diagnosis	HR HPV-DNA test result	HC2 viral load (RLU/CO)*	E6/E7 mRNA test result	Type specific mRNA test result**	HPV CISH† signal	P16/Ki67 Dual stain result
1	CIN1	Positive	63.5	Negative	—	*P*	Negative
2	CIN1	Positive	516.61	Negative	—	*D*	Negative
3	*CIN3*	Positive	*15.79*	Negative	—	*Negative*	Positive
4	CIN2	Positive	146.77	Positive	16	*D/P*	Positive
5	CIN2	Positive	1283.97	Negative	—	*D/P*	Positive
6	CIN1	Positive	298.55	Negative	—	*D*	Negative
7	CIN3	Positive	*1529.35*	Positive	16, 31	*D/P*	Positive
8	CIN3	Positive	2207.8	Positive	31	*D/P*	Positive
9	CIN1	Positive	2.06	Negative	—	*D*	Negative
10	*CIN2*	Positive	*216.93*	Positive	31	*D/P*	Positive
11	CIN1	Positive	6.7	Negative	—	*Negative*	Negative
12	CIN2	Positive	84.32	Positive	31	*Negative*	Positive
13	CIN3	Positive	10.56	Positive	16	*D/P*	Positive
14	CIN3	Positive	338.02	Positive	16	*D/P*	Positive
15	CIN1	Positive	1211.84	Positive	33	*D/P*	Positive
16	CIN3	Positive	3.3	Positive	16	*P*	Positive
17	CIN1	Positive	155.79	Positive	16	*D*	Negative
18	CIN1	Positive	28.81	Negative	—	*Negative*	Positive
19	CIN2	Positive	34.82	Negative	—	*D*	Positive
20	CIN3	Positive	913.36	Negative	—	*D*	Positive
21	CIN2	Positive	1536.02	Positive	16	*P*	Negative
22	CIN2	Positive	107.22	Positive	18, 45	*D/P*	Positive
23	CIN1	Positive	75.86	Negative	—	*D/P*	Negative
24	CIN2	Positive	675.75	Positive	16	*D/P*	Positive
25	CIN2	Positive	596.84	Positive	16	*D/P*	Positive
26	CIN3	Positive	1914.17	Positive	16	*D/P*	Positive
27	CIN2	Positive	570.26	Positive	16, 45	*D/P*	Positive
28	CIN1	Positive	783.56	Negative	—	*D*	Negative
29	CIN1	Negative	—	Negative	—	*Negative*	Negative
30	CIN3	Positive	3.93	Positive	16	*P*	Positive
31	CIN3	Positive	968.56	Positive	31	*D/P*	Positive
32	CIN1	Positive	926.05	Positive	31	*Invalid*	Negative
33	CIN2	Negative	—	Positive	31	*Invalid*	Positive
34	CIN1	Positive	45	Negative	—	*D*	Negative
35	CIN3	Positive	117	Positive	16	*D/P*	Positive
36	CIN1	Positive	237.48	Positive	16	*Invalid*	Negative
37	CIN1	Positive	5.31	Positive	18, 31	*Negative*	Negative
38	CIN1	Positive	204.42	Positive	45	*Negative*	Negative
39	CIN3	Positive	663.26	Positive	33	*Negative*	Positive
40	CIN3	Positive	38.61	Positive	16	*Negative*	Positive
41	CIN1	Positive	10.11	Positive	33	*D/P*	Positive
42	CIN1	Positive	137.88	Negative	—	*D*	Negative
43	CIN3	Positive	6.21	Positive	16	*Negative*	Positive
44	CIN2	Positive	2663.26	Positive	31	*D/P*	Positive
45	SCC	Positive	1549.74	Positive	33	*D/P*	Positive
46	CIN2	Positive	894.17	Positive	16	*P*	Positive

Table 1: Continued.

Case	Histological diagnosis	HR HPV-DNA test result	HC2 viral load (RLU/CO)*	E6/E7 mRNA test result	Type specific mRNA test result**	HPV CISH† signal	P16/Ki67 Dual stain result
47	CIN1	Positive	20.47	Negative	—	*Negative*	Negative
48	CIN1	Positive	26.23	Negative	—	*Negative*	Negative
49	CIN1	Positive	787.16	Positive	31	*Negative*	Negative
50	CIN1	Positive	676.46	Positive	16	*D/P*	Negative
51	CIN3	Positive	2.36	Positive	16	*P*	Positive
52	CIN3	Positive	1.45	Positive	18	*P*	Positive
53	CIN3	Positive	111.95	Positive	16, 18	*D/P*	Positive
54	CIN3	Positive	544.41	Positive	16	*D/P*	Positive
55	CIN2	Positive	663.21	Positive	16	*D/P*	Positive
56	CIN1	Negative	—	Negative	—	*Negative*	Negative
57	CIN2	Positive	1569.56	Positive	18	*D/P*	Positive
58	CIN3	Positive	758.66	Positive	16	*D/P*	Positive
59	CIN2	Positive	130.13	Positive	16	*D/P*	Positive
60	CIN3	Positive	87.01	Positive	16	*P*	Positive
61	CIN3	Positive	968.56	Positive	31	*D/P*	Positive
62	CIN2	Positive	6.21	Positive	16	*P*	Positive
63	CIN3	Positive	24.01	Positive	16	*P*	Positive

*Relative light unit in relation to control (RLU/CO).
**HPV genotype(s) detected by Nuclisens EasyQ HPV mRNA test.
†D: diffuse; P: punctated; D/P: mixed diffuse/punctated.

Table 2: Diagnostic performances of HPV-DNA test (HC2) and E6/E7 mRNA test.

Molecular testing	Diagnostic performances (95% CI*)	
	Sensitivity	Specificity
HPV-DNA test	97.4% (85.1–100)	8% (1.2–26)
HPV-mRNA test	90.7% (81.6–99.4)	64% (44.4–79.7)

*Confidence intervals (CI).

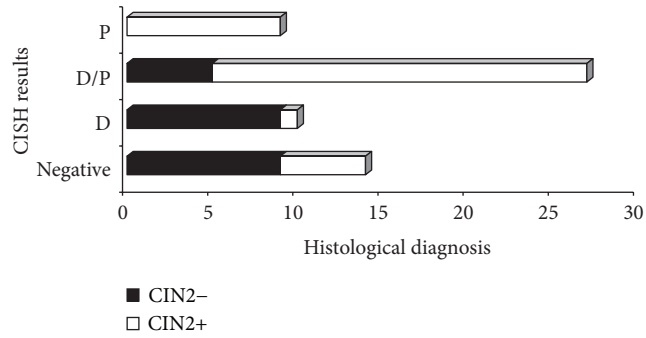

Figure 2: Correlation between CISH results and histological diagnosis (P < 0.0001). P: punctate pattern; D/P: diffuse and punctated (mixed) pattern; D: diffuse pattern. CIN2+: Cervical intraepithelial neoplasia grade 2 or greater (including CIN2, CIN3, and invasive squamous cell carcinoma); CIN2–: less than Cervical Intraepithelial Neoplasia grade 2 (including CIN1 and negative for dysplasia.

Sensitivity and specificity of CISH analysis were 86.5% (95% CI: 71.4–94.4) and 39.1% (95% CI: 22.2–59.3), respectively. A positive CISH result conferred a ≥CIN2+ risk (OR) of 4.11 (95% CI: 2–13.9).

CISH results were assessed against HPV-DNA test (Figure 3). All CISH-positive cases also resulted HPV-DNA positive. Among HPV-DNA positive patients, 76.7% (N = 46/60) were CISH positive. Within CISH-negative cases, 85.7% (N = 12/14) were HPV-DNA positive, while 14.3% (N = 2/14) were HPV-DNA negative (P = .001). Overall percent agreement between CISH and DNA test was 80% (k = 0.20, P < 0.05).

CISH results were also assessed against HPV E6/E7 mRNA expression. Among mRNA+ cases, 77.8% (N = 35/45) were CISH positive. Of those, 2.9% (N = 1/35) showed a diffuse pattern, 71.4% (N = 25/35) a mixed pattern, and 25.7% (N = 9/35) a punctated pattern. Among the 11 mRNA/CISH+ cases, only 2 cases (18%) demonstrated a punctated pattern (P < 0.0001). Overall percent agreement between CISH and mRNA test was 70% (k = 0.24, P < 0.05).

Since HPV-DNA test is currently considered the most reliable method to detect papillomavirus infection in both cytological and histological samples, the performances of CISH and mRNA test were compared to HPV-DNA test performance. DNA testing achieved an area under the curves (AUC) of 0.53 (95% CI, 0.4–0.65) CISH and of 0.64 (95% CI, 0.5–0.75) and mRNA testing of 0.79 (95% CI, 0.67–0.89) (Figure 4). Difference between HPV-DNA test and mRNA test was statistically significant (P < 0.0001), while difference between RNA testing and CISH did not reach significance (P = 0.06).

Table 3: Association between CISH signal patterns and grading of cervical lesions ($P < 0.01$).

CISH result	Number of cases (%)				Total
	CIN1	CIN2	CIN3	SCC	
Invalid	2 (8)	1 (6.3)	0	0	**3 (4.8)**
Negative	9 (36)	1 (6.3)	4 (19)	0	**14 (22.2)**
Diffuse	9 (36)	1 (6.3)	0	0	**10 (15.9)**
Diffuse-punctated	5 (20)	11 (68.7)	11 (52.4)	0	**27 (42.8)**
Punctated	0	2 (12.4)	6 (28.6)	1 (100)	**9 (14.3)**
Total	**25 (39.7)**	**16 (25.4)**	**21 (33.3)**	**1 (1.6)**	**63**

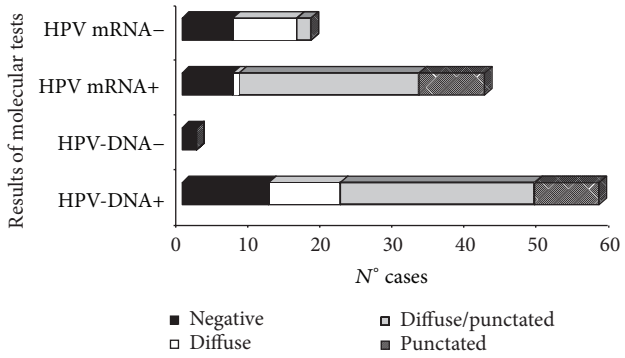

Figure 3: Correlation between CISH signal and results from molecular tests ($k = 0.20$, $P < 0.05$).

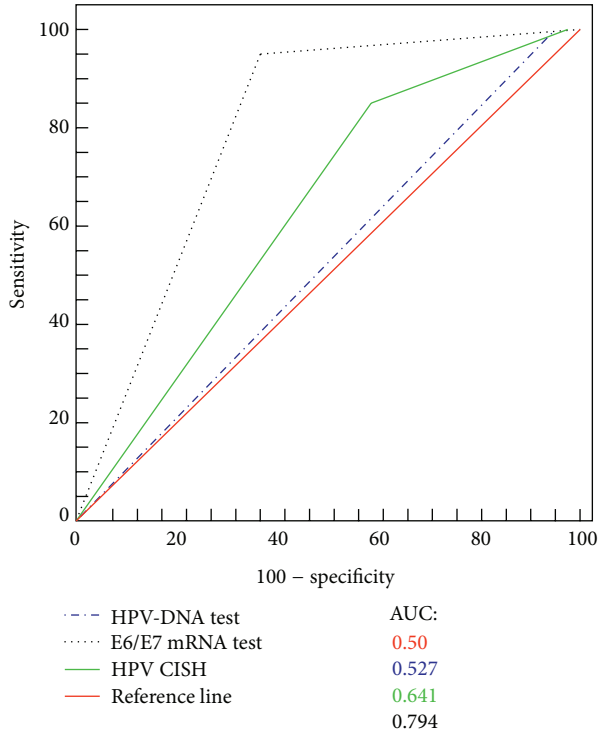

Figure 4: Receiving operating characteristic curves (ROC), comparing CISH, HPV-DNA test, and E6/E7 mRNA diagnostic performances. The red line indicates a reference threshold with area under the ROC curve of 0.5.

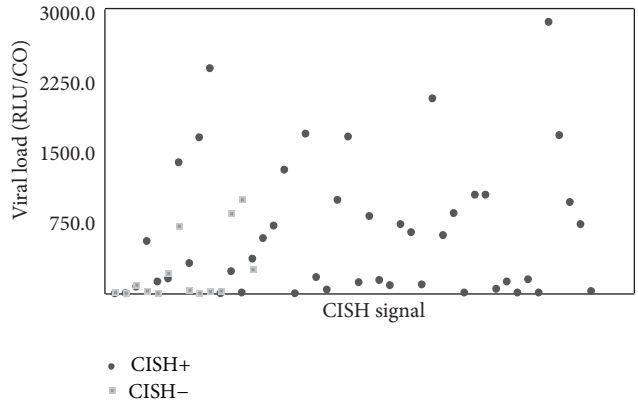

Figure 5: Correlation between CISH signal and HPV viral load, as detected by HC2 test ($P = 0.01$). RLU/CO value provided an estimation of the number of HPV-DNA copies of each sample. RLU/CO: ratio between relative light units and control.

CISH Results and HPV Viral Load. Among cytological samples testing HPV-DNA positive, the mean of viral loads was 502.9 ± 620.5 RLU/CO, the median being 155.79 RLU/CO (range 1.45–2663.29 RLU/CO).

Considering the categories of viral load values as described in Section 2, 31.7% ($N = 19/60$) of the cases showed low viral load, 6.7% ($N = 4/60$) intermediate load, and 61.6% ($N = 37/60$) high viral load. The rate of CISH positivity has been found to be lower in cases with low viral load level (58%) than in those with intermediate (75%) and high (86.6%) load levels (Cochran-Armitage trend test, $P = 0.01$) (Figure 5).

Correlation between CISH punctate signal pattern and viral load categories showed that the rate of this pattern was higher in specimens with low viral loads than in those having intermediate or high loads (Fisher exact test, $P = 0.05$).

p16 and p16/Ki67 Dual Stain Analysis. Both p16 immunohistochemistry and p16/Ki67 analysis were performed on the entire FFPE series.

A positive p16 result was defined as a diffuse moderate-to-strong cytoplasmic and nuclear staining. There was no difference in the intensity of staining between the different epithelial layers. Brown staining of normal metaplastic or endocervical cells was considered as negative p16 test.

When the diagnosis of cervical lesion was categorized into four, that is, CIN1, CIN2, CIN3, and SCC, a complete concordance for all the two observers was obtained in 32

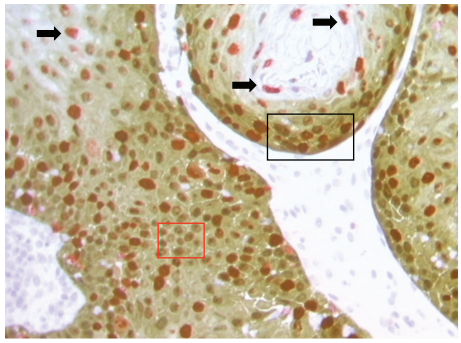

Figure 6: p16/Ki67 dual stain (40x magnification). Red square: brown chromogen marked cytoplasmic/nuclear p16 expression. Black arrows: red chromogen marked Ki-67 expression within nuclei. Black square: simultaneous expressions of both markers were revealed within the same cells.

cases (51%), including 8 CIN1, 11 CIN2, 12 CIN3, and 1 SCC ($k = 0.06$). The lower agreement was observed for CIN1 diagnosis, the higher for SCC ($P = 0.08$) (Table 4). Sensitivity and specificity of p16 IHC were 96.4 (95% CI: 85.1–100) and 100% (95% CI: 83.9–100), respectively.

Considering p16/Ki67 dual stain immunohistochemistry (Figure 6), all 63 histological samples gave interpretable results. p16 expression was observed in 48 of 63 cases (76.2%). Ki67 expression has been found in all histological specimens. Particularly, 13/25 CIN1 cases (52%) showed weak Ki67 expression in the basal layer of cervical epithelium. The remaining 12 CIN1 cases showed strong nuclear Ki67 expression in the lower part of the epithelium (one-third), associated with cytoplasmic expression of p16 within the same cells. As the CIN grade was higher, stronger Ki67 expression was observed, particularly in 87.5% of CIN2 ($N = 14/16$) cases (within two-third of cervical epithelium) and in 100% of CIN3 cases (within the three-third of the epithelium). Expression level of p16 positively correlated with that of Ki67 ($P < 0.01$). In the unique case of SCC, strong dual-stain positivity has been also shown by neoplastic cells infiltrating the stroma.

The use of p16/Ki67 IHC significantly improved consensus among pathologists, which reached 100% ($k = 1$). Sensitivity and specificity of dual stain were 100% (95% CI: 88.8–100) and 84% (95% CI: 64.6–94.1), respectively.

Since in cervical tissue p16 is considered a surrogate biomarker of HPV-E7 expression, we correlated both p16 and p16/Ki67 staining results with HPV-E6/E7 status, as determined by mRNA test (Table 5). p16 expression was observed in 77.8% ($N = 35/45$) of mRNA-positive cases. Among mRNA-negative cases, p16 showed no immunoreactivity in 88.9% ($N = 16/18$) of patients. Concordance between p16 and E6/E7 mRNA test was 81% ($k = 0.59$).

Dual stain positivity has been found in 88.9% ($N = 40/45$) of mRNA-positive patients, negativity being detected in 88.8% ($N = 16/18$) of mRNA-negative cases. Concordance between p16/Ki67 dual stain and mRNA test was 89% ($k = 0.74$).

Concordance between dual stain and CISH (punctated and mixed pattern) was 83.3% ($k = 0.64$).

3. Discussion

Although HPV-DNA and E6/E7 mRNA tests still remain the current standards for the confirmation of HPV infections in cytological specimens, no consensus exists about technology that should be used for the detection of Papillomavirus in formalin-fixed paraffin-embedded samples [14]. This fact presents the clinicians with the dilemma of selecting the more suitable method. Molecular techniques (such as PCR) certainly represent the gold standard method, reaching a sensitivity of 1 DNA copy/cell [14]. However, DNA extraction requires trained laboratory personnel and is still highly time-consuming and labour intensive for routine application. In addition, to detect HPV-DNA, a wide range of consensus primers, such as MY09/11, PGMY09/11, GP5+/6+, and SPF, are available [15]. Amplification with each of these primers provides amplification products of different sizes, thus providing different levels of sensitivity in viral detection. Particularly on FFPE material, because of the damaged and fragmented DNA, it is possible that the use of these primers could reach a high rate of false negative results [14]. It has been already shown that the maximum accuracy of PCR is obtained using fresh frozen tissues [16].

All consensus PCR primers for the detection of HPV-DNA would target L1 region. This region is deleted when HPV-DNA is integrated into the host cell genome [17]. So, when HPV integration would occur, PCR should probably give false negative results.

Finally, due to its high sensitivity, PCR would detect HPV infection without any correlation with the prognosis of cervical lesion.

ISH is certainly less sensitive than PCR [18], but the visualization of HPV-DNA signals within nuclei of cervical lesions could offer both detection and localization of HPV-DNA without damage of morphology. In addition, ISH helps to distinguish between episomal HPV from integrated one, the last being the necessary condition for neoplastic progression [19]. However, the low analytic sensitivity of ISH, ranging from 10 to 50 copy/cell, would be a weakness in case of high-grade cervical lesions in which, due to the frequent integration status of HPV, DNA copy number is usually less than 50 copy/cell. [7, 8]. Then, the choice of ISH technique would be extremely important. Non-tyramide-based methods showed too low sensitivity rate [20, 21]. On the other hand, the higher sensitivity of tyramide-based ISH could lead to interpretation bias, especially due to non-specific staining [22]. Hence, our aim is to analyse the performances of an optimized chromogenic ISH tyramide-based biotin-free assay.

In our FFPE series, sensitivity of CISH was about 87%, higher if compared to series using non-tyramide-based methods [19, 22, 23]. CISH positive cases were characterized by a clear background. The rate on invalid results was very low (4.8%) and due to scant FFPE specimens. CISH positivity always matched with HPV-DNA positivity. 20% of HPV-DNA positive cases demonstrated negativity at CISH analysis. The latter data may probably be due to the limited number of oncogenic genotypes detected by CISH probe (HPV 16, 18, 31, 33, and 54), in comparison to those detected by HC2.

Table 4: p16 immunostaining: interobserver agreement within histological categories of cervical lesions.

p16 interobservers agreement	Histological diagnosis				
	CIN1 (%)	CIN2 (%)	CIN3 (%)	SCC (%)	Total
Positive	8 (32)	11 (68.8)	12 (57.1)	1 (100)	**32 (50.8)**
Negative	17 (68)	5 (31.2)	9 (42.9)	0	**31 (49.2)**
Total	**25 (39.7)**	**16 (25.4)**	**21 (33.3)**	**1 (1.6)**	**63**

Table 5: Correlation between p16 and p16/Ki67 immunohistochemistry and E6/E7 mRNA test.

Immunohistochemistry	E6/E7 mRNA test		
	Positive (%)	Negative (%)	Total
p16 positive	35 (77.8)	2 (11.1)	**37 (58.7)**
p16 negative	10 (22.2)	16 (88.9)	**26 (41.3)**
Total	**45**	**18**	**63**
p16/Ki67 dual stain positive	40 (88.9)	2 (11.1)	**42 (66.7)**
p16/Ki67 dual stain negative	5 (11.1)	16 (88.8)	**21 (33.3)**
Total	**45**	**18**	**63**

Anyhow, HPV types identified by CISH would represent five of the six most oncogenic genotypes, the sixth being HPV-45 [1, 24–26].

It is now well known that HPV integration is common in CIN2+ lesions while is uncommon or absent in CIN1 [27]. Studies on cervical carcinomas and SCCs cell lines demonstrated that oncogenic E6/E7 oncogenes are frequently overexpressed during HPV integration [27]. In our study, 100% of cases with punctate signal matched with CIN2+, while 94.7% of CIN2+ showed E6/E7 oncogenic expression (E6/E7 mRNA positivity). Percent agreement between CISH and mRNA test was high. Thus, we may conclude that CISH punctate signal confirmed as a sign of viral integration [18]. The only two CISH+/mRNA cases were probably due to HPV genotype 54, detected by CISH but not detected by mRNA test.

In our series, when present, diffuse signal has been detected within cells of the mid/superficial layers. This pattern was mainly associated with CIN2−/mRNA negative cases and confirmed as a marker of productive HPV infections. Diffuse and punctate signals within the same lesion have also been found. This mixed pattern was associated with CIN2+ in 81.5% of the cases. This fact would be due to the polyclonal nature of cervical intraepithelial lesions. The unique case of infiltrating SCC showed punctate signal only, confirming the monoclonality of invasive neoplasia.

Although our cohort encompassed a limited number of cases, our preliminary results underline the usefulness of the tyramide-based CISH protocol which we used. This technology does not suffer of nonspecific background, simultaneously allowing the detection of HPV genome within morphological context. In addition, the use of a chromogen in alternative to fluorescence revealed to be more convenient for routine purpose, given the wide availability of light microscopy in pathology settings. Finally, CISH protocol could prove helpful also during the followup of patients with cervical lesions, as a feasible alternative to HPV-DNA and E6/E7 mRNA tests on FFPE specimens.

Recent researches on cervical cancer widely analysed biomarkers resulting associated with the various stages of HPV infection [3]. One of these strongly related to transforming HPV infection would be p16. Overexpression of p16 seems to increase with increasing degree of cervical lesion [28, 29]. A meta-analysis on p16 immunostaining on cytological and histological cervical specimens estimated that 2% of normal tissues and 38% of CIN1 showed diffuse staining, compared with 68% of CIN2 and 82% of CIN3 [30]. p16 immunostaining demonstrated to be cheap and easy to perform in pathology laboratories. The semiquantitative scoring system described by Klaes et al. [31], is actually the most widely used approach for the evaluation of this marker on histological specimens. However, estimation of results is often based on colorimetric and morphological criteria which are often subjective. This lack of standardization would make the use of this biomarker somehow difficult [30]. The assessment of p16 staining can be also hampered by false positive results [32, 33]. Endometrial, metaplastic, and endocervical cells, as well as tubo-endometrioid metaplasia would stain p16-positive [34], since a non-HPV dependent p16 expression pathway may also exist [4, 35]. For all the above mentioned reasons, there would be considerable reluctance among histopathologists to incorporate p16 IHC into routine gynae-pathology. Specifically, in our series the evaluation of p16 immunoreactivity generated a great variability in the interpretation and reached a low agreement level (51%).

Nowadays, there is a considerable interest in the evaluation of the combination p16/Ki67, which would allow to differentiate dysplastic cells from nondysplastic ones, and meaningless HPV infection from transforming ones. In the present study, we performed p16/Ki67 dual stain immunohistochemistry on FFPE series of specimens encompassing all grades of morphological abnormalities. In our experience,

this genotype-independent method has proved to be feasible and highly efficient in producing valid results. Even though in a limited series, dual stain results were always unequivocal. Moreover, inter-observer agreement was highest (100%), since only cells simultaneously showing p16/Ki67 expression have been considered as positive, irrespective of morphology. Finally, in our series dual stain improved specificity of p16 alone.

In this setting, 98% of CIN2+ stained mRNA positive, while 100% stained p16/Ki67-positive. The only invasive cancer showed dual stain and E6/E7 mRNA positivity. It seems likely that dual stain positive/mRNA positive CIN2+ could represent cervical lesions at higher risk of progression toward invasive cancer [36]. This fact could not be determined in the present setting, since all CIN2+ lesions were surgically removed [37].

4. Conclusion

HPV are recognized as a necessary cause of CIN, but only a minority of HPV infections even results in cervical lesions. Although the majority of infections may be cleared by immune system, integration of HPV sequence into the host genome may induce CIN progression. The detection of HPV genome within cervical lesions and the assessment of its physical status are then crucial in prognostic terms.

To the authors' knowledge, this is the first study evaluating the novel HPV tyramide-based CISH technology and the innovative CINtec PLUS p16/Ki-67 double stain immunohistochemistry on histological tissues, as well as the first investigation comparing both methods to molecular tests actually considered as the gold standards for HPV detection.

Molecular assays may be expensive and require a high level of expertise, which are often difficult to reach in routinely laboratory. Although larger studies are needed, our data demonstrate the usefulness of CISH and p167Ki67 immunostaining in surgical pathology settings.

In particular, CISH could be a feasible method to localize HPV genome on paraffin-embedded specimens. This technology would help to distinguish episomal from integrated HPV, thus allowing conclusions regarding the prognosis of the lesion. Likewise, the genotype-independent p16/Ki67 dual staining approach, which demonstrated greater efficacy than p16 alone, would confer a higher level of standardization to the diagnostic procedure.

Finally, due to their strong correlation with tests which are currently considered the standards for HPV detection in cytological specimens, both CISH and dual stain technologies would be considered a viable potential alternative to molecular assays in the evaluation of the biology of cervical lesions.

Nevertheless, these preliminary data need to be confirmed in a larger clinical cohort.

Disclosure

The authors specify that this paper has not been published, submitted, or accepted for publication elsewhere.

Conflict of Interests

All the authors declare that they have no conflict of interests.

Authors' Contribution

Roberta Zappacosta and Antonella Colasante contributed equally to this paper.

References

[1] R. Zappacosta and S. Rosini, "Cervical cancer screening: from molecular basis to diagnostic practice, going through new technologies," *Technology in Cancer Research and Treatment*, vol. 7, no. 3, pp. 161–174, 2008.

[2] J. Cuzick, C. Clavel, K. Petry et al., "Overview of the European and North American studies on HPV testing in primary cervical cancer screening," *International Journal of Cancer*, vol. 119, no. 5, pp. 1095–1101, 2006.

[3] J. Cuzick, M. Arbyn, R. Sankaranarayanan et al., "Overview of human papillomavirus-based and other novel options for cervical cancer screening in developed and developing countries," *Vaccine*, vol. 26, no. 10, pp. K29–K41, 2008.

[4] P. Giorgi Rossi, M. Benevolo, A. Vocaturo et al., "Prognostic value of HPV E6/E7 mRNA assay in women with negative colposcopy or CIN1 histology result: a follow-up study," *PLOS One*, vol. 8, no. 2, pp. 54–62, 2013.

[5] M. Guo, Y. Gong, M. Deavers et al., "Evaluation of a commercialized in situ hybridization assay for detecting human papillomavirus DNA in tissue specimens from patients with cervical intraepithelial neoplasia and cervical carcinoma," *Journal of Clinical Microbiology*, vol. 46, no. 1, pp. 274–280, 2008.

[6] M. M. Dabić, L. Hlupić, D. Babić, S. Jukić, and S. Seiwerth, "Comparison of polymerase chain reaction and catalyzed signal amplification in Situ hybridization methods for human papillomavirus detection in paraffin-embedded cervical preneoplastic and neoplastic lesions," *Archives of Medical Research*, vol. 35, no. 6, pp. 511–516, 2004.

[7] M. F. Evans, S. L. Mount, B. G. Beatty, and K. Cooper, "Biotinyl-tyramide-based in situ hybridization signal patterns distinguish human papillomavirus type and grade of cervical intraepithelial neoplasia," *Modern Pathology*, vol. 15, no. 12, pp. 1339–1347, 2002.

[8] J. D. Meissner, "Nucleotide sequences and further characterization of human papillomavirus DNA present in the CaSki, SiHa and HeLa cervical carcinoma cell lines," *Journal of General Virology*, vol. 80, no. 7, pp. 1725–1733, 1999.

[9] K. U. Petry, D. Schmidt, S. Scherbring et al., "Triaging Pap cytology negative, HPV positive cervical cancer screening results with p16/Ki-67 Dual-stained cytology," *Gynecologic Oncology*, vol. 121, no. 3, pp. 505–509, 2011.

[10] D. Schmidt, C. Bergeron, K. J. Denton, and R. Ridder, "p16/ki-67 dual-stain cytology in the triage of ASCUS and LSIL papanicolaou cytology: results from the European equivocal or mildly abnormal Papanicolaou cytology study," *Cancer Cytopathology*, vol. 119, no. 3, pp. 158–166, 2011.

[11] A. Tinelli, G. Leo, M. Pisanò et al., "HPV viral activity by mRNA-HPV molecular analysis to screen the transforming infections in precancer cervical lesions," *Current Pharmaceutical Biotechnology*, vol. 10, no. 8, pp. 767–771, 2009.

[12] J. R. Landis and G. G. Koch, "The measurement of observer agreement for categorical data," *Biometrics*, vol. 33, no. 1, pp. 159–174, 1977.

[13] E. R. DeLong, D. M. DeLong, and D. L. Clarke-Pearson, "Comparing the areas under two or more correlated receiver operating characteristic curves: a nonparametric approach," *Biometrics*, vol. 44, no. 3, pp. 837–845, 1988.

[14] P. J. F. Snijders, A. J. C. van den Brule, and C. J. L. M. Meijer, "The clinical relevance of human papillomavirus testing: relationship between analytical and clinical sensitivity," *Journal of Pathology*, vol. 201, no. 1, pp. 1–6, 2003.

[15] R. Zappacosta, D. Caraceni, L. Ciccocioppo et al., "Is HPV-DNA testing a useful tool in predicting low-grade squamous intraepithelial lesion outcome? A retrospective longitudinal study," *International Journal of Immunopathology and Pharmacology*, vol. 23, no. 1, pp. 317–326, 2010.

[16] W. Qu, G. Jiang, Y. Cruz et al., "PCR detection of human papillomavirus: comparison between MY09/MY11 and GP5+/GP6+ primer systems," *Journal of Clinical Microbiology*, vol. 35, no. 6, pp. 1304–1310, 1997.

[17] M. Arbyn, P. Sasieni, C. J. L. M. Meijer, C. Clavel, G. Koliopoulos, and J. Dillner, "Chapter 9: clinical applications of HPV testing: a summary of meta-analyses," *Vaccine*, vol. 24, supplement 3, pp. S78–S89, 2006.

[18] M. F. Evans and K. Cooper, "Human papillomavirus integration: detection by in situ hybridization and potential clinical application," *Journal of Pathology*, vol. 202, no. 1, pp. 1–4, 2004.

[19] M. Montag, T. J. F. Blankenstein, N. Shabani, A. Brüning, and I. Mylonas, "Evaluation of two commercialised in situ hybridisation assays for detecting HPV-DNA in formalin-fixed, paraffin-embedded tissue," *Archives of Gynecology and Obstetrics*, vol. 284, no. 4, pp. 999–1005, 2011.

[20] K. T. Kuo, C. H. Hsiao, C. H. Lin, L. Kuo, S. Huang, and M. Lin, "The biomarkers of human papillomavirus infection in tonsillar squamous cell carcinoma-molecular basis and predicting favorable outcome," *Modern Pathology*, vol. 21, no. 4, pp. 376–386, 2008.

[21] A. Luginbuhl, M. Sanders, and J. D. Spiro, "Prevalence, morphology, and prognosis of human papillomavirus in tonsillar cancer," *Annals of Otology, Rhinology and Laryngology*, vol. 118, no. 10, pp. 742–749, 2009.

[22] M. F. Evans, H. A. Aliesky, and K. Cooper, "Optimization of biotinyl-tyramide-based in situ hybridization for sensitive background-free applications on formalin-fixed, paraffin-embedded tissue specimens," *BMC Clinical Pathology*, vol. 3, no. 1, pp. 1–17, 2003.

[23] M. F. Evans, A. Matthews, D. Kandil, C. S. Adamson, W. E. Trotman, and K. Cooper, "Discrimination of "Driver" and "Passenger" HPV in tonsillar carcinomas by the polymerase chain reaction, chromogenic in situ hybridization, and $p16^{INK4a}$ immunohistochemistry," *Head and Neck Pathology*, vol. 5, no. 4, pp. 344–348, 2011.

[24] G. M. Clifford, J. S. Smith, M. Plummer, N. Muñoz, and S. Franceschi, "Human papillomavirus types in invasive cervical cancer worldwide: a meta-analysis," *British Journal of Cancer*, vol. 88, no. 1, pp. 63–69, 2003.

[25] L. Kraus, T. Molden, R. Holm et al., "Presence of E6 and E7 mRNA from human papillomavirus types 16, 18, 31, 33, and 45 in the majority of cervical carcinomas," *Journal of Clinical Microbiology*, vol. 44, no. 4, pp. 1310–1317, 2006.

[26] S. de Sanjosé, M. Diaz, X. Castellsagué et al., "Worldwide prevalence and genotype distribution of cervical human papillomavirus DNA in women with normal cytology: a meta-analysis," *Lancet Infectious Diseases*, vol. 7, no. 7, pp. 453–459, 2007.

[27] G. Gallo, M. Bibbo, L. Bagella et al., "Study of viral integration of HPV-16 in young patients with LSIL," *Journal of Clinical Pathology*, vol. 56, no. 7, pp. 532–536, 2003.

[28] N. Murphy, M. Ring, C. C. B. B. Heffron et al., "$p16^{INK4a}$, CDC6, and MCM5: predictive biomarkers in cervical preinvasive neoplasia and cervical cancer," *Journal of Clinical Pathology*, vol. 58, no. 5, pp. 525–534, 2005.

[29] S. S. Wang, M. Trunk, M. Schiffman et al., "Validation of $p16^{INK4a}$ as a marker of oncogenic human papillomavirus infection in cervical biopsies from a population-based cohort in Costa Rica," *Cancer Epidemiology Biomarkers and Prevention*, vol. 13, no. 8, pp. 1355–1360, 2004.

[30] I. Tsoumpou, M. Arbyn, M. Kyrgiou et al., "$p16^{INK4a}$ immunostaining in cytological and histological specimens from the uterine cervix: a systematic review and meta-analysis," *Cancer Treatment Reviews*, vol. 35, no. 3, pp. 210–220, 2009.

[31] R. Klaes, T. Friedrich, D. Spitkovsky et al., "Overexpression of $p16^{INK4a}$ as a specific marker for dysplastic and neoplastic epithelial cells of the cervix uteri," *International Journal of Cancer*, vol. 92, no. 2, pp. 276–284, 2001.

[32] I. Tsoumpou, G. Valasoulis, C. Founta et al., "High-risk human papillomavirus DNA test and $p16^{INK4a}$ in the triage of LSIL: a prospective diagnostic study," *Gynecologic Oncology*, vol. 121, no. 1, pp. 49–53, 2011.

[33] K. J. Denton, C. Bergeron, P. Klement, M. J. Trunk, T. Keller, and R. Ridder, "The sensitivity and specificity of $p16^{INK4a}$ cytology vs HPV testing for detecting high-grade cervical disease in the triage of ASC-US and LSIL Pap cytology results," *American Journal of Clinical Pathology*, vol. 134, no. 1, pp. 12–21, 2010.

[34] C. M. Martin and J. J. O'Leary, "Histology of cervical intraepithelial neoplasia and the role of biomarkers," *Best Practice & Research Clinical Obstetrics and Gynaecology*, vol. 25, no. 5, pp. 605–615, 2011.

[35] J. L. Meyer, D. W. Hanlon, B. T. Andersen, O. F. Rasmussen, and K. Bisgaard, "Evaluation of $p16^{INK4a}$ expression in ThinPrep cervical specimens with the CINtec $p16^{INK4a}$ assay: correlation with biopsy follow-up results," *Cancer*, vol. 111, no. 2, pp. 83–92, 2007.

[36] M. del Pino, S. Garcia, V. Fusté et al., "Value of $p16^{INK4a}$ as a marker of progression/regression in cervical intraepithelial neoplasia grade 1," *American Journal of Obstetrics and Gynecology*, vol. 201, no. 5, pp. 488e1–488e7, 2009.

[37] L. M. Stewart, M. H. Einstein, W. K. Huh et al., "Guidelines for the management of abnormal cervical cancer screening tests and cancer precursors," *Journal of Lower Genital Tract Disease*, vol. 17, pp. 1–27, 2013.

Hindawi Publishing Corporation
BioMed Research International
Volume 2013, Article ID 685641, 9 pages
http://dx.doi.org/10.1155/2013/685641

Review Article

Usefulness of Traditional Serum Biomarkers for Management of Breast Cancer Patients

Peppino Mirabelli and Mariarosaria Incoronato

Fondazione SDN IRCCS, Via E. Gianturco 113, 80143 Naples, Italy

Correspondence should be addressed to Peppino Mirabelli; pemirabelli@gmail.com

Received 10 June 2013; Revised 6 September 2013; Accepted 9 September 2013

Academic Editor: Natasa Tosic

The measurement of serum tumor markers levels in breast cancer (BC) patients is an economic and noninvasive diagnostic assay frequently requested by clinical oncologists to get information about the presence or absence of disease as well as its evolution. Despite their wide use in clinical practice, there is still an intense debate between scientific organizations about the real usefulness for patient monitoring during followup as well as response to therapy evaluation in case of advanced BC. In this review, we want to highlight the current recommendations published by scientific organizations about the use of "established" BC serum markers (CEA, TPA, TPS, CIFRA-21, CA15-3, and s-HER2) in clinical oncology practice. Moreover, we will focus on recent papers evidencing the usefulness of tumor markers levels measurement as a guide for the prescription and diagnostic integration of molecular imaging exams such as those performed by hybrid 18-fluorofeoxyglucose-positron emission tomography with integrated computed tomography. This technology is nowadays able to detect early cancer lesions undetectable by conventional morphological imaging investigation and most likely responsible for increasing of serum tumor markers levels.

1. Introduction

Serum tumor markers are soluble molecules released into the blood stream by cancer cells or other cell types belonging to tumor microenvironment [1]. The measurement of these molecules is considered an economic and noninvasive diagnostic assay able to give information about the presence or absence of disease as well as its evolution. In particular, the ideal serum tumor marker should be able to (i) early detect disease; (ii) predict response or resistance to specific therapies; (iii) monitor the patient after primary therapy [2]. In case of breast cancer (BC), different serum markers were tested for these purposes, and to date, the most used in clinical practice are carcinoembryonic antigen (CEA), the soluble form of MUC-1 protein (CA15-3), circulating cytokeratins such as tissue polypeptide antigen (TPA), tissue polypeptide specific antigen (TPS) and cytokeratin 19 fragment (CIFRA-21-1), and the proteolytically cleaved ectodomain of the human epidermal growth factor receptor 2 (s-HER2). Although all of these markers are routinely used in clinical practice, none is useful for screening programs and/or early diagnosis of BC [1, 2]. In addition, an intense debate is still present between scientific organizations regarding their usefulness for patient monitoring during follow-up as well as evaluating response to therapy in case of advanced BC. Nevertheless, thanks to the introduction in clinical practice of molecular imaging exams able to identify cancer lesions previously undetectable by conventional morphological imaging instruments, tumor markers are now reevaluated as an early warning able to highlight patients at risk to relapse [3]. The aim of this review is to highlight the current recommendations about the use of "established" serum markers (CEA, TPA, TPS, CA15-3, and s-HER2) as well as to discuss their usefulness for the prescription and diagnostic integration [4] of molecular imaging exams such as those performed by hybrid 18-fluorodeoxyglucose-positron emission tomography with integrated computed tomography (FDG-PETCT).

2. Established Biomarkers: Structure and Function

2.1. Carcinoembryonic Antigen. In a historical paper published in 1965, Gold and Freedman identified an antigen absent in human normal adult colon specimens and brightly displayed in human fetal and cancer colon tissues; therefore, they called this antigen carcinoembryonic antigen (CEA) [5]. About 30 years later, it was found that CEA consists of a large family of glycoproteins whose structure was similar to that of immunoglobulin super family [6]. Nowadays, CEA antigen is known as cluster of differentiation (CD)66e or CEACAM5 [6, 7]. This protein, with a size of about 100–200 kDa, is a member of the immunoglobulin superfamily with an N-terminal domain including 29 potential glycosylation sites and is attached to the membrane by a glycosyl phosphatidylinositol (GPI) anchor [6, 7]. As reported in Figure 1(a), the extracellular region is composed of six domains homologous to the immunoglobulin constant domain of the C-2 set (IgC2-like) and one immunoglobulin variable domain (IgV-like) [6, 7]. The mechanism responsible for its release in the extracellular matrix is still object of study; however, *in vitro* experiments disclosed that CEA, like other GPI anchored proteins, could be released due to the GPI anchor cleavage catalysis mediated by an endogenous glycosylphosphatidylinositol-specific phospholipase D (GPI-PLD) type enzyme [8].

The function of CEA is still not completely understood. Most probably, it is involved in adhesion to the extracellular matrix and to other cell types thanks to the homophilic and heterophilic interactions with CD66a (CEACAM1) and CD66c (CEACAM6) [9]. Interestingly, recent findings suggest its involvement also in cancer growth, invasion, and metastasis [10, 11]. Indeed, overexpression of CEA and CEACAM6 inhibits anoikis and apoptosis in colon and pancreatic cancer cells [12], disrupts cell polarization and tissue architecture [13], enhances liver metastasis [13], increases chemoresistance [14] as well as recombinant overexpression of CEACAM5 and -6 proteins in transgenic mice (CEABAC mice), and promotes the formation of colon tumours and lung tumours [15].

2.2. MUC-1 Protein. CA15-3 is the soluble form of MUC-1 protein, that is, a large type I transmembrane glycoprotein. As reported in Figure 1(b), MUC-1 is featured by a large tandem repeat domain highly polymorphic that can include a minimum of 21 up to 125 repeats between individuals; each repeat is composed of 20 amino acids rich in serine, threonine, and proline residues, and the cytoplasmic portion is composed of 72 amino acids containing 7 tyrosine residues forming a potential clathrin-mediated endocytic signal sequence [16]. The cytoplasmic tail of MUC-1 is involved in signal transduction by interaction with signaling molecules such as beta-catenin and growth factor receptor-bound protein/Son of Sevenless (Grb/SOS) [16]. Interestingly, MUC-1 is able to exceed the distance spanned by most cell surface proteins being this protein formed by a rigid structure that protrudes 200–500 nm from the cell surface [16].

As regards the functional role of MUC-1, initially, it was supposed to be mainly involved in the protection, lubrication, and hydration of external surfaces of epithelial tissue layers, as well as lining ducts and lumens in different parts of the body [16, 17]. Indeed, MUC-1 is strongly expressed by epithelia of glands and ducts as well as goblet and columnar cells of epithelial tissues where it has a protective role by inhibiting the microbial access to the cell wall and blocking degradative enzymes activity [17, 18]. Also, in case of cellular transformation, a growing number of pieces of scientific evidence proved that MUC-1 should be also considered *de facto* an oncogene. Indeed, its levels are upregulated in epithelial cancer cells of different origin and increase with cancer development and metastasis [18]. In particular, MUC-1, like other transmembrane mucins, contributes to oncogenesis by promoting receptor tyrosine kinase signalling, loss of epithelial cell polarity, constitutive activation of growth and survival pathways (e.g., the Wnt-β-catenin and nuclear factor-κB pathways), and downregulation of stress-induced death pathways [19–22]. Moreover, it has a critical role for cancer immunosurveillance being able to block the access of immune cells to tumors, so that cancer cells are protected from possible clearance mediated by the immune system [23, 24]. Although MUC-1 expression is strictly associated with BC aggressiveness, it is not routinely performed for histological classification of BC, and its use in clinical setting is focused on the serum evaluation of its soluble form called CA15-3.

2.3. HER-2. The discovery of human epidermal growth factor receptor 2 (HER-2; also known as ERBB2) by King et al. in 1985 is considered a milestone for cancer research [25, 26]. Indeed, after its discovery, HER-2 gene was found to be amplified in different number of epithelial cancers, and its protein overexpression has been linked to central tumor cell proliferation and survival pathways. HER2 is a member of the ERBB tyrosine kinase receptor family that includes ERBB1 (EGFR), ERBB3 (HER3), and ERBB4 (HER4). The HER2 receptor is a type 1 transmembrane protein of 1233aa with an extracellular domain of 630aa containing seven potential N-linked glycosylation sites, a transmembrane region of 23aa, and a cytoplasmatic portion of 580aa with a tyrosine-kinase-containing domain (Figure 1(c)) [26].

Unlike the other members of ERBB family, no direct ligand binding has been observed for HER2 receptor, and it is known that its activation relies on (i) heterodimerization with another family member (i.e., EGFR upon EGF ligand binding) or (ii) homodimerization with itself when expressed at very high levels [27]. In case of heterodimerization, HER2 is necessary for ligand binding stabilization and phosphorylation of tyrosine residues that leads to downstream second messenger pathways activation such as those mediated by mitogen activated protein kinase (MAPK), phospholipase-Cγ and phosphatidylinositol 3 kinase (PI3K) [26]. The homodimerization of HER2 is primarily detectable in case of cellular transformation that leads to HER2 overexpression, particularly in case of BC where HER2 gene was found amplified in 20% of cases up to 25–50 copies. This amplification

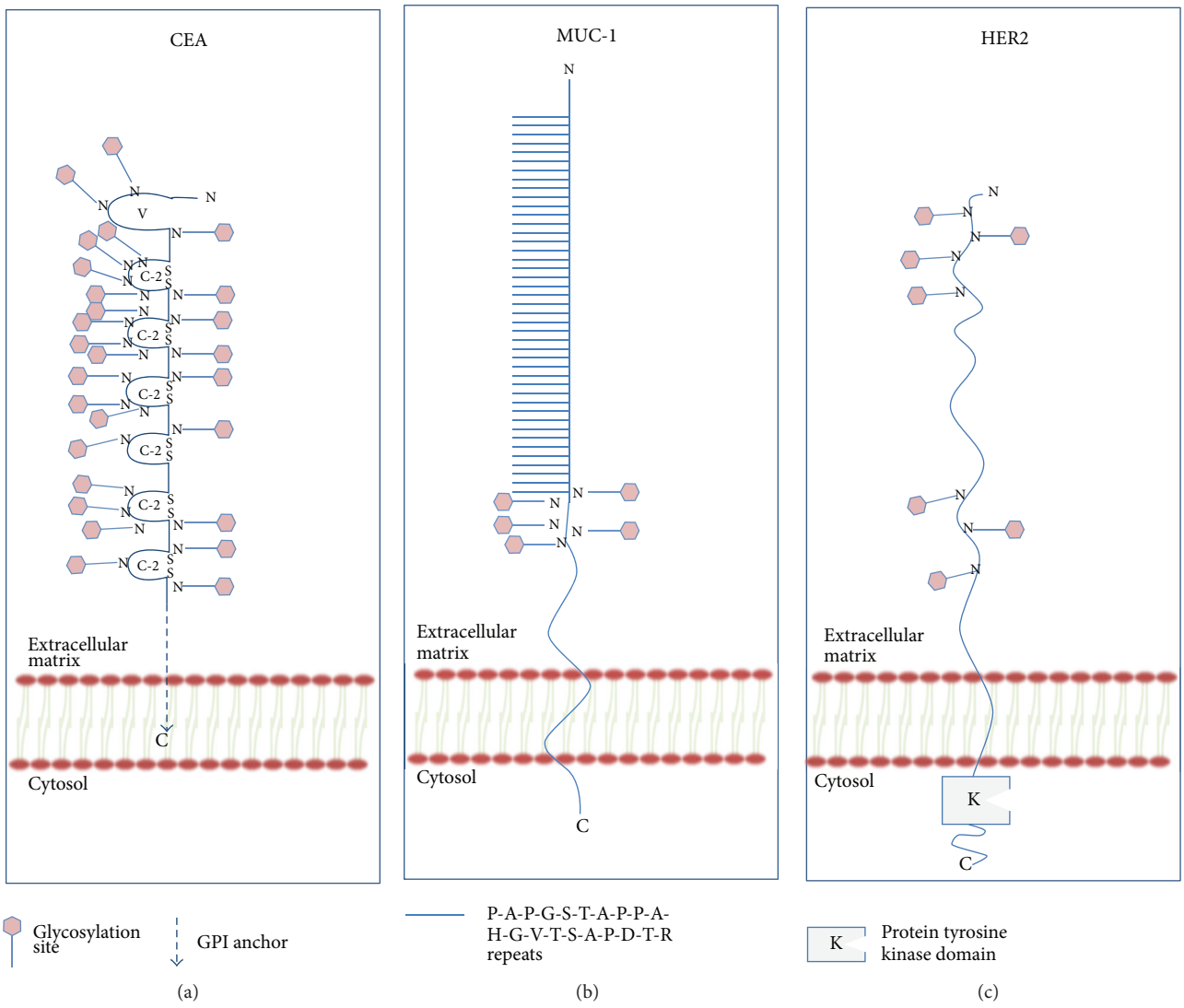

Figure 1: Schematic representation of CEA (a), MUC-1 (b), and HER2 (c) proteins. Of note, proteins are not to scale.

is responsible for 40–100-fold increase in HER-2 protein resulting in 2 million receptors expressed at the surface of tumor cell [26]. The abnormal activation of HER2 in case of homodimerization in cancer tissues leads to a cascade of signaling events causing the activation of a series of transcription factors able to regulate many genes generally involved in cell proliferation, survival, differentiation, and invasion [26]. Due to these peculiar characteristics, the detection of HER-2 has become a routine prognostic and predictive factor in BC and is recommended by the American Society of Clinical Oncology/College of American Pathologists international guidelines [28].

2.4. Cytokeratins (TPA, TPS, and CYFRA 21.1). Cytokeratins (CKs) are a class of intermediate filaments primary involved in cytoskeletal organization of epithelial cells for the fixation of the nucleus and maintenance of cellular morphology for cell protection from mechanical and nonmechanical stressors [29]. CKs comprise 20 related polypeptides classified in two groups: type I includes acidic CKs (CK 9–20) and type II includes neutral-basic CKs (CK 1–8) [29]. Type I and II CKs are always present in stoichiometric amounts, and their expression is differentiation dependent; for instance, in a lot of normal simple epithelial cells (glandular epithelia, transitional cell epithelium, and hepatocytes), CK8 and its obligate partner CK18 constitute the primary pair. The keratin expression pattern of normal epithelia is largely maintained also in the neoplastic counterpart. Therefore, keratins have long and extensively been used as immunohistochemical markers in diagnostic tumor pathology and most cancers of glandular epithelia origin, including BC, express CK8, CK18, and CK19 as specific cancer tissue biomarkers [29, 30]. Interestingly, during the last years, a growing number of pieces of experimental evidence disclosed that CKs have also an important role in cancer pathophysiology. In particular, in case of hormonally responsive BC, it has been shown that CK18 has a regulatory role as it can effectively associate with and sequester the estrogen

receptor-alpha (ER-α) target gene and ERα coactivator LRP16 in the cytoplasm, thus attenuating ERα-mediated signaling and estrogen-stimulated cell cycle progression in BC cells [31]. Moreover, in case of BC, CK8 and CK18 are frequently found downregulated in metastatic tissue biopsies where their ubiquitin-immunoreactive degradation products are detectable and related with tumor aggressiveness [32]. Also, CK-8, -17, and -19 are upregulated in BC cells featured by defective autophagy, a condition where disease-promoting mechanisms such as toxic protein aggregation, oxidative stress, genomic damage, and inflammation are increased [33, 34]. In oncological patients, cytokeratins serum levels are informative of disease status and are frequently used for clinical management. For this purpose, the CKs tested primarily into the blood stream are CK8, CK18, and CK19 and the most widely used assays are (i) TPA for the evaluation of CK8, CK18, and CK19; (ii) TPS for the measurement of CK8 and CK18; and (iii) CYFRA 21.1 for CK19.

3. Tumor Markers for Diagnosis and Prognosis of BC

3.1. CEA. The first tumor marker used for diagnostic purposes of different human cancer (colorectal, pancreatic, breast, ovary, head and neck, bladder, kidney, and prostate cancers) was the CEA antigen, found overexpressed in serum of oncological patients compared to healthy individuals [35]. Further studies showed that CEA measurement was not useful for screening or for diagnosis of early BC since it was too insensitive and nonspecific to reliably differentiate patients with early BC from those with benign disease or disease free [36–38]. However, in case of symptomatic BC patients CEA sensitivity increases, and some authors evidenced that CEA levels at diagnosis are able to correlate with the stage of disease [39, 40]. Additionally, as a prognostic tool, the positive pretherapeutic levels of CEA may be useful to highlight those patients with a worse prognosis and at risk to have a recurrence after primary therapy [41, 42].

3.2. CA15-3. The soluble form of MUC-1 (CA15-3) was identified as a more specific BC marker with respect to CEA. Also, this marker disclosed low sensitivity and specificity for the detection of BC, since its sensitivity is 10–15%, 20–25%, and 30–35% for stages I, II, and III, respectively [43]. Therefore, the screening of CA15-3 in BC patients is not recommended. As for CEA, the increasing levels of CA15-3 may be useful to detect patients with advanced disease [44]. Indeed, the simultaneous positivity of both markers allows early diagnosis of metastases in up to 60–80% of patients with advanced disease [45].

3.3. s-HER-2. In the last ten years, particular attention has been devoted to the detection of the soluble form of HER-2 in serum from BC patients. Indeed, as demonstrated by several *in vitro* and *in vivo* experiments, the ectodomain of HER-2 can be proteolytically cleaved from the intact receptor and released as soluble molecule (s-HER-2) [46–48]. In normal healthy individuals, low concentrations of s-HER-2 can be detected in serum; however, in some BC patients, s-HER2 levels are increased according to the tumor burden and HER-2 status [49]. Even if s-HER-2, like other circulating tumor markers, has limited usefulness for diagnosis and/or screening of BC, the US Food and Drug Administration (FDA) introduced its serum levels measurement for monitoring trastuzumab treatment in BC patients with HER-2 positive tissue and serum expression [50]. Particularly, in these patients, it has been shown that decreasing values of s-HER-2 can be related to a positive response to biological therapy, whereas increasing levels are able to predict resistance or may act as an early warning indicating that standard doses of trastuzumab are insufficient [51].

3.4. Cytokeratins. The screening of circulating cytokeratins in BC patients at diagnosis is actually not recommended; however, recent observations showed that the detection rate of hepatic metastases in patients with BC can be raised up to 90% by simultaneous testing the serum levels of CA15-3, CEA, and circulating cytokeratins (TPA, TPS, and CYFRA 21.1) [45, 46].

4. Tumor Markers for Surveillance after Primary BC Treatment

4.1. International Guidelines Recommendations. Serum tumor markers are frequently required by clinical oncologists as an economic and noninvasive test for patient management during followup after primary BC therapy for an early detection of recurrence or metastases [63, 64]. They should be useful to discriminate those patients at risk to have a recurrence after primary BC treatment; however, their usefulness is still object of intense debate in the scientific community [63, 64]. This criticism has been raised during the 1990s, when two large multicenter randomized prospective trials, accounting each for about 1000 patients, showed that patients subjected only to periodic clinical visit and mammography showed the same outcome respect to those following an intense regimen including radiology and biomarkers screening [65, 66]. Furthermore, this *caveat* has been recently confirmed and stressed by the ASCO guidelines for Breast Cancer Follow-Up and Management After Primary Treatment (Table 1) [52]. In particular, these guidelines recommend that an optimal followup has to be primarily done by a careful history and physical patient examination performed by an experienced physician together with a regular mammography, particularly in case of breast conserving surgical therapy. Conversely, tumor markers exams, bone scans, chest radiographs, liver ultrasounds, CT, and even FDG-PET scanning as well as magnetic resonance imaging are not recommended by ASCO for routine BC followup in asymptomatic patients with no specific findings on clinical examination [52]. Despite these recommendations, other scientific organizations suggest serum tumor markers testing for postoperative surveillance as well as therapy monitoring in patients with advanced BC (Table 1). In particular, the European Group on Tumor Markers (EGTM; http://www.egtm.eu/recommendations.html) [57] and the

Table 1: Current recommendations edited by international scientific organizations for the use of serum cancer biomarkers in clinical oncology.

Expert panel	Recommendation	Year of publication	Reference
ASCO	The use of CA15-3 and CEA is not recommended for routine surveillance of patients with breast cancer after primary therapy	2013	[52]
ESMO	Serum tumor markers (such as CA15-3 and/or CEA), if initially elevated, may be helpful in monitoring response, particularly in the case of nonmeasurable disease. However, a change in tumor markers alone should not be used as the only determinant for treatment decisions	2012	[53]
ACR	Localizing "occult" disease especially in the presence of clinical indicators such as elevated tumor markers	2012	[54]
EANM	Establishing and localizing disease sites as a cause for elevated serum markers (e.g., colorectal, thyroid, ovarian, cervix, melanoma, breast, and germ-cell tumours)	2010	[55]
NACB	CEA and CA15-3 are useful for therapy monitoring especially in patients with nonevaluable disease	2008	[56]
EGTM	CA15-3 and CEA are the most useful serum markers in patients with breast cancer. Serial determinations of these markers are useful in assessing prognosis, early detection of relapse (metastasis), and therapy monitoring	2005	[57]

Table 2: Studies proving the usefulness of performing PETCT scan on patients during followup with rising tumor markers for the detection of cancer lesions undetectable by conventional morphological imaging.

Study/year	Results	Remarks	Tumor markers	Reference
Filippi et al. Nucl Med Commun. 2011	FDG PETCT was positive in 36 out of 46 patients with rising biomarkers	The FDG-PET/CT scan plays an important role in restaging breast cancer patients with rising tumor markers and negative or equivocal findings in conventional imaging techniques	CEA and CA15-3	[58]
Evangelista et al. Eur J Nucl Med Mol Imaging. 2011	PETCT scan analysis was positive in 30 out of 40 patients with elevated tumor marker	FDG PETCT is more sensitive than CT for the evaluation of disease relapse; PETCT might be considered a complementary imaging technique during followup in patients with breast cancer	CA15-3	[59]
Champion et al. Cancer 2011	PETCT scans were positive in 181 patients (79.5%) and normal in 47 patients with rising CA15-3 and/or CEA	FDG PETCT imaging is an efficient technique to detect breast cancer recurrence suspected on tumor marker rising in asymptomatic patients	CEA and CA15-3	[60]
Grassetto et al. Eur J Radiol. 2011	Tumor deposits were detected in 40/89 patients by FDG PETCT	FDG PETCT may have a potential role in asymptomatic patients with rising markers and negative conventional imaging	CA15-3	[61]
Katayama et al. Ann Nucl Med. 2012	PETCT scan analysis was positive in 23 out of 47 patients with elevated tumor marker	The change in the tumor marker levels was substantially correlated with the PET findings and moderately correlated with the CT findings	CEA, I-CTP, CA15-3, BCA225, and NCC-ST-439	[62]

National Academy of Clinical Biochemistry (NACB) [56] indicate that rising of tumor markers serum levels, with particular attention to CA15-3 in case of BC, is able to detect asymptomatic patients at risk to have metastases prior to the onset of clinical or radiological findings. In this way, the relationship between serum levels of biomarkers and imaging findings is still an argument of great interest for both laboratory medicine and radiology [3].

4.2. Tumor Markers and FDG-PETCT. For a long time, biochemical markers results were compared to those obtained by conventional morphological imaging modalities. In these circumstances, a high rate of false negatives was reported, and less than 20% of tumor marker elevations were associated with clinical and radiological findings. Consequently, these data have aroused doubts and criticisms in the scientific community about the value of tumor marker-guided follow-up also in case of BC [56]. During the last years, a growing number of scientific studies (Table 2) proved that whole-body FDG-PETCT scan is able to reduce the number of false negative cases by evidencing early tumor lesions previously undetectable by conventional morphological imaging exams. In this regard, it is important to consider two studies

published in 2011 by Filippi et al. [58] and Evangelista et al. [59] who evidenced for the first time that hybrid FDG-PETCT scan was able to pick up cancer lesions, undetectable by conventional CT alone, in a cohort of about 40 asymptomatic BC patients with rising serum tumor markers. These observations were soon after corroborated in a third study by Champion et al. analyzing a large cohort of asymptomatic BC patients with rising CA15-3 and/or CEA tumor markers [60]. The ability of tumor markers to integrate PETCT exams for an optimal BC patient management during followup was also evidenced by Grassetto et al. who retrospectively studied 89 asymptomatic BC patients with rising CA15-3 levels and negative conventional imaging exams [61] and found that 40 out of 89 patients were positive at FDG-PETCT scan with tumor lesions detectable at level of chest wall, internal mammary nodes, lungs, liver, and skeleton. Moreover, in 23 out of 40 patients, a solitary lesion was detectable. Ultimately, in 2012, a study by Katayama et al. proved that change in tumor marker levels is primarily correlated with PET findings than CT, however, the hybrid pattern obtained by combining PET and CT imaging allow an optimal detection of FDG uptake to monitor disease progression, particularly in case of bone metastases, respect to other conventional imaging modalities [62].

5. Monitoring Response to Therapy in Advanced BC

Monitoring of therapy in patients with advanced BC is a critical issue in order to define cases responding to therapy from nonresponding ones [67]. Currently, the criteria of International Union against Cancer (UICC) are still used for assessing response to therapy, and they include physical examination, measurement of lesions, radiology, and isotope scanning [68]. Tumor markers levels measurement was not included in UICC criteria; however, two later multicenter studies showed that changes in serial concentrations of tumor markers, particularly CA15-3, correlate with response to therapy as well as with UICC criteria [69, 70]. In this regard, the actual guidelines from the European School of Oncology (ESO) suggest that "if tumor markers such as CA15-3 and CEA are elevated at time of treatment initiation, they can be helpful for therapy monitoring and long-term surveillance but they cannot be used solely for decision making with respect to change of therapy" [71]. Contrary to what is stated by ESO guidelines, the ASCO guidelines [52] do not suggest tumor marker measurement for monitoring response to therapy. However, since in about 10–20% of advanced BC the UICC criteria are not applicable (i.e., in patient with bone disease), the ASCO suggests tumor markers level measurement to have an early therapy response evaluation, but that tumor marker level alone is not sufficient for any therapy decision making.

6. Conclusions and Future Perspectives

The current routinely used serum tumor markers have limited usefulness for diagnosis and/or screening of BC due to their very low sensitivity and specificity as well as to the fact that they can be raised also in case of some benign conditions. For example, benign breast or ovarian disease and endometriosis may be associated with CA15-3 rising, while other conditions such as inflammatory bowel disease, pancreatitis, and gastritis may cause CEA increase [72]. Tumor markers level measurement at diagnosis may be only useful to point out those patients with advanced BC and then at risk to have liver involvement; however, it is not excluded that metastatic BC cases may present with normal serum concentrations.

As regards the usefulness of tumor markers for monitoring patients during followup, the debate is still open between scientific organizations (Table 1). In fact, the actual ASCO and ESMO guidelines do not suggest the use of tumor markers for monitoring BC patients during followup, and both confirm that they should be used only for advanced BC therapy monitoring, especially in cases where cancer lesions response, to therapy are not clinically evaluable. Conversely, the European Group for Tumor Markers (EGTM) [57] in agreement with the National Academy of Clinical Biochemistry (NACB) [57] sustains that serial evaluation of tumor markers levels is important for BC patient monitoring in order to get an early diagnosis of recurrence, since tumor markers rising often precede clinical or radiological signs of disease. Finally, the American College of Radiology (ACR) [54] and the European Association for Nuclear Medicine (EANM) [55] suggest that tumor markers increasing during followup may be an early warning able to highlight those patients needing molecular imaging investigations. In particular, according to recent studies (Table 2), both organizations reevaluated the role of tumor markers as an early warning able to highlight those patients at risk to have a recurrence due to clusters of tumor cells undetectable by conventional morphological imaging modalities. We believe that this last consideration is important since the biochemical markers results could integrate the diagnostic pathway for an early diagnosis of BC recurrence and, consequently, provide a better therapeutic intervention.

In our personal experience, CA15-3 proved to be a good serum tumor marker for those BC patients needing accurate molecular imaging investigations (PETCT) during followup. Our observations are in agreement with recent published studies suggesting that CA15-3 rising often precedes clinical or radiological signs of disease recurrence [61, 73]. Nevertheless, CA15-3 as well as other established biomarkers cited in this review does not fulfill the features of an ideal biomarker especially in terms of diagnostic sensitivity and specificity. On the basis of these diagnostics gaps, many research groups are conducting studies aimed at identifying new biomarkers able to diagnose BC at an early stage using minimally invasive approaches. In particular, during the last years, circulating noncoding molecules of RNA (miRNAs) are emerging as an innovative class of cancer biomarkers since found aberrantly expressed in different human cancers (tissues and serum) and featured by unprecedented levels of diagnostic specificity and sensitivity [74–77]. Despite this exciting discovery, common BC specific miRNAs have yet to emerge across studies, and it is too soon to interpret their functional role. In addition, comparing the circulating miRNAs profiling identified by

different studies from different countries, only few of these miRNAs were corroborated by independent research groups [78]. On the basis of these pieces of evidence, it is essential to invest in larger study cohorts to validate a reproducible circulating-derived miRNAs signature to achieve true translational relevance and bring circulating miRNAs into routine diagnostics for early detection of BC, to predict outcome and in treatment planning.

References

[1] P. Marić, P. Ozretić, S. Levanat, S. Orešković, K. Antunac, and L. Beketić-Orešković, "Tumor markers in breast cancer: evaluation of their clinical usefulness," *Collegium Antropologicum*, vol. 35, no. 1, pp. 241–247, 2011.

[2] S. E. Bates, "Clinical applications of serum tumor markers," *Annals of Internal Medicine*, vol. 115, no. 8, pp. 623–638, 1991.

[3] M. Plebani, "Biochemical and imaging biomarkers: the search for the Holy Grail," *Clinical Chemistry and Laboratory Medicine*, vol. 48, no. 8, pp. 1055–1056, 2010.

[4] C. J. McMahon, V. Crowley, N. McCarroll, R. Dunne, and M. T. Keogan, "Elevated tumour marker: an indication for imaging?" *Annals of Clinical Biochemistry*, vol. 47, no. 4, pp. 327–330, 2010.

[5] P. Gold and S. O. Freedman, "Demonstration of tumor-specific antigens in human colonic carcinomata by immunological tolerance and absorption techniques," *The Journal of Experimental Medicine*, vol. 121, pp. 439–462, 1965.

[6] S. Hammarström, "The carcinoembryonic antigen (CEA) family: structures, suggested functions and expression in normal and malignant tissues," *Seminars in Cancer Biology*, vol. 9, no. 2, pp. 67–81, 1999.

[7] K. Kuespert, S. Pils, and C. R. Hauck, "CEACAMs: their role in physiology and pathophysiology," *Current Opinion in Cell Biology*, vol. 18, no. 5, pp. 565–571, 2006.

[8] A. Pakdel, F. Naghibalhossaini, P. Mokarram, M. Jaberipour, and A. Hosseini, "Regulation of carcinoembryonic antigen release from colorectal cancer cells," *Molecular Biology Reports*, vol. 39, no. 4, pp. 3695–3704, 2012.

[9] C. H. F. Chan and C. P. Stanners, "Recent advances in the tumour biology of the GPI-anchored carcinoembryonic antigen family members CEACAM5 and CEACAM6," *Current Oncology*, vol. 14, no. 2, pp. 70–73, 2007.

[10] R. D. Blumenthal, H. J. Hansen, and D. M. Goldenberg, "Inhibition of adhesion, invasion, and metastasis by antibodies targeting CEACAM6 (NCA-90) and CEACAM5 (carcinoembryonic antigen)," *Cancer Research*, vol. 65, no. 19, pp. 8809–8817, 2005.

[11] M. Gemei, P. Mirabelli, R. Di Noto et al., "CD66c is a novel marker for colorectal cancer stem cell isolation, and its silencing halts tumor growth in vivo," *Cancer*, vol. 119, no. 4, pp. 729–738, 2013.

[12] C. Ilantzis, L. Demarte, R. A. Screaton, and C. P. Stanners, "Deregulated expression of the human tumor marker CEA and CEA family member CEACAM6 disrupts tissue architecture and blocks colonocyte differentiation," *Neoplasia*, vol. 4, no. 2, pp. 151–163, 2002.

[13] M. S. Duxbury, H. Ito, M. J. Zinner, S. W. Ashley, and E. E. Whang, "CEACAM6 gene silencing impairs anoikis resistance and in vivo metastatic ability of pancreatic adenocarcinoma cells," *Oncogene*, vol. 23, no. 2, pp. 465–473, 2004.

[14] M. S. Duxbury, H. Ito, E. Benoit, T. Waseem, S. W. Ashley, and E. E. Whang, "A novel role for carcinoembryonic antigen-related cell adhesion molecule 6 as a determinant of gemcitabine chemoresistance in pancreatic adenocarcinoma cells," *Cancer Research*, vol. 64, no. 11, pp. 3987–3993, 2004.

[15] C. H. F. Chan, D. Cook, and C. P. Stanners, "Increased colon tumor susceptibility in azoxymethane treated CEABAC transgenic mice," *Carcinogenesis*, vol. 27, no. 9, pp. 1909–1916, 2006.

[16] M. Brayman, A. Thathiah, and D. D. Carson, "MUC1: a multifunctional cell surface component of reproductive tissue epithelia," *Reproductive Biology and Endocrinology*, vol. 2, article 4, 2004.

[17] D. W. Kufe, "Mucins in cancer: function, prognosis and therapy," *Nature Reviews Cancer*, vol. 9, no. 12, pp. 874–885, 2009.

[18] D. W. Kufe, "MUC1-C oncoprotein as a target in breast cancer: activation of signaling pathways and therapeutic approaches," *Oncogene*, vol. 32, pp. 1073–1081.

[19] J. Ren, N. Agata, D. Chen et al., "Human MUC1 carcinoma-associated protein confers resistance to genotoxic anticancer agents," *Cancer Cell*, vol. 5, no. 2, pp. 163–175, 2004.

[20] J. Ren, A. Bharti, D. Raina, W. Chen, R. Ahmad, and D. Kufe, "MUC1 oncoprotein is targeted to mitochondria by heregulin-induced activation of c-Src and the molecular chaperone HSP90," *Oncogene*, vol. 25, no. 1, pp. 20–31, 2006.

[21] H. Rajabi, M. Alam, H. Takahashi et al., "MUC1-C oncoprotein activates the ZEB1/miR-200c regulatory loop and epithelial-mesenchymal transition," *Oncogene*, 2013.

[22] D. Kufe, "Oncogenic function of the MUC1 receptor subunit in gene regulation," *Oncogene*, vol. 29, no. 42, pp. 5663–5666, 2010.

[23] S. Tsuboi, "Tumor defense systems using O-glycans," *Biological and Pharmaceutical Bullettin*, vol. 35, no. 10, pp. 1633–1636, 2012.

[24] Y. Suzuki, M. Sutoh, S. Hatakeyama et al., "MUC1 carrying core 2 O-glycans functions as a molecular shield against NK cell attack, promoting bladder tumor metastasis," *International Journal of Oncology*, vol. 40, no. 6, pp. 1831–1838, 2012.

[25] C. R. King, M. H. Kraus, and S. A. Aaronson, "Amplification of a novel v-erbB-related gene in a human mammary carcinoma," *Science*, vol. 229, no. 4717, pp. 974–976, 1985.

[26] L. J. Tafe and G. J. Tsongalis, "The human epidermal growth factor receptor 2 (HER2)," *Clinical Chemistry and Laboratory Medicine*, vol. 50, no. 1, pp. 23–30, 2012.

[27] C. Gutierrez and R. Schiff, "HER2: biology, detection, and clinical implications," *Archives of Pathology and Laboratory Medicine*, vol. 135, no. 1, pp. 55–62, 2011.

[28] A. C. Wolff, M. E. H. Hammond, J. N. Schwartz et al., "American Society of Clinical Oncology/College of American Pathologists guideline recommendations for human epidermal growth factor receptor 2 testing in breast cancer," *Archives of Pathology and Laboratory Medicine*, vol. 131, no. 1, pp. 18–43, 2007.

[29] V. Karantza, "Keratins in health and cancer: more than mere epithelial cell markers," *Oncogene*, vol. 30, no. 2, pp. 127–138, 2011.

[30] H.-A. Lehr, A. Folpe, H. Yaziji, F. Kommoss, and A. M. Gown, "Cytokeratin 8 immunostaining pattern and E-cadherin expression distinguish lobular from ductal breast carcinoma," *The American Journal of Clinical Pathology*, vol. 114, no. 2, pp. 190–196, 2000.

[31] Y. Meng, Z. Wu, X. Yin et al., "Keratin 18 attenuates estrogen receptor α-mediated signaling by sequestering LRP16 in cytoplasm," *BMC Cell Biology*, vol. 10, article 96, 2009.

[32] K. Iwaya, H. Ogawa, Y. Mukai, A. Iwamatsu, and K. Mukai, "Ubiquitin-immunoreactive degradation products of cytokeratin 8/18 correlate with aggressive breast cancer," *Cancer Science*, vol. 94, no. 10, pp. 864–870, 2003.

[33] S. Kongara and V. Karantza, "The interplay between autophagy and ROS in tumorigenesis," *Frontiers in Oncology*, vol. 171, 2012.

[34] S. Kongara, O. Kravchuk, I. Teplova et al., "Autophagy regulates keratin 8 homeostasis in mammary epithelial cells and in breast tumors," *Molecular Cancer Research*, vol. 8, no. 6, pp. 873–884, 2010.

[35] E. W. Martin Jr., W. E. Kibbey, and I. DiVecchia, "Carcinoembryonic antigen. Clinical and historical aspects," *Cancer*, vol. 37, no. 1, pp. 62–81, 1976.

[36] D. E. Haagensen Jr., S. J. Kister, and J. P. Vandevoorde, "Evaluation of carcinoembryonic antigen as a plasma monitor for human breast carcinoma," *Cancer*, vol. 42, no. 3, pp. 1512–1519, 1978.

[37] A. Rimsten, H. O. Adami, B. Wahren, and B. Nordin, "Carcinoembryonic antigen in serum of unselected breast-cancer patients and of non-hospitalized controls," *British Journal of Cancer*, vol. 39, no. 2, pp. 109–115, 1979.

[38] D. Y. Wang, R. E. Knyba, and R. D. Bulbrook, "Serum carcinoembryonic antigen in the diagnosis and prognosis of women with breast cancer," *European Journal of Cancer and Clinical Oncology*, vol. 20, no. 1, pp. 25–31, 1984.

[39] A. K. Agrawal, M. Jelen, J. Rudnicki et al., "The importance of preoperative elevated serum levels of CEA and CA15-3 in patients with breast cancer in predicting its histological type," *Folia Histochemica et Cytobiologica*, vol. 48, no. 1, pp. 26–29, 2010.

[40] B.-W. Park, J.-W. Oh, J.-H. Kim et al., "Preoperative CA 15-3 and CEA serum levels as predictor for breast cancer outcomes," *Annals of Oncology*, vol. 19, no. 4, pp. 675–681, 2008.

[41] J. S. Lee, S. Park, J. M. Park et al., "Elevated levels of preoperative CA 15-3 and CEA serum levels have independently poor prognostic significance in breast cancer," *Annals of Oncology*, vol. 24, no. 5, pp. 1225–1312, 2013.

[42] P. Gaglia, B. Caldarola, R. Bussone et al., "Prognostic value of CEA and ferritin assay in breast cancer: a multivariate analysis," *European Journal of Cancer and Clinical Oncology*, vol. 24, no. 7, pp. 1151–1155, 1988.

[43] M. J. Duffy, "Serum tumor markers in breast cancer: are they of clinical value?" *Clinical Chemistry*, vol. 52, no. 3, pp. 345–351, 2006.

[44] A. Nicolini, A. Carpi, P. Ferrari et al., "The role of tumour markers in improving the accuracy of conventional chest X-ray and liver echography in the post-operative detection of thoracic and liver metastases from breast cancer," *British Journal of Cancer*, vol. 83, no. 11, pp. 1412–1417, 2000.

[45] V. Liska, L. Holubec Jr., V. Treska et al., "Evaluation of tumour markers as differential diagnostic tool in patients with suspicion of liver metastases from breast cancer," *Anticancer Research*, vol. 31, no. 4, pp. 1447–1451, 2011.

[46] S. Mori, Y. Mori, T. Mukaiyama et al., "In vitro and in vivo release of soluble erbB-2 protein from human carcinoma cells," *Japanese Journal of Cancer Research*, vol. 81, no. 5, pp. 489–494, 1990.

[47] B. C. Langton, M. C. Crenshaw, L. A. Chao, S. G. Stuart, R. W. Akita, and J. E. Jackson, "An antigen immunologically related to the external domain of gp185 is shed from nude mouse tumors overexpressing the c-erbB-2 (HER-2/neu) oncogene," *Cancer Research*, vol. 51, no. 10, pp. 2593–2598, 1991.

[48] D. Baskić, P. Ristić, S. Pavlović et al., "Serum HER2 and CA 15-3 in breast cancer patients," *Journal of BUON*, vol. 9, no. 3, pp. 289–294, 2004.

[49] B. Leyland-Jones and B. R. Smith, "Serum HER2 testing in patients with HER2-positive breast cancer: the death knell tolls," *The Lancet Oncology*, vol. 12, no. 3, pp. 286–295, 2011.

[50] W. P. Carney, R. Neumann, A. Lipton, K. Leitzel, S. Ali, and C. P. Price, "Monitoring the circulating levels of the HER2/neu oncoprotein in breast cancer," *Clinical Breast Cancer*, vol. 5, no. 2, pp. 105–116, 2004.

[51] J. Trapé, X. Filella, M. Alsina-Donadeu, L. Juan-Pereira, À. Bosch-Ferrer, and R. Rigo-Bonnin, "Increased plasma concentrations of tumour markers in the absence of neoplasia," *Clinical Chemistry and Laboratory Medicine*, vol. 49, no. 10, pp. 1605–1620, 2011.

[52] J. L. Khatcheressian, P. Hurley, E. Bantug et al., "Breast cancer follow-up and management after primary treatment: American Society of Clinical Oncology clinical practice guideline update," *Journal of Clinical Oncology*, vol. 31, no. 7, pp. 961–965, 2013.

[53] F. Cardoso, N. Harbeck, L. Fallowfield, S. Kyriakides, and E. Senkus, "Locally recurrent or metastatic breast cancer: ESMO clinical practice guidelines for diagnosis, treatment and follow-up," *Annals of Oncology*, vol. 23, supplement 7, pp. vii1–vii9, 2012.

[54] "ACR-SPR Practice guideline for performing FDG-PET/CT in oncology," 2012, http://www.acr.org/guidelines/.

[55] R. Boellaard, M. J. O'Doherty, W. A. Weber et al., "FDG PET and PET/CT: EANM procedure guidelines for tumour PET imaging: version 1.0," *European Journal of Nuclear Medicine and Molecular Imaging*, vol. 37, no. 1, pp. 181–200, 2010.

[56] C. M. Sturgeon, M. J. Duffy, U. H. Stenman et al., "National Academy of Clinical Biochemistry laboratory medicine practice guidelines for use of tumor markers in testicular, prostate, colorectal, breast, and ovarian cancers," *Clinical Chemistry*, vol. 54, no. 12, pp. 11–79, 2008.

[57] R. Molina, V. Barak, A. van Dalen et al., "Tumor markers in breast cancer-European Group on Tumor Markers recommendations," *Tumour Biology*, vol. 26, no. 6, pp. 281–293, 2005.

[58] V. Filippi, J. Malamitsi, F. Vlachou et al., "The impact of FDG-PET/CT on the management of breast cancer patients with elevated tumor markers and negative or equivocal conventional imaging modalities," *Nuclear Medicine Communications*, vol. 32, no. 2, pp. 85–90, 2011.

[59] L. Evangelista, Z. Baretta, L. Vinante et al., "Tumour markers and FDG PET/CT for prediction of disease relapse in patients with breast cancer," *European Journal of Nuclear Medicine and Molecular Imaging*, vol. 38, no. 2, pp. 293–301, 2011.

[60] L. Champion, E. Brain, A.-L. Giraudet et al., "Breast cancer recurrence diagnosis suspected on tumor marker rising," *Cancer*, vol. 117, no. 8, pp. 1621–1629, 2011.

[61] G. Grassetto, A. Fornasiero, D. Otello et al., "18F-FDG-PET/CT in patients with breast cancer and rising Ca 15-3 with negative conventional imaging: a multicentre study," *European Journal of Radiology*, vol. 80, no. 3, pp. 828–833, 2011.

[62] T. Katayama, K. Kubota, Y. Machida, A. Toriihara, and H. Shibuya, "Evaluation of sequential FDG-PET/CT for monitoring bone metastasis of breast cancer during therapy: correlation between morphological and metabolic changes with tumor markers," *Annals of Nuclear Medicine*, vol. 26, no. 5, pp. 426–435, 2012.

[63] C. M. Sturgeon, L. C. Lai, and M. J. Duffy, "Serum tumour markers: how to order and interpret them," *BMJ*, vol. 339, no. 7725, pp. 852–858, 2009.

[64] M. Brooks, "Breast cancer screening and biomarkers," *Methods in Molecular Biology*, vol. 472, pp. 307–321, 2009.

[65] M. R. Del Turco, D. Palli, A. Cariddi, S. Ciatto, P. Pacini, and V. Distante, "Intensive diagnostic follow-up after treatment of primary breast cancer: a randomized trial," *Journal of the American Medical Association*, vol. 271, no. 20, pp. 1593–1597, 1994.

[66] A. Liberati, "Impact of follow-up testing on survival and health-related quality of life in breast cancer patients: a multicenter randomized controlled trial," *Journal of the American Medical Association*, vol. 271, no. 20, pp. 1587–1592, 1994.

[67] F. Cardoso, A. Costa, L. Norton et al., "1st International consensus guidelines for advanced breast cancer (ABC 1)," *Breast*, vol. 21, no. 3, pp. 242–252, 2012.

[68] J. L. Hayward, R. D. Rubens, and P. P. Carbone, "Assessment of response to therapy in advanced breast cancer. A project of the programme on clinical oncology of the International Union against Cancer, Geneva, Switzerland," *British Journal of Cancer*, vol. 35, no. 3, pp. 292–298, 1977.

[69] J. F. R. Robertson, W. Jaeger, J. J. Syzmendera et al., "The objective measurement of remission and progression in metastatic breast cancer by use of serum tumor markers," *European Journal of Cancer*, vol. 35, no. 1, pp. 47–53, 1999.

[70] J. Kurebayashi, R. Nishimura, K. Tanaka et al., "Significance of serum tumor markers in monitoring advanced breast cancer patients treated with systemic therapy: a prospective study," *Breast Cancer*, vol. 11, no. 4, pp. 389–395, 2004.

[71] B. Melichar, "Biomarkers in the treatment of cancer: opportunities and pitfalls," *Clinical Chemistry and Laboratory Medicine*, vol. 24, pp. 1–5, 2013.

[72] N. U. Lin, C. Thomssen, F. Cardoso et al., "International guidelines for management of metastatic breast cancer (MBC) from the European School of Oncology (ESO)-MBC Task Force: surveillance, staging, and evaluation of patients with early-stage and metastatic breast cancer," *Breast*, vol. 22, no. 3, pp. 203–210, 2013.

[73] L. Evangelista, A. R. Cervino, C. Ghiotto, A. Al-Nahhas, D. Rubello, and P. C. Muzzio, "Tumor marker-guided PET in breast cancer patients: a recipe for a perfect wedding: a systematic literature review and meta-analysis," *Clinical Nuclear Medicine*, vol. 37, no. 5, pp. 467–474, 2012.

[74] D. Madhavan, K. Cuk, B. Burwinkel, and R. Yang, "Cancer diagnosis and prognosis decoded by blood-based circulating microRNA signatures," *Frontiers in Genetics*, vol. 21, no. 4, article 116, 2013.

[75] K. Cuk, M. Zucknick, J. Heil et al., "Circulating microRNAs in plasma as early detection markers for breast cancer," *International Journal of Cancer*, vol. 132, no. 7, pp. 1602–1612, 2013.

[76] H. Zhao, J. Shen, L. Medico, D. Wang, C. B. Ambrosone, and S. Liu, "A pilot study of circulating miRNAs as potential biomarkers of early stage breast cancer," *PLoS ONE*, vol. 5, no. 10, Article ID e13735, 2010.

[77] M. Chan, C. S. Liaw, S. M. Ji et al., "Identification of circulating MicroRNA signatures for breast cancer detection," *Clinical Cancer Research*, vol. 19, no. 16, pp. 4477–4487, 2013.

[78] R. S. Leidner, L. Li, and C. L. Thompson, "Dampening enthusiasm for circulating microRNA in breast cancer," *PLoS ONE*, vol. 8, no. 3, Article ID e57841, 2013.

Hindawi Publishing Corporation
BioMed Research International
Volume 2013, Article ID 531640, 6 pages
http://dx.doi.org/10.1155/2013/531640

Research Article

Carbohydrate 19.9 Antigen Serum Levels in Liver Disease

Gaetano Bertino,[1] Annalisa Maria Ardiri,[1] Giuseppe Stefano Calvagno,[1] Giulia Malaguarnera,[2] Donatella Interlandi,[1] Marco Vacante,[3] Nicoletta Bertino,[1] Francesco Lucca,[3] Roberto Madeddu,[4] and Massimo Motta[3]

[1] *Department of Medical and Pediatric Sciences, Hepatology Unit, University of Catania, 95123 Catania, Italy*
[2] *International Ph.D. Program in Neuropharmacology, University of Catania, 95123 Catania, Italy*
[3] *Research Center "The Great Senescence", University of Catania, 95125 Catania, Italy*
[4] *Department of Biomedical Sciences, University of Sassari, 07100 Sassari, Italy*

Correspondence should be addressed to Giulia Malaguarnera; giulia.malaguarnera@live.it

Received 23 June 2013; Revised 10 September 2013; Accepted 12 September 2013

Academic Editor: Aleksandra Nikolic

Background. Carbohydrate 19.9 antigen (CA19.9) has been used in the diagnosis and followup of gastrointestinal tumours. The aim of this prospective longitudinal study was the evaluation of CA19.9 levels in patients with chronic hepatitis and hepatic cirrhosis hepatitis C virus and B virus correlated. *Materials and Methods*. 180 patients were enrolled, 116 with HCV-related chronic liver disease (48% chronic hepatitis, 52% cirrhosis) and 64 with HBV-related chronic liver disease (86% chronic hepatitis, 14% cirrhosis). Patients with high levels of CA19.9 underwent abdominal ecography, gastroendoscopy, colonoscopy, and abdominal CT scan. *Results.* 51.7% of patients with HCV-related chronic liver disease and 48.4% of those with HBV-related chronic liver disease presented high levels of CA19.9. None was affected by pancreatic or intestinal neoplasia, cholestatic jaundice, or other diseases potentially able to induce Ca19.9 elevations. CA19.9 levels were elevated in 43.3% of HCV chronic hepatitis, in 56.3% of HCV cirrhosis, in 45.1% of HBV chronic hepatitis, and in 58% of HBV cirrhosis. *Conclusions.* CA19.9 commonly increases in the serum of patients with chronic viral hepatitis. Elevation of CA 19.9 is not specific for neoplastic disease and is related to the severity of fibrosis and to the viral aetiology of hepatitis.

1. Introduction

CA19.9 is a glycoprotein expressed by several epithelial cancers, as well as in normal pancreatic and biliary duct epithelia, and it is used currently in the diagnosis and followup of gastrointestinal tumours [1, 2]. High levels of CA19.9 have been observed in patients with gastric adenocarcinoma, in colon, biliary duct, and pancreatic carcinomas [3–6]. Patients affected by chronic diseases such as pancreatitis, renal failure, and chronic liver disease showed a significant reduction of CA19.9 specificity [7]. The CA19.9 immuno-reactivity was observed in bile ductules and interlobular bileducts of non-neoplastic areas surrounding hepatocellular carcinoma [8].

CA19.9 levels increase in non-neoplastic and organ-specific diseases such as acute and chronic pancreatitis, cholelithiasis, cholecystitis, achalasia, acute hepatitis, hepatic cirrhosis, and respiratory diseases and in systemic diseases such as diabetes mellitus and rheumatic and autoimmune disorders. CA19.9 serum levels can be used as marker for the followup of chronic organ-specific inflammations, such as prostatitis [9–16]. An increase in CA19.9 serum levels has been reported in nonneoplastic liver disease such as simple liver cysts, severe steatosis, autoimmune hepatitis, chronic alcoholic hepatitis, and hepatic cirrhosis [16, 17], where CA19.9 levels seem to correlate with the grade of fibrosis and cholestasis [17].

The aim of this study was to evaluate serum CA19.9 levels in a cohort of subjects affected by chronic HCV-correlated (CHC) and HBV-correlated hepatitis (CHB), in order to evaluate whether elevated CA19.9 serum levels can be considered a non casual event and/or could depend on the viral infection (HCV or HBV). We also investigated

the correlation between CA19.9 serum levels and the severity of the liver disease.

2. Methods and Materials

2.1. Patients. Eligible patients for this prospective longitudinal study were those who were 18 years of age or older, were infected by HCV genotype 1b (as determined with the use of the INNO-LiPA assay), and had a quantifiable (>6.90E + 07 IU/mL) serum HCV RNA level (as determined by polymerase chain reaction, COBAS AmpliPrep/COBAS TaqMan—ROCHE) and those who were infected by HBV, with positivity to HBsAg (as determined with CLIA technique) and quantifiable HBV DNA serum level (as determined with the use of PCR-based analysis). Both HCV- or HBV-infected populations must had elevated serum alanine transaminase levels and findings on liver biopsy consistent with chronic infection. Cirrhotic patients had to have a Child-Pugh score less than 7 to be eligible. Ineligible patients were those who had other liver diseases, as well as those who were affected by cancer, severe jaundice, pulmonary and renal chronic diseases, prostatic diseases, autoimmune diseases, and diabetes mellitus. None of the patients made excessive use of alcohol (>20 g/die) or hepatotoxic drugs. Study recruitment was performed in observation and respect of Helsinki Declaration. All patients gave their informed consent for the study participation and for each invasive procedure they underwent. All sensitive data were collected and protected in respect of present privacy statements. From November 2007 to January 2009, 180 eligible patients have been enrolled (108 males, 72 females). The entire cohort is split into two groups depending on the viral aetiology: Group 1 contains HCV-infected subjects (74 males, 42 females; mean age 54, range 35–73 years); Group 2 contains HBV-infected subjects (34 males, 30 females; mean age 53, range 34–75 years). Clinical evaluations, hematochemical, virological, instrumental, and histological analysis were performed on these patients.

2.2. Laboratory Analysis. The following serum analyses are reported in details: renal function tests, serum K^+ and Na^+, fasting and postprandial glucose, PSA (prostatic specific antigen) serum assay, AST and ALT (aspartate aminotransferase and alanine aminotransferase), γGT (gamma glutamil tranferase), alkaline phosphatase, total, conjugated and unconjugated bilirubin, cholinesterase, serum proteins, prothrombin, fibrinogen, and prothrombin time (PT) analysis were performed. Chemical and physical urine exam was also performed. All patients underwent a complete virological assay for HBV and HCV. HBsAg (hepatitis B surface antigen), anti-HBc IgG (hepatitis B "core" IgG antibody), HBeAg (Hepatitis B "e" antigen), HBeAb (hepatitis B "e" antibody), HBV-DNA (hepatitis B virus DNA), anti-Delta (Delta virus antibody) assays were performed. Genomic analysis for HBV-DNA and HBV genotypes was performed using COBAS AmpliPrep and INNOLIPA Genotyping assay. Anti-HCV antibodies were determined by ELISA (Enzyme-Linked immunosorbent assay ELISA assay-Ortho Diagnostic Systems, Raritan, NJ, USA). HCV-RNA (Hepatitis C Virus RNA) levels were detected by polymerase chain reaction (PCR) of HCV-RNA 5′UTR using COBAS AmpliPrep/COBAS TaqMan (Roche Diagnostics Systems, Branchburg, N.J). HCV viral genotypes were determined by restriction analysis of HCV-RNA 5′ UTR, using Simmonds' classification [18]. Anti-nuclear (ANA), anti-mitochondrial (AMA), anti-smooth muscle (SMA), anti-liver/kidney microsome type 1 (LKM1) auto-antibodies were measured using immunofluorescence assay (IFA) and semi-quantitative ELISA immobilizing enzyme test. Thyroid function was evaluated by levels of TSH (Thyroid-Stimulating Hormone) (WHO 2nd IPR 80/558-ECL), free T3 (free-Triiodothyronine) and free T4 (free-Tetraiodothyronine T4) that were determined by immunoradiometric assay (IRMA) and antibodies against thyroid peroxidase and thyroglobulin were measured by IFA. Serum C3 and C4 assay was performed. Serum levels of iron (n.v. 55–160 mg/dL in men, 45–150 mg/dL in women), saturated transferring (n.v. 2–36 g/L), total transferrin (total iron binding capacity, TIBC n.v. 218–411 mg/dL), unsatured transferrin (unsatured iron binding capacity, UIBC n.v. 110–290 mg/dL) and ferritin (n.v. 18–370 ng/mL) were determined, and saturation of transferrin was calculated as: serum level of iron/TIBC × 100 v.n. 0–40. Genetic testing to identify hemochromatosis HFE gene mutations was performed in order to exclude subjects with hereditary hemochromatosis. CA19.9 measurement was performed in all patients by ECL method Elexis COBAS (n.v. 0.0–39.0 UI/mL) using a commercial kit (CA19.9 diagnostic immunoassay-ROCHE) based on company's instructions. The standard cut-off value (100 UI/mL) grants a sensitivity and specificity of 96% and 90%, respectively. All liver function tests, hematochemical and hormonal measurements, and virological analysis have been executed in the laboratory of our hospital with automated and standardized methods, in conformity to the quality certified standards EN ISO 9001 : 2000.

2.3. Histological Assessment of the Liver. Patients underwent ultrasound-assisted percutaneous biopsy: tissue specimens were obtained with Menghini modified needles (automatic aspiration needle for liver biopsy, ACR 16G, 11 cm, manufactured by Sterylab Srl, Milan; Italy). A Specimen 5 cm long and containing at least 6 portal spaces was considered significant. Histological evaluation of the grade of necroinflammatory activity (grading) and fibrosis (staging) of hepatic tissue was carried out using the METAVIR scoring system [19].

Patients who resulted positive to high serum levels of CA19.9 were subjected to perform abdominal and thyroid ecography, thorax radiography, Esophagogastroduodenoscopy (EGD), colonoscopy, and thorax and abdominal spiral TC. Clinical, instrumental, and laboratory investigations allowed to exclude other causes of serum CA19.9 elevation: pancreatic, intestinal, ovarian, mammalian, and prostate tumours, chronic respiratory disease, autoimmune diseases, rheumatic disease, inflammatory bowel diseases, cholestatic jaundice, and hereditary hemochromatosis. Baseline characteristics of the study cohort are shown in Table 1.

Table 1: Baseline characteristics of the study cohort.

Characteristic	Group 1 HCV patients ($N = 116$) N (%)	Group 2 HBV patients ($N = 64$) N (%)	
Sex—n° (%)			
Male	74 (63.8)	34 (53.1)	
Female	42 (36.2)	30 (46.9)	
Age (years)	54 ± 2.3	53 ± 2.6	
Race	caucasian	caucasian	
Body-mass index (Kg/m^2)	26.5 ± 1.0	27.6 ± 1.2	
Blood pressure (sys/dia)—mmHg	128 ± 0.8/84 ± 0.3	132 ± 1.1/81 ± 0.7	
Weight (Kg)	68.5 ± 1.3	71.2 ± 0.6	
AST—IU/L (n.v. 8–18)	63 ± 0.7	73 ± 0.6	
ALT—IU/L (n.v. 8–18)	75 ± 1.2	81 ± 0.8	
γGT—IU/L (n.v. 2–30)	34 ± 1.4	32 ± 1.1	
Cholinesterase—IU/L (n.v. 4900–11900)	5982 ± 102.5	5878 ± 190.3	
Alkaline Phosphatase—IU/L (n.v. 35–100)	86 ± 0.8	89 ± 1.0	
Total bilirubin—mg/dL (n.v. 0.2–1.2)	1.06 ± 0.5	1.07 ± 0.3	
Conjugated bilirubin—mg/dL (n.v. 0.0–0.4)	0.16 ± 0. 2	0.14 ± 0.1	
Viremia			
Mean—log IU/mL	6.40 ± 0.86	6.31 ± 0.92	
Genotype	1b (100)	D	39 (81.2)
		A	4 (8.3)
		D + A	2 (4.2)
		D + F	2 (4.2)
		D + F + A	1 (2.1)
Fasting glucose—mg/dL (n.v. 74–106)	86 ± 1.3	79 ± 1.5	
Serum urea—mg/dL (n.v. 6–40)	42 ± 2.1	39 ± 2.3	
Serum creatinin—mg/dL (n.v. 0.7–1.3)	0.7 ± 0.1	0.6 ± 0.2	
Serum proteins—mg/dL (n.v. 6–8)	7.1 ± 0.6	7.4 ± 0.3	
Fibrinogen—mg/dL (n.v. 200–400)	325 ± 10.3	316 ± 11.5	
Prostatic Specific Antigen—ng/mL (n.v. < 0.4)	1.3 ± 0.7	1.8 ± 0.5	
ANA, AMA, SMA, LKM1	Negative	Negative	
C3-C4—mg/dL	91 ± 1.6	89 ± 1.9	
PLTs count-cell/mm^3	218 ± 19 × 10^3	216 ± 21 × 10^3	
Prothrombin time-sec	10 ± 0.3	9.8 ± 0.2	
Prothrombin-%	112 ± 0.9	104 ± 1.3	
INR—% (n.v. 0.9–1.2)	1.2 ± 0.2	1.1 ± 0.6	
Child-Pugh score	≤5	≤5	
CA19.9—IU/mL (v.n. < 39)	76.8 ± 42.3	78.8 ± 41.6	

Values are expressed as the mean ± SD. The body-mass index is the weight in kilograms divided by the square of the height in meters.
* Viremia stands for quantitative HCV-RNA in Group 1 and HBV-DNA in Group 2 respectively.

3. Statistical Analysis

Continuous variables have been presented with mean values ± standard deviation (SD). Dichotomic variations will be expressed as frequencies, and significance was examined by a nonparametric statistical method (Mann-Whitney U Test). $P < 0.05$ was considered statistically significant.

4. Results

In group 1 (HCV infected subjects), none of patients (0/116; 0%) was found to have METAVIR score F0; 56/116 (48.3%) patients resulted affected by chronic hepatitis (CH, METAVIR F1–F3) and 60/116 (51.7%) by hepatic cirrhosis HCV-correlated (METAVIR F4). 60/116 (51.7%)

Table 2: Distribution of patients with elevated serum Ca19.9 according to METAVIR score.

METAVIR*	Group 1 HCV patients ($N = 60$) N (%)	Group 2 HBV patients ($N = 31$) N (%)
F1–F3	26 (43.3)[A]	14 (45.2)[B]
F4	34 (56.7)[C]	17 (54.8)[D]
total	60 (51.7)[E]	31 (48.4)[F]

P values**: A vs B = ns; C vs D = ns; A vs C ≤0.05, B vs D ≤0.05 and E vs D ≤0.001

*Liver biopsy specimens were assessed by local pathologist for histology status and reviewed by one expert pathologist, blinded about specimens group assignment.

**P was calculated using a non parametric test (Mann-Whitney U test).

patients presented high serum levels of CA19.9 (mean value 76.8 UI/mL, SD = 42.3 UI/mL); 26/60 (43.3%) patients with score from F1 to F3; 34/60 (56.7%) with score F4 (cirrhosis). In group 2 (HBV infected subject), all patients were HBeAg negative, anti-HBe positive, and anti-Delta negative; HBV-DNA was detectable in 48/64 (75%) patients. D genotype was found in 39/48 (81.2%) cases, genotype A in 4/48 (8.3%), genotype D + A in 2/48 (4.2%), genotype D + F in 2/48 (4.2%), genotype D + F + A in 1/48 (2.1%). 33/64 (51.7%) patients showed METAVIR F0; 14/64 (21.9%) showed METAVIR F1-F3 (CH); 17/64 (26.6%) showed METAVIR F4 (cirrhosis). In this group, all patients with score ≥ F1 (31/64; 48.4%), showed high serum levels of CA19.9 (mean value 78.8 UI/mL, SD = 41.6 UI/mL). No patients were found with F0 score in group 1 as well as no increase of CA19.9 serum level was observed in patients with METAVIR score F0 in group 2 (33/64; 51.7%). Our results showed that the increase of CA19.9 serum levels in patients with hepatic cirrhosis is statistically significant ($P < 0.05$) in comparison to CA19.9 increase in patients with chronic hepatitis, in both groups 1 and 2 (Tables 1 and 2). Furthermore, our results show a highly significant difference ($P < 0.001$) about the increase of CA19.9 serum levels considering the viral aetiology (HCV versus HBV) of the liver damage when a comparison is made between the overall amount of patients with elevated CA19.9 serum levels in both groups.

5. Discussion

Our data have shown that high levels of CA19.9 are a frequent event in viral chronic hepatitis HCV- and HBV-related diseases, 51.7% and 48.4%, respectively. They often cannot be considered as a sign of neoplastic disease and are statistically correlated with the severity of the disease ($P < 0.05$) and with an increase of the fibrotic process. In fact, elevations of CA19.9 serum levels can be secondary to the necroinflammatory processes, to small bile ducts alterations, to the presence of regeneration nodules, and to the hyper production of raw collagen, which all are typical expression signs of chronic hepatitis progression to liver cirrhosis.

A number of studies have investigated the clinical utility of CA19.9 in diagnosing pancreatic cancer, cholangiocarcinoma, and other malignancies [20, 21]. Previous studies have shown that serum CA19.9 levels are also elevated in a broad range of benign and malignant conditions, including inflammatory bowel disease, rheumatoid arthritis, pancreatitis, achalasia, heavy tea consumption, Sjogren's syndrome, Hashimoto's thyroiditis, cholangiocarcinoma, colorectal, hepatocellular, esophageal, and lung and ovarian carcinomas [21–23].

CA19.9 is a mucinic type glycoprotein that is present only in traces in serum and is normally absent in other tissues such as pulmonary epithelium, perialveolar interstitial space, and liver. It is reasonable that any noxa (viral or toxic) which is able to promote tissue inflammatory damage and, sequentially, reparative features with fibrotic tissue deposition and parenchymal regeneration (as it happens in chronic liver disease, with intra- and interacinar fibrosis, nodular regeneration, and biliary neoductulation) can induce CA19.9 synthesis [24]. CA19.9 immunoreactivity was observed in cell membranes facing biliary canaliculi and in biliary ductules of hepatic bioptic specimens of patients with chronic hepatitis and liver cirrhosis [8]. Immunohistochemical analysis for CA19.9 showed high reactivity in hepatic inflammatory areas, in particular, in bile ductule cells and hepatocytes in ductular metaplasia, suggesting that these cells can be involved in CA19.9 synthesis, and its serum levels increase [8, 25–27].

The first outcome of our study is that it is necessary to carefully evaluate the use of CA19.9 as a tumoral marker in the presence of a chronic liver disease, because a high percentage of false positives can occur. Our data also focused on the possibility to use CA19.9 as indirect marker of hepatic fibrosis.

Some works in the literature report a statistically significant correlation between CA19.9 serum levels and some standard parameters of hepatic function: a positive correlation can be shown with levels of AST, ALT, alkaline phosphatase and bilirubin [17]. Other studies showed a correlation between CA19.9 (alone or together with CA 125) and the grade of hepatic fibrosis. In these studies two groups of patients have been examined, one with a F3-F4 METAVIR score (portal fibrosis without septa, or septal without cirrhosis) and one with a F4 METAVIR score (severe septal fibrosis with cirrhosis). CA19.9 serum levels (alone or together with other serum markers) can be used to individuate patients with severe fibrosis and cirrhosis [28].

Transaminases have been the first indirect hepatic fibrosis markers. They have been eventually associated to each other in the aspartate aminotransferase/alanine aminotransferase ratio (AAR) index [28]. Wai and other authors have proposed a further evolution of AAR index, by combining AST to platelet count [aspartate aminotransferase platelet ratio index (APRI)] [29–33].

6. Conclusion

The increase of CA19.9 serum levels are frequent in chronic viral hepatitis. In our population of patients with viral chronic hepatitis and cirrhosis, CA19.9 serum levels elevation does

not indicate a contemporary neoplastic disease, but correlates in a statistically significant way ($P < 0.05$) with the grade of liver fibrosis, appearing to be more evident in patients with higher fibrosis score, thus correlating with the severity of the liver disease. A previous study showed similar results but was conducted on subjects with HCV and did not evaluate subject with HBV [34–36]. A novelty in this study could be represented by the elevation of CA19.9 serum levels that seems to be related to the viral aetiology, showing a high statistical significance when HCV-infected are compared to the HBV-infected patients ($P < 0.001$). This could be explained by a more fibrogenic property of HCV than HBV, but more researches must be conducted to better assess the specific role of the virus for Ca19.9 neosynthesis, while a direct interaction between HCV proteins and hepatic stellate cells (HSCs) may contribute to HCV-induced liver fibrosis. Further investigations may clarify if CA19.9 can assume the role of indirect marker of hepatic fibrosis and be not only as neoplastic biomarker.

We propose that CA19.9 could be used in the combinations with the other markers already in use, in order to increase the diagnostic accuracy of the available tests, rising both the positive (PPV) and the negative (NPV) predictive values.

Conflict of Interests

The authors declare that they have no competing interests. GM was supported by the International Ph.D. programme in Neuropharmacology, University of Catania.

References

[1] Y. Motoo, Y. Satomura, I. Mouri et al., "Serum levels of pancreatitis-associated protein in digestive diseases with special reference to gastrointestinal cancers," *Digestive Diseases and Sciences*, vol. 44, no. 6, pp. 1142–1147, 1999.

[2] M. F. Plemenos, C. Dimas, A. Kotsios, K. Gennatas, and A. Kondi-Pafiti, "Prognostic significance of the immunohistochemical localization and serological detection of CA19-9 tumor antigen in colon carcinoma," *Journal of B.U.ON*, vol. 9, no. 1, pp. 73–76, 2004.

[3] K. Markocka-Maczka, "Ca 19-9 antigen in differentiation of pancreatic inflammatory and neoplastic tumors," *Wiadomosci Lekarskie*, vol. 56, no. 11-12, pp. 537–540, 2003.

[4] M. Ducreux, V. Boige, and D. Malka, "CA 19-9 and pancreatic carcinoma, a revival?" *Onkologie*, vol. 30, no. 1-2, pp. 12–13, 2007.

[5] A. Nouts, P. Lévy, H. Voitot, and P. Bernades, "Diagnostic value of Ca 19-9 antigen in patients with chronic pancreatitis or pancreatic adenocarcinoma: effects of complications," *Gastroentérologie Clinique et Biologique*, vol. 22, no. 2, pp. 152–159, 1998.

[6] N. Tanaka, S. Okada, H. Ueno, T. Okusaka, and M. Ikeda, "The usefulness of serial changes in serum CA19-9 levels in the diagnosis of pancreatic cancer," *Pancreas*, vol. 20, no. 4, pp. 378–381, 2000.

[7] J. Nowak, D. Jakubowska, A. Wiczkowski et al., "Carbohydrate antigens CA 19-9, CA 242, CA 50 in liver diseases," *Wiadomości Lekarskie*, vol. 51, no. 11-12, pp. 484–491, 1998.

[8] Y. Kitagawa, M. Iwai, A. Muramatsu et al., "Immunohistochemical localization of CEA, CA19-9 and DU-PAN-2 in hepatitis C virus-infected liver tissues," *Histopathology*, vol. 40, no. 5, pp. 472–479, 2002.

[9] O. Uygur-Bayramiçli, R. Debak, E. Orbay et al., "Type 2 diabetes mellitus and CA 19-9 levels," *World Journal of Gastroenterology*, vol. 13, no. 40, pp. 5357–5359, 2007.

[10] É. Szekanecz, Z. Śandor, P. Antal-Szalmás et al., "Increased production of the soluble tumor-associated antigens CA19-9, CA125, and CA15-3 in rheumatoid arthritis: potential adhesion molecules in synovial inflammation?" *Annals of the New York Academy of Sciences*, vol. 1108, pp. 359–371, 2007.

[11] R. Safadi, M. Ligumsky, E. Goldin, Y. Ilan, Y. S. Haviv, and S. Nusair, "Increased serum CA 19-9 antibodies in Sjogren's syndrome," *Postgraduate Medical Journal*, vol. 74, no. 875, pp. 543–544, 1998.

[12] E. Giannini, P. Borro, F. Botta et al., "Cholestasis is the main determinant of abnormal CA 19-9 levels in patients with liver cirrhosis," *International Journal of Biological Markers*, vol. 15, no. 3, pp. 226–230, 2000.

[13] K. H. Park, J. S. Kim, J. H. Lee et al., "Significances of serum level and immunohistochemical stain of CA19-9 in simple hepatic cysts and intrahepatic biliary cystic neoplasms," *The Korean Journal of Gastroenterology*, vol. 47, no. 1, pp. 52–58, 2006.

[14] X. Vandemergel, F. Vandergheynst, and G. Decaux, "Very high elevation of CA19-9 level in a patient with steatosis," *Acta Gastro-Enterologica Belgica*, vol. 68, no. 3, pp. 380–381, 2005.

[15] M. Montalto, L. Santoro, M. Vastola et al., "Normalisation of high CA 19-9 values in autoimmune hepatitis after steroidal treatment," *International Journal of Immunopathology and Pharmacology*, vol. 18, no. 3, pp. 603–607, 2005.

[16] E. De Goede and S. H. Yap, "An exceptional high concentration of serum CA 19.9 in a patient with alcoholic liver disease," *Gut*, vol. 41, no. 4, pp. 579–580, 1997.

[17] S. Maestranzi, R. Przemioslo, H. Mitchell, and R. A. Sherwood, "The effect of benign and malignant liver disease on the tumour markers CA19-9 and CEA," *Annals of Clinical Biochemistry*, vol. 35, no. 1, pp. 99–103, 1998.

[18] P. Simmonds, A. Alberti, H. J. Alter et al., "A proposed system for the nomenclature of hepatitis C viral genotypes," *Hepatology*, vol. 19, no. 5, pp. 1321–1324, 1994.

[19] P. Bedossa and T. Poynard, "An algorithm for the grading of activity in chronic hepatitis C. The METAVIR Cooperative Study Group," *Hepatology*, vol. 24, no. 2, pp. 289–293, 1996.

[20] T. Kodama, H. Satoh, H. Ishikawa, and M. Ohtsuka, "Serum levels of CA19-9 in patients with nonmalignant respiratory diseases," *Journal of Clinical Laboratory Analysis*, vol. 21, no. 2, pp. 103–106, 2007.

[21] W. Steinberg, "The clinical utility of the CA 19-9 tumor-associated antigen," *American Journal of Gastroenterology*, vol. 85, no. 4, pp. 350–355, 1990.

[22] A. Andriulli, T. Gindro, P. Piantino et al., "Prospective evaluation of the diagnostic efficacy of CA 19-9 assay as a marker for gastrointestinal cancers," *Digestion*, vol. 33, no. 1, pp. 26–33, 1986.

[23] G. Bertino, A. Ardiri, M. Malaguarnera, G. Malaguarnera, N. Bertino, and G. S. Calvagno, "Hepatocellualar carcinoma serum markers," *Seminars in Oncology*, vol. 39, pp. 410–433, 2012.

[24] M. Schöniger-Hekele and C. Müller, "The combined elevation of tumor markers CA 19-9 and CA 125 in liver disease patients is highly specific for severe liver fibrosis," *Digestive Diseases and Sciences*, vol. 51, no. 2, pp. 338–345, 2006.

[25] G. Malaguarnera, I. Paladina, M. Giordano, M. Malaguarnera, G. Bertino, and M. Berretta, "Serum markers of intrahepatic cholangiocarcinoma," *Disease Markers*, vol. 34, pp. 219–228, 2013.

[26] G. Malaguarnera, M. Giordano, I. Paladina et al., "Markers of bile duct tumors," *World Journal of Gastrointestinal Oncology*, vol. 3, pp. 49–59, 2011.

[27] G. Malaguarnera, M. Giordano, I. Paladina, M. Berretta, A. Cappellani, and M. Malaguarnera, "Serum markers of hepatocellular carcinoma," *Digestive Diseases and Sciences*, vol. 55, no. 10, pp. 2744–2755, 2010.

[28] E. Giannini, D. Risso, F. Botta et al., "Validity and clinical utility of the aspartate aminotransferase-alanine aminotransferase ratio in assessing disease severity and prognosis in patients with hepatitis C virus-related chronic liver disease," *Archives of Internal Medicine*, vol. 163, no. 2, pp. 218–224, 2003.

[29] C.-T. Wai, J. K. Greenson, R. J. Fontana et al., "A simple noninvasive index can predict both significant fibrosis and cirrhosis in patients with chronic hepatitis C," *Hepatology*, vol. 38, no. 2, pp. 518–526, 2003.

[30] N. V. Chrysanthos, G. V. Papatheodoridis, S. Savvas et al., "Aspartate aminotransferase to platelet ratio index for fibrosis evaluation in chronic viral hepatitis," *European Journal of Gastroenterology and Hepatology*, vol. 18, no. 4, pp. 389–396, 2006.

[31] F. Imbert-Bismut, V. Ratziu, L. Pieroni, F. Charlotte, Y. Benhamou, and T. Poynard, "Biochemical markers of liver fibrosis in patients with hepatitis C virus infection: a prospective study," *The Lancet*, vol. 357, no. 9262, pp. 1069–1075, 2001.

[32] K. A. Gebo, H. F. Herlong, M. S. Torbenson et al., "Role of liver biopsy in management of chronic hepatitis C: a systematic review," *Hepatology*, vol. 36, no. 5 I, pp. S161–S172, 2002.

[33] R. Bataller, Y.-H. Paik, J. N. Lindquist, J. J. Lemasters, and D. A. Brenner, "Hepatitis C virus core and nonstructural proteins induce fibrogenic effects in hepatic stellate cells," *Gastroenterology*, vol. 126, no. 2, pp. 529–540, 2004.

[34] G. Bertino, A. M. Ardiri, P. Boemi et al., "Meaning of elevated CA 19-9 serum levels in chronic hepatitis and HCV-related cirrhosis," *Minerva Gastroenterologica e Dietologica*, vol. 53, no. 4, pp. 305–309, 2007.

[35] T. Stroffolini, A. Spadaro, V. Di Marco et al., "Current practice of chronic hepatitis B treatment in Southern Italy," *European Journal of Internal Medicine*, vol. 23, pp. 124–127, 2012.

[36] G. Bertino, A. Ardiri, P. M. Boemi et al., "Epoetin alpha improves the response to antiviral treatment in HCV-related chronic hepatitis," *European Journal of Clinical Pharmacology*, vol. 66, pp. 1055–1063, 2010.

Hindawi Publishing Corporation
BioMed Research International
Volume 2013, Article ID 726239, 11 pages
http://dx.doi.org/10.1155/2013/726239

Review Article

Immune Monitoring in Cancer Vaccine Clinical Trials: Critical Issues of Functional Flow Cytometry-Based Assays

Iole Macchia, Francesca Urbani, and Enrico Proietti

Department of Hematology, Oncology and Molecular Medicine, Istituto Superiore di Sanità, 00161 Rome, Italy

Correspondence should be addressed to Iole Macchia; iole.macchia@iss.it

Received 20 June 2013; Accepted 19 August 2013

Academic Editor: Jelena Urosevic

The development of immune monitoring assays is essential to determine the immune responses against tumor-specific antigens (TSAs) and tumor-associated antigens (TAAs) and their possible correlation with clinical outcome in cancer patients receiving immunotherapies. Despite the wide range of techniques used, to date these assays have not shown consistent results among clinical trials and failed to define surrogate markers of clinical efficacy to antitumor vaccines. Multiparameter flow cytometry- (FCM-) based assays combining different phenotypic and functional markers have been developed in the past decade for informative and longitudinal analysis of polyfunctional T-cells. These technologies were designed to address the complexity and functional heterogeneity of cancer biology and cellular immunity and to define biomarkers predicting clinical response to anticancer treatment. So far, there is still a lack of standardization of some of these immunological tests. The aim of this review is to overview the latest technologies for immune monitoring and to highlight critical steps involved in some of the FCM-based cellular immune assays. In particular, our laboratory is focused on melanoma vaccine research and thus our main goal was the validation of a functional multiparameter test (FMT) combining different functional and lineage markers to be applied in clinical trials involving patients with melanoma.

1. Introduction

The primary objective of immune monitoring in cancer vaccine clinical trials is to find a correlation between the efficient induction of tumor-specific T-cell responses and clinical efficacy, due to the importance of the host immune system in controlling tumor progression. However, although in several cancer vaccine trials there is indication of increased frequency of tumor-specific T-cells, no validated biomarkers exist for cancer immunotherapy as yet [1].

One reason for the lack of correlation between the immune parameters measured and objective clinical response might be the complexity of the immune responses required for a successful tumor eradication which cannot be dissected through the most frequently used T-cell assays.

Antitumor cell-mediated immunity is a key biomarker for most vaccines and immunotherapies and involves the activity of specialized cells including antigen specific cytotoxic T lymphocytes (CTLs) [2] and $CD4^+$ helper T lymphocytes [3] as well as components of innate immunity such as macrophages, dendritic cells (DC), natural killer cells (NK), and granulocytes.

In addition, since the success of immune response against cancer is due to the balance between the effector and the suppressive compartments, immunological monitoring should also include analysis of immune suppressive cells (ISCs) such as regulatory T-cells (TREGs), myeloid-derived suppressor cells (MDSCs), and tumor-associated macrophages (TAMs) [4–6]. These cells play an important role in cancer progression and responses to immunotherapy. However, due to their tremendous phenotypic and functional heterogeneity, their usefulness as biomarkers of outcome or response to therapy has to await for further development of monitoring assays that better reflect their biologic significance in cancer.

In addition, a recent report [7] indicates that regulatory B cells (BREGs), a small subset of suppressor cells, may have profound effects on the development of T-cell responses,

further complicating the interpretation of antitumor immune suppression in disease.

Local and systemic antitumor immune responses can show markedly different patterns and many functional responses could be missed when only peripheral blood lymphocytes (PBLs) and not tumor infiltrating lymphocytes (TILs) are evaluated; therefore, more emphasis should be put on immune monitoring also at the effector site by taking a biopsy of a metastatic lesion [8]. To this end, the concept of "Immunoscore," initially described for colorectal cancer patients, has been recently introduced as an essential prognostic and potentially predictive tool to classify cancers, beside the traditional tumor staging classification (AJCC/UICC-TNM) [9–13]. This parameter might facilitate clinical decision making including rational stratification of patient treatment. Usually the immunoscore approach refers to the analysis of the location, density, and functional orientation of different immune cell populations infiltrating the tumor, including macrophages, DC, mast cells, NK cells, naïve and memory lymphocytes, B cells, and T lymphocytes (which include various subsets of T-cell: T_H1, T_H2, T_H17, regulatory T-cells (T_{REGS}), T follicular helper cells (T_{FH}), and cytotoxic T-cells). Such "immune contexture" annotated in a large collections of human tumors has allowed the identification of components that are beneficial for patients and those that are deleterious [14]. For instance, in a study by Pagès et al. [15], high densities of T-cells ($CD3^+$), cytotoxic T-cells ($CD8^+$), and of memory T-cells ($CD45RO^+$) were clearly associated with a longer disease-free survival (DFS) (after surgical resection of the primary tumour) and/or overall survival (OS).

However, the analysis of tumor microenvironment is not always feasible and the only samples available are those obtained from peripheral blood. Furthermore, sometimes peripheral responses should be of some relevance and could integrate and increase information given by the tumor microenvironment. For this reason, we believe that, in addition to scoring T-cells at tumor sites, the frequency and functions of T-cells circulating in the peripheral blood of cancer patients should be examined as potential biomarkers, by means of validated and standardized immune assays.

Concerning the quality of T-cell response, several papers showed that the multifunctionality of effector cells is an important factor to predict the immunological protection [25]. In particular, it has been demonstrated that the functional profile of HIV-specific $CD8^+$ T-cells in progressors is limited compared to that of nonprogressors, which consistently maintain highly functional $CD8^+$ T-cells and that the frequency and proportion of the HIV-specific T-cell response with highest functionality inversely correlates with viral load in the progressors [26]. In addition, other reports indicated that vaccine-induced multifunctional $CD4^+$ and $CD8^+$ T-cells produce greater amounts of IFN-γ than cells that secrete IFN-γ alone [27].

In the setting of cancer immunotherapy, the induction of polyfunctional NY-ESO-1-specific T-cell responses, following anti-CTLA-4 treatment of metastatic melanoma patients, has been recently shown to enhance T-cell responses and to induce durable clinical responses [28]. Further, a recent paper [29] demonstrated that the triple combination of IFN-γ, IL-2, and TNF-α represents a Th1 pattern of polycytokine secretion with greater antigen sensitivity and superior tumor recognition.

In order to get new insights in exploitation of vaccine-induced polyfunctional T-cells, standardization and validation of multiparameter assays are required.

In this review, we will overview the current technology used for immune monitoring during cancer immunotherapy in melanoma patients, focusing on a polychromatic FCM-based approach for *ex vivo* detection of tumor-antigen specific T lymphocytes producing multiple functional molecules simultaneously. To this aim, we will provide few experimental examples to discuss critical process steps encountered during validation of an FMT developed in our laboratory, consisting of a six-color panel for assessment of polyfunctionality of tumor-specific $CD8^+$ T-cells in cryopreserved human peripheral blood mononuclear cells (PBMCs).

2. Overview of Immunoassays

The objective of any immune monitoring study is to collect interpretable, reliable, and reproducible data for the detection, quantification, and characterization of immune responses directed at specific antigens.

The principal techniques utilized for immune monitoring are reviewed in [30].

Measuring cytokine production and profile represents an integral part of immune monitoring during immunotherapeutic treatments [31]. First-generation immune-monitoring techniques included proliferation and cytotoxicity assays following short-term *in vitro* expansion; more recently, tetramer and Elispot (second-generation assays) allowed to assess directly *ex vivo* the frequency of vaccine specific T-cells and their ability to produce cytokines, usually IFN-γ [32]. However, this type of analyses is limited by the lack of information about the functional state of the cells. In the setting of cancer patients, where tumor escape mechanisms may induce T-cell anergy by altering lymphocyte signalling and effector functions [33], the need for third-generation assays aimed at evaluating the functional properties of rare cell populations of vaccine-induced T-cells with a multiparameter approach is becoming increasingly evident. To this aim, the development of polychromatic flow cytometry for immune monitoring has significantly contributed to progress in the field of human immunology.

In this paper, we will focus on some of the most widely used FCM-based assays for measurement of antigen-specific T-cells. In particular, intracellular cytokine staining (ICS) represents one of the main FCM-based assays and it has been previously validated by Horton et al. and De Rosa et al. [24, 34].

The CD107 mobilization assay measures the exposure of CD107 (LAMP: lysosomal associated membrane protein) a and b, present in the membrane of cytotoxic granules of CTLs, onto the cell surface as a result of degranulation and it can be used as an alternative to ^{51}Cr release assay. In fact, a good correlation has been demonstrated between degranulation

and cytotoxic activity of tumor-specific $CD8^+$ T-cell clones and $CD8^+$ T-cells, as measured in an FCM-based killing assay [35, 36]. Further, CD107-expressing $CD8^+$ T-cells are shown to mediate cytolytic activity in an antigen-specific manner. Soluble major histocompatibility class I tetramers are a widely utilized tool for the direct *ex vivo* detection, characterization, and isolation of antigen-specific T-cells in a variety of clinical settings such as infectious, autoimmune, or neoplastic diseases [37–41].

To provide a more complete assessment of the functionality of $CD8^+$ T-cells expressing cognate T-cell receptors (TCR), measurement of CD107a and b expression can be combined with MHC-class I tetramer labeling and ICS [35].

In order to insure reproducibility and worldwide comparisons for conclusive longitudinal monitoring in multicenter studies, standardized operating procedure (SOPs), as well as standardized reagents and analysis protocols, need to be used [42].

Effective large-scale assay harmonization efforts have already been conducted for commonly used immunological assays of peripheral blood immune cell populations [43, 44].

Advances in multiparameter flow cytometric technologies and reagent applications for characterization and functional analysis of cells modulating the immune network have been recently reviewed in [45].

Researchers from Europe and the United States have started a project called Minimal Information About T-cell Assays (MIATA) [46] to standardize and harmonize commonly used assays such as the enzyme linked immunosorbent spot assay (Elispot) [47] and major histocompatibility complex tetramer assays [48]. The establishment of universally accepted guidelines for performing and presenting immunological assays in scientific publications will create a framework that will allow the comparison of immune responses across clinical trials. Many groups performed also optimization and harmonization of intracellular cytokine assays [49–52].

3. Key Issues Involved in FCM-Based Assays and Development of FMT

Flow cytometry is a powerful and versatile technique, ideal for phenotyping, enumerating, and assessing the function of rare and precisely defined cell subsets at the single cell level. Functions assessed by flow cytometry include cytokine/chemokine production, CD107 expression, multimer analysis, natural cytotoxicity, antibody dependent cell cytotoxicity (ADCC), and proliferation. Critical steps for immune monitoring by flow cytometry which may affect yield, viability, and immunologic function of cells, include shipping blood variables such as temperature [16] and time delay of drawn blood processing, freezing/thawing conditions [17, 19, 51], type of anticoagulant used for blood collection, and type of density-gradient centrifugation used for the isolation of peripheral blood mononuclear cells. Other variables facing multicolor assay depend on antibodies and fluorochromes used, fixation and permeabilization reagents, instrument setup, data acquisition and analysis, reporting of results, internal quality control, external quality assessment, and flow sorting [53] (Table 1).

The importance of *ex vivo* analysis versus *in vitro* analysis has been addressed by [54].

The principal challenge for FCM-based assays for immune monitoring in cancer clinical trials is often due to the need of detecting rare subsets of cells avoiding the spurious positive events. This goal can be achieved by using a multiparameter approach in order to minimize the false positive and negative events by gating and subgating the cells of interest which express multiple markers simultaneously. Other critical issues are represented by *in vitro* T-cell culture methods when immune responses are analyzed in expanded T-cell cultures instead of *ex vivo*. To this aim, optimization of a cell culture method for analysis of polyfunctional T-cells has been previously dissected [55].

By setting up a procedure to assess polyfunctionality of tumor-associated antigen- (TAA-)specific cells in clinical trials, we observed a reduction of cell number at the end of the experiment, probably due to a loss of cells at different steps of cell processing (unpublished data). These observations led us to initiate a set of controlled *in vitro* studies to investigate the impact of different reagents and methods on recovery, viability, and immunological function of cells.

Our final goal was the optimization and validation of a reliable method, which we named FMT, for assessment of antigen specificity and effector functions against the melanocyte differentiation antigen Melan-A/MART-1. This protocol, adapted from [56], was based on a six-color panel combining CD8, MHC-tetramer, CD107a, and intracellular cytokine staining for three soluble factors with distinct properties (CD107, TNF-α, and IL-2), in response to the peptide Melan-A/MART-1 or other stimuli.

In previous experiments, based on previous reports indicating that different fixation/permeabilization buffers may affect the results of intracellular cytokine detection [21], we performed the FMT for CD107, TNF-α, and IL-2, after stimulation with *Staphylococcus* Enterotoxin B (SEB) and PHA and we compared two distinct standardized commercial lysing/permeabilization buffers: the Lysing/Perm solutions and the Intrasure kit (both purchased from BD Biosciences) (Figure 1).

Overall, we found that the fixation/permeabilization with the Intrasure kit resulted in a stronger response for all the parameters analyzed and that stimulation with SEB yielded the higher percentages of $CD8^+$ T-cells producing one, two, or three factors (Figure 1). Based on these results, we decided to use in our next experiments the Intrasure permeabilization kit and SEB as positive control.

Next, we investigated the impact of DNAse, which is usually used to digest extracellular DNA and reduce cellular clumping, on cell recovery and viability as well as its effect on cell function (Table 2).

Compared to previous reports [20] facing this issue, we try to keep the DNAse during the all steps of the FMT procedure, from thawing to culturing, even during washing steps.

Our results indicated that using DNAse after thawing PBMCs samples and during the entire procedure increased

Table 1

Critical issue		References
Blood collection, shipment, and processing	Temperature of storage	[16]
	Time from blood draw to sample processing	[17, 18]
	Freezing/thawing conditions	[19]
DNAse during culture		[20]
Perm/lysing reagents		[21]
Flow cytometric issues	Antibodies and fluorochromes	[22, 23]
	Spectral overlap and color compensation Instrument setup	
	Data acquisition and analysis	[24]

Table 2

	w/o DNAse NT	w/o DNAse SEB	w/o DNAse MART-1
% of $CD8^+$ $MART\text{-}1^{+*}$	0.0036	0.0039	0.0046
Number of $CD8^+$ $MART\text{-}1^{+¶}$	34	29	38
	DNAse in culture NT	DNAse in culture SEB	DNAse in culture MART-1
% of $CD8^+$ $MART\text{-}1^+$	0.013	0.0081	0.0077
Number of $CD8^+$ $MART\text{-}1^+$	129	80	75
	DNAse always NT	DNAse always SEB	DNAse always MART-1
% of $CD8^+$ $MART\text{-}1^+$	0.015	0.017	0.011
Number of $CD8^+$ $MART\text{-}1^+$	143	153	103

*Percentage or ¶number of cells as assessed in an FMT assay, performed on PBMCs from healthy donors, treated and labeled as in Figure 1, with the addition of HLA-A2/peptide tetramer staining at the beginning of culture (HLA-A2∗0201 peptide phycoerythrin (PE) tetrameric complexes specific for the Melan-A/MART-1 antigen).

the absolute number and percentages of $CD8^+$/MART-1+ cells as shown in Table 2 that summarizes the effect of DNAse on cell recovery at the end of FMT, by enumerating TAA-specific (Melan-A/MART-1) $CD8^+$ T-cells in the presence or not of DNAse (DN25- SIGMA).

Soluble tetrameric MHC/peptide complexes have opened the possibility to directly identify and monitor antigen-specific $CD8^+$ T-cells at the tumor site and in blood [40]. Multiparameter monitoring of antigen-specific T-cell responses that combines *ex vivo* tetramer staining with various phenotyping and functional assays provides a novel approach to assess the functional potential of tumor-specific T lymphocytes and may also facilitate the optimization of vaccination protocols.

Dextramers are multimers based on a dextran backbone bearing multiple fluorescein and streptavidin moieties, used for the analysis of relatively low frequency antigen-specific T-cells in peripheral blood. The functionality and optimization of dextramers have been previously demonstrated on human $CD8^+$ T-cell clones with four independent antigen specificities [57].

Staining of a $CD8^+$ line from a healthy donor with either MART-1-specific tetramers or pentamers or dextramers shows that dextramers produce a stronger signal against Melan-A antigen and a lower background signal than their tetramer and pentamer counterparts (Figure 2). Thus, dextramers could become the reagents of choice as the antigen-specific T-cell labeling transitions from basic research to clinical application.

Finally, validation of the FMT for analysis of the functionality of T-cells directly *ex vivo* was performed on a melanoma patient with discrete percentage of $CD8^+$ $MART\text{-}1^+$ specific T-cells.

In this assay, we evaluated the production of multiple cytokines (IFNα, TNFγ, and IL-2) and upregulation of LAMP-1 (CD107a) by tumor- (Melan-A/MART-1) specific T-cells. (Figures 3(a) and 3(b)).

On our side, our FMT experiments were acquired on a BD-Canto instrument by DIVA software. We chose to analyze them by a classical approach, using a standard software dedicated to flow cytometry analysis, Flow Jo (Treestar, MA, USA) and generating graphical representation by Excel (Microsoft, WA, USA) elaboration. Gating strategy might have a potential impact on the analysis of antigen-specific polyfunctional T-cell responses. In our setting, our population of interest was defined meeting the criteria of a lymphocyte morphology, based on forward- and side-scatter parameters, singlet morphology, based on forward height scatter and forward area

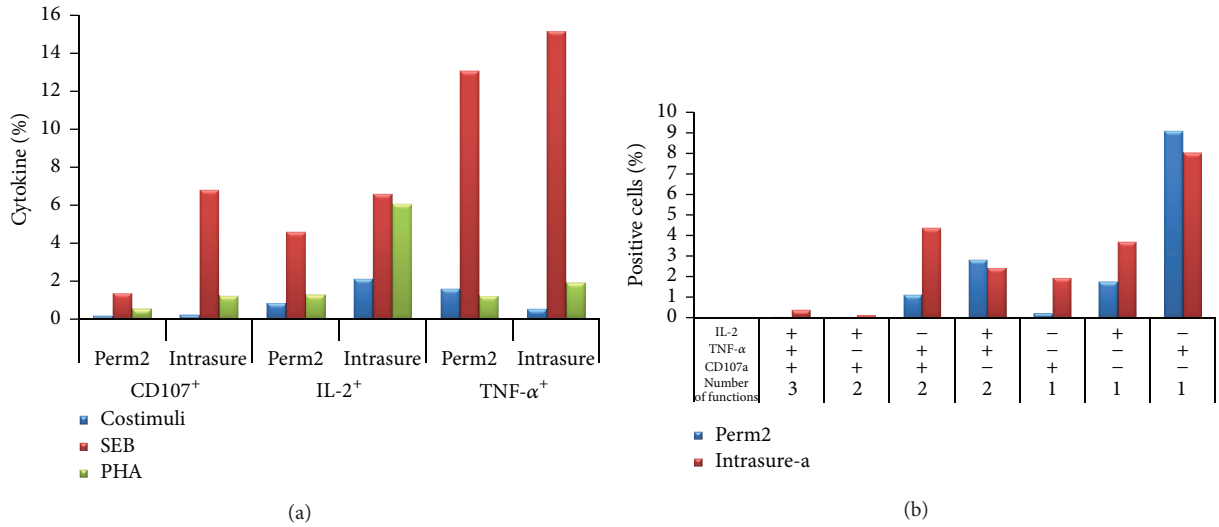

Figure 1: Comparison of intracellular and cell surface markers after treatment of cells with two different fixation/permeabilization buffers. Assessment of cytokine secretion and cytotoxic factor expression in $CD8^+$ T-cells. Briefly, thawed PBMC from a healthy donor was cultured (1 hour at 37°C) in presence of anti-CD107a and *Staphylococcus* enterotoxin B (SEB; Sigma-Aldrich, Munich, Germany, used at 2 μg/mL) or PHA (HA16, Murex Biotech, Dartford, UK, used at 1.5 μg/mL) in presence of costimulatory antibodies (CD28 and CD49d). After the addition of brefeldin A (Golgi Plug) and monensin (Golgi stop) (Becton Dickinson, San Jose, CA, USA), cells were incubated for additional 5 hours. Following stimulation, final 2 mM EDTA was added to each well and incubated for 15 minutes. Cells were then incubated for 30 min at 4°C with surface antibodies (CD8), fixed, and permeabilized with the previously mentioned lysing/permeabilization buffers and stained with fluorescently labelled antibodies directed against IL-2 and TNF-α. Samples were then acquired on a FacsCanto flow cytometer instrument (BD Biosciences) and analyzed by FACSDiva and/or FlowJo software (Tree Star, Ashland). (a) Bar graph showing the percentages of total $CD107a^+$, TNF-α^+, and IL-2^+ analyzed within $CD8^+$ gated cells. (b) Bar graph showing the polyfunctionality of $CD8^+$ T-cells upon SEB stimulation (Boolean analysis). As negative controls, we included untreated cell (only costimuli).

scatter, positivity of surface antigen expression (tetramer and CD8). Expression of 4 parameters, CD107a and the intracellular cytokines, IL-2, IFN-γ, and TNF-α, was simultaneously investigated by a 6-colors staining to assess polyfunctionality of the gated population. This sequential gating strategy is shown in Figure 3(a), along with some bidimensional plots showing some of the possible representation of parameters under study.

The possible combinations of positivity/negativity of these 4 parameters generate a large number of variables (30 for each sample). An effective way to give a graphic representation of such a lot of variables is to use histograms and pie chart (Figure 3(b)). Pie charts give a quick shot of the proportion of responding cells producing one or more functions without specifying which is the particular function [58]. We drew these graphics by elaborating FlowJo results export using a standard Excel (Microsoft, WA, USA) worksheet, adapting the Simplified Presentation of Incredibly Complex Evaluations software's approach (SPICE, Version 2.9, Mario Roederer, Vaccine Research Center, NIAID, NIH), one of the most largely utilized free Apple Mac-based data mining software [54, 58, 59].

4. Tools and Software for Analysis of Flow Cytometric Data

Traditional methods to analyze flow cytometric data involve gating of populations in one- or two-dimensional displays and manually selecting populations of interest. However, such methods are highly subjective and time consuming. Particularly, with the advent of multiple lasers flow cytometry analyzer, it is possible to have up to 18 colors of fluorescence detection simultaneously in the same sample. This leads to an enormous amount of variables, due to the all possible combinations of each parameter acquired. So that, critical is the analysis approach: bioinformatics will be surely the way to manage this kind of data in the next future. Looking back to the classical way to analyze FCS files, by manual, sequential gating, in the past years an enormous number of dedicated software has been developed by industries and academies (most of these last being freeware) [60].

Just to cite the most common among them, BD-DIVA, Miltenyi-MACSQuantify, Millipore-GuavaSuite, (acquisition and analysis commercial software, being interfaces of flow cytometer), FlowJo (one of the most common analyser software for flow cytometry), BeckmanCoulter-Kaluza, Weasel (commercial analysis software), and WinMDI, (free academic analysis software); each of them is endowed with peculiar tools and utility.

A detailed list of cytometry software and educational materials in cytometry is provided by the "original cytometry software catalog," developed and managed by Dr. Eric Martz and by the Purdue University Cytometry Laboratories (http://www.cyto.purdue.edu/flowcyt/software/Catalog.htm).

Reviewing the new computational approach of analysis, often based on automated gating and high level of statistical

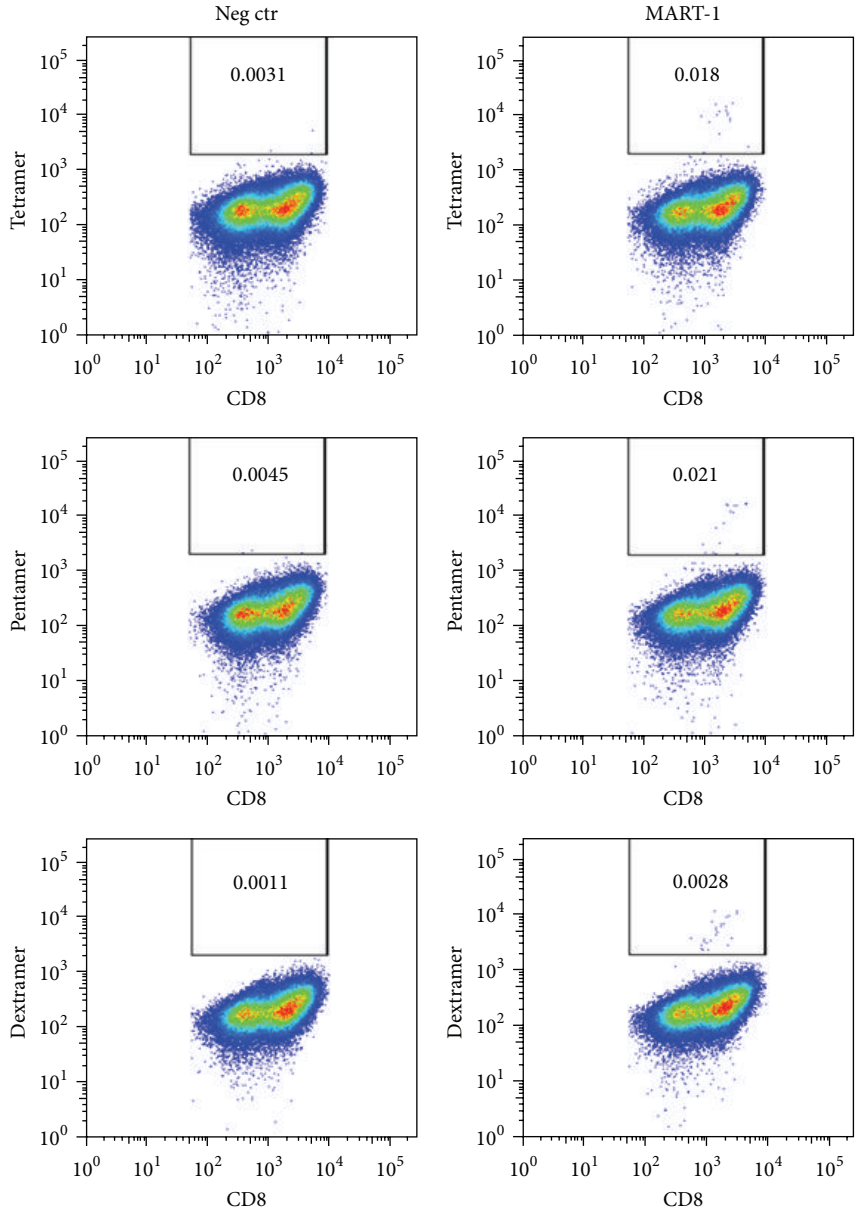

Figure 2: Comparison of different MHC multimers for detection of antigen-specific T-cells: dot plots representing percentages of $CD8^+$ $MART\text{-}1^+$ $tetramer^+$/$pentamer^+$/$dextramers^+$ cells, analyzed within the singlets-live gate of a $CD8^+$ expanded line obtained from a healthy donor.

analysis and representation output, several groups have developed different strategies.

Among them, open source tools like Bioconductor flowFlowJo, able to extracting information from a FlowJo workspace and deliver the data into *R* (one of the most common statistical processor) in the flowCore paradigm, have been developed to allow the management of high throughput data [61].

Probability binning algorithm extensively described by Roederer et al. in [62] is today a powerful tool employed, th2solution phenotype [63].

One unique approach, an algorithm called SPADE, utilizes downsampling, clustering, minimum spanning tree, and upsampling algorithms to generate two-dimensional branched visualizations [64, 65]. The branched tree structure incorporates information from all measurements in the data, partially addressing scalability issues. However, SPADE has many of the same subjective inputs as conventional clustering algorithms (e.g., number of clusters) and also may have issues of reproducibility and generation of nonbiological branches.

Similar to the SPADE software, the Euroflow Consortium software called INFINICYT uses nearest-neighbor analysis to associate the data around the center of the mass of cells. Adopting Euclidean distance analysis, this software associates a normal profile for a cell type (through phenotyping of multiple normal samples) to identify and characterize an

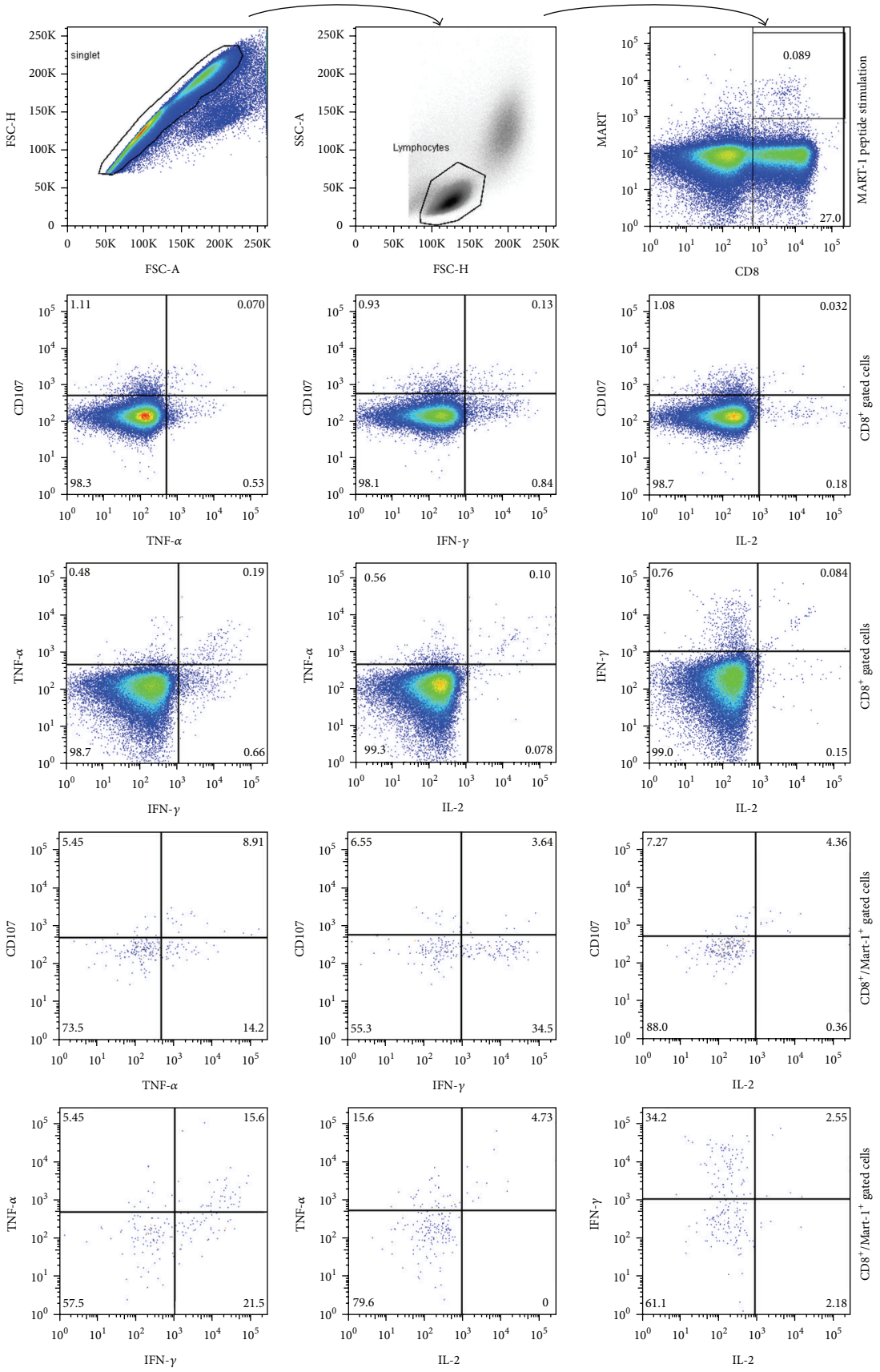

(a)

Figure 3: Continued.

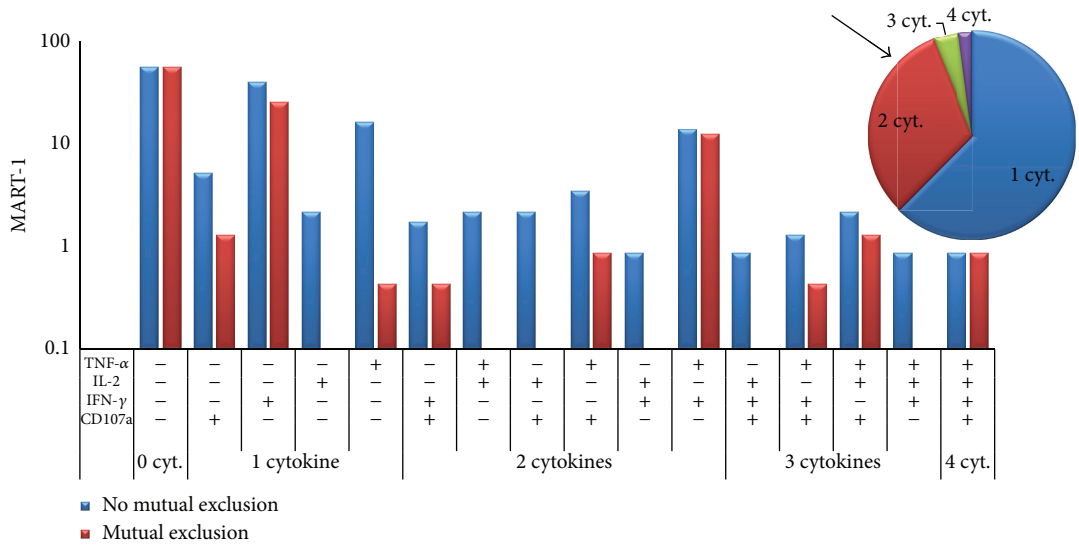

(b)

Figure 3: Validation of FMT (representative example of a melanoma patient). (a) Sequential gating strategy. Representative example dot plots and FACSDIVA analysis. Forward-scatter (FSC) area versus FSC height parameters were used to exclude cell doublets; cells were gated by forward and side scatter for lymphocytes; gated populations are plotted as CD8 (horizontal axis) versus tetramer staining (vertical axis). Direct *ex vivo* analysis cytokine production (IFNα, TNFγ, IL-2) and degranulation CD107a/LAMP-1) within CD8$^+$ population or CD8$^+$/MART-1 tetramer gated T-cells after stimulation with Melan-A/MART-1 peptide. (b) Histogram plots representing the individual functional combinations as a proportion of the total responding cells after stimulation with Melan-A/MART-1 peptide. *Mutual exclusion, red bars*: Percentage of cells expressing a certain combination of parameters (+) and not expressing the parameter indicated as (−). *No mutual exclusion, blue bars*: percentage of cells expressing a certain combination of parameters (+) independently from the expression of the parameter indicated with (−). The *pie slices* indicate the average proportion of the response producing 1, 2, 3, or 4 functions (regarding in this case "no mutual exclusion" variables). Each slice indicates one of the functions.

abnormal profile (http://www.infinicyt.com/). Developed as a diagnostic tool, this approach is limited by the relative frequency of the cell subset of interest and restriction of the parameter chosen to determine the normal profile that was used to create the database.

An additional way to look at the data is using the probability state modeling (PSM) method and the visualization tools in GemStone (http://www.vsh.com/products/gemstone/) software for the analysis of multidimensional flow cytometry data. A probability state model is a set of generalized Q functions, one for each correlated measurement, where the common cumulative probability axis can be a surrogate for time or cellular progression. By exploiting the unique characteristics of Q functions, PSM can model any number of correlated measurements and present one comprehensive yet understandable view of the results. In summary, these various software packages work to reduce the complexity into a relatively small set of model parameters that are amenable to group statistics and comparisons.

A model-based analysis based on statistical mixture models has been recently reported by [66], for cell subtype identification in flow cytometry.

Multivariate analysis of flow cytometric data using decision trees is interestingly described in [67], where, in order to examine whether the production of a certain cytokine is depended on other cytokines, datasets from intracellular staining for six cytokines with complex patterns of co-expression were analyzed.

A number of these approaches involve some variation of clustering analysis, which can have important limitations. Other approaches have been developed in addition to clustering, including principal components analysis (PCA) and Bayesian inference. These approaches have been evaluated through the FlowCAP initiative (http://flowcap.flowsite.org/).

To standardize the *universe* of Flow Data, MIFlowCyt (minimal information about a flow cytometry) experiment standard has been approved by the International Society for Advancement of Cytometry for the reporting of any flow cytometry results (http://flowcyt.sourceforge.net/miflowcyt/).

Our comment on computational approach, using of command line languages, algorithm design is that it is a potent and precious tool but quite far from the mean expertise of a flow cytometer user, which should have a specific training and/or collaborating with a bioinformatician. Maybe the future will reserve us more user friendly interfaces dedicated to computational analysis of flow data.

5. Consortia and Useful Links for Harmonization and Standardization of FCM-Based Assays

Many immune monitoring Consortia have been recently created worldwide to help facilitate and harmonize immune

monitoring approaches in the cancer immunotherapy field and establish rigorous quality control standards for serial monitoring of immunologic functions.

Among them, the Cancer Immunotherapy Consortium (CIC) of the Cancer Research Institute (CRI) in USA and the Association for Cancer Immunotherapy (CIMT) in Europe supported the web-based reporting framework on "Minimal Information about T-Cell Assays" MIATA [46], a project aimed at generating recommendations on the minimum information required to allow an objective and thorough interpretation of published results from immunological T-cell assays. (http://www.miataproject.org/). As mentioned before, up to date, this framework has completed proficiency panels and published harmonization guidelines for the top immune assays (Elispot, peptide-multimer assays, intracellular cytokine staining, and Luminex) [48, 68].

In addition, several links might help researcher to find their response to common questions regarding technical issues about FCM based-assays. Just to cite some of them, the Maecker lab weblog (http://www.miataproject.org/) provides research and training materials for flow cytometry and immune monitoring; the (http://cytobank.org/facselect/) might help to assist with optimization of staining conditions; the ICH Q2(R1) document (http://www.ich.org/products/guidelines/quality/article/quality-guidelines.html) is a guideline for validation of analytical procedures. In addition, a number of companies, such as the IST (http://immunositetechnologies.com/services/automation/immune-monitoring-automation.html) offer their expertise to design, develop, validate, and run polychromatic flow assays.

6. Conclusions

The development of new vaccines and immunotherapeutic strategies against cancer requires the sophisticated assessment of immune parameters (biomarkers) to reliably measure antitumor immune responses.

A wide range of advanced monitoring assays is currently used to determine phenotypical and functional characteristics of antitumor T-cells in cancer immunotherapy trials, including T-cell proliferation, cytokine profile, CTL assays, CTL-associated molecules (CD107, perforin, granzyme B, and CD154), and MHC-multimer analysis. However, these assays still fail to establish the possible correlation between immune response and clinical outcome. The lack of this correlation might reflect the methodological limitations of immunologic assays or the postvaccination absence of antitumor responses sufficiently robust to induce disease-free or overall survival.

Multiparameter flow cytometry expands platform for assessing functional profiles and patterns of immune responses. In particular, the use of polychromatic flow cytometry is likely to assume a role in defining the correlates of protection for vaccine efficacy as well as in monitoring immunotherapies in diseases such as HIV and cancer. In fact, it allows simultaneous detection of various parameters such as enumeration at the single cell level of different T-cell subsets (naïve, effector, central memory, effector memory), as well as cells belonging to the innate and myeloid compartment and providing information about the breadth and the quality of the induced immune response. The recent literature relates simultaneous expression of multiple functions (polyfunctionality) to immunity, since measurement of IFN-γ alone underestimates the total response [69].

Nevertheless, despite advances in the development of immune monitoring assays during the past decade, further advances are needed to implement throughput and standardization of such assays according to Good Laboratory Practice guidelines, such as those recently formulated based on recommendations from the iSBTc-SITC/FDA/NCI Workshop on Immunotherapy Biomarkers [70].

The goal of the present paper was to provide further insights into the development of standardized FCM-based immune assays. In particular, we revised the most common and critical issues of FCM-based technologies used for immune monitoring and evaluated the applicability of a six-color flow cytometric assay, previously developed in our laboratory, for immune monitoring in the setting of melanoma studies. This assay simultaneously measures effector cell degranulation and cytokine production by Melan-A/MART-1 specific $CD8^+$ T-cells. We were able to define some of the crucial aspects regarding sample processing and evaluated various staining and gating strategies. Concerning flow data analysis, we might conclude that different approaches of analysis and visual representations should be performed in order to obtain a complete picture of results about polyfunctionality of tumor specific T-cells.

Ethical Approval

Shown experiments were carried out according to the principles set out in the Declaration of Helsinki in 1964 and all subsequent revisions. Blood donors received and signed appropriate informed consent.

Acknowledgment

The authors would like to thank Dr. Federica Moschella for her valuable comments and scientific contribution.

References

[1] T. L. Whiteside, "Immune responses to cancer: are they potential biomarkers of prognosis?" *Frontiers in Oncology*, vol. 3, article 107, 2013.

[2] M. Vergati, C. Intrivici, N.-Y. Huen, J. Schlom, and K. Y. Tsang, "Strategies for cancer vaccine development," *Journal of Biomedicine and Biotechnology*, vol. 2010, Article ID 596432, 13 pages, 2010.

[3] M. J. Dobrzanski, "Expanding roles for CD4 T-cells and their subpopulations in tumor immunity and therapy," *Frontiers in Oncology*, vol. 3, article 63, 2013.

[4] M. Vergati, J. Schlom, and K. Y. Tsang, "The consequence of immune suppressive cells in the use of therapeutic cancer vaccines and their importance in immune monitoring," *Journal of Biomedicine and Biotechnology*, vol. 2011, Article ID 182413, 8 pages, 2011.

[5] B. M. Olson and D. G. McNeel, "Monitoring regulatory immune responses in tumor immunotherapy clinical trials," *Frontiers in Oncology*, vol. 3, article 109, 2013.

[6] I. Marigo, L. Dolcetti, P. Serafini, P. Zanovello, and V. Bronte, "Tumor-induced tolerance and immune suppression by myeloid derived suppressor cells," *Immunological Reviews*, vol. 222, no. 1, pp. 162–179, 2008.

[7] A. Biragyn and C. Lee-Chang, "A new paradigm for an old story: the role of regulatory B cells in cancer," *Frontiers in Immunology*, vol. 3, article 206, 2012.

[8] E. P. M. Tjin, D. Konijnenberg, G. Krebbers et al., "T-cell immune function in tumor, skin, and peripheral blood of advanced stage melanoma patients: implications for immunotherapy," *Clinical Cancer Research*, vol. 17, no. 17, pp. 5736–5747, 2011.

[9] J. Galon, F. Pagès, F. M. Marincola et al., "The immune score as a new possible approach for the classification of cancer," *Journal of Translational Medicine*, vol. 10, article 1, 2012.

[10] J. Galon, F. Pag ès, F. M. Marincola et al., "Cancer classification using the Immunoscore: a worldwide task force," *Journal of Translational Medicine*, vol. 10, article 205, 2012.

[11] L. H. Sobin and C. C. Compton, "TNM seventh edition: what's new, what's changed: communication from the International Union Against Cancer and the American Joint Committee on Cancer," *Cancer*, vol. 116, no. 22, pp. 5336–5339, 2010.

[12] C. Wittekind, C. C. Compton, F. L. Greene, and L. H. Sobin, "TNM residual tumor classification revisited," *Cancer*, vol. 94, no. 9, pp. 2511–2516, 2002.

[13] P. A. Ascierto, M. Capone, W. J. Urba et al., "The additional facet of immunoscore: immunoprofiling as a possible predictive tool for cancer treatment," *Journal of Translational Medicine*, vol. 11, article 54, 2013.

[14] W. H. Fridman, F. Pagès, C. Sautès-Fridman, and J. Galon, "The immune contexture in human tumours: impact on clinical outcome," *Nature Reviews Cancer*, vol. 12, no. 4, pp. 298–306, 2012.

[15] F. Pagès, A. Kirilovsky, B. Mlecnik et al., "In situ cytotoxic and memory T cells predict outcome in patients with early-stage colorectal cancer," *Journal of Clinical Oncology*, vol. 27, no. 35, pp. 5944–5951, 2009.

[16] W. C. Olson, M. E. Smolkin, E. M. Farris et al., "Shipping blood to a central laboratory in multicenter clinical trials: effect of ambient temperature on specimen temperature, and effects of temperature on mononuclear cell yield, viability and immunologic function," *Journal of Translational Medicine*, vol. 9, article 26, 2011.

[17] M. L. Disis, C. Dela Rosa, V. Goodell et al., "Maximizing the retention of antigen specific lymphocyte function after cryopreservation," *Journal of Immunological Methods*, vol. 308, no. 1-2, pp. 13–18, 2006.

[18] H. T. Maecker, J. Moon, S. Bhatia et al., "Impact of cryopreservation on tetramer, cytokine flow cytometry, and ELISPOT," *BMC Immunology*, vol. 6, article 17, 2005.

[19] A. Weinberg, L.-Y. Song, C. Wilkening et al., "Optimization and limitations of use of cryopreserved peripheral blood mononuclear cells for functional and phenotypic T-cell characterization," *Clinical and Vaccine Immunology*, vol. 16, no. 8, pp. 1176–1186, 2009.

[20] B. E. McLaughlin, N. Baumgarth, M. Bigos et al., "Nine-color flow cytometry for accurate measurement of T cell subsets and cytokine responses. Part I: panel design by an empiric approach," *Cytometry A*, vol. 73, no. 5, pp. 400–410, 2008.

[21] L. Papagno, J. R. Almeida, E. Nemes, B. Autran, and V. Appay, "Cell permeabilization for the assessment of T lymphocyte polyfunctional capacity," *Journal of Immunological Methods*, vol. 328, no. 1-2, pp. 182–188, 2007.

[22] H. T. Maecker and J. Trotter, "Flow cytometry controls, instrument setup, and the determination of positivity," *Cytometry A*, vol. 69, no. 9, pp. 1037–1042, 2006.

[23] T. Kalina, J. Flores-Montero, V. H. van der Velden et al., "Euroflow standardization of flow cytometer instrument settings and immunophenotyping protocols," *Leukemia*, vol. 26, no. 9, pp. 1986–2010, 2012.

[24] S. C. De Rosa, D. K. Carter, and M. J. McElrath, "OMIP-014: validated multifunctional characterization of antigen-specific human T cells by intracellular cytokine staining," *Cytometry A*, vol. 81, no. 12, pp. 1019–1021, 2012.

[25] G. Makedonas and M. R. Betts, "Polyfunctional analysis of human t cell responses: importance in vaccine immunogenicity and natural infection," *Springer Seminars in Immunopathology*, vol. 28, no. 3, pp. 209–219, 2006.

[26] M. R. Betts, M. C. Nason, S. M. West et al., "HIV nonprogressors preferentially maintain highly functional HIV-specific CD8+ T cells," *Blood*, vol. 107, no. 12, pp. 4781–4789, 2006.

[27] M. L. Precopio, M. R. Betts, J. Parrino et al., "Immunization with vaccinia virus induces polyfunctional and phenotypically distinctive $CD8^+$ T cell responses," *Journal of Experimental Medicine*, vol. 204, no. 6, pp. 1405–1416, 2007.

[28] J. Yuan, S. Gnjatic, H. Li et al., "CTLA-4 blockade enhances polyfunctional NY-ESO-1 specific T cell responses in metastatic melanoma patients with clinical benefit," *Proceedings of the National Academy of Sciences of the United States of America*, vol. 105, no. 51, pp. 20410–20415, 2008.

[29] S. Wilde, D. Sommermeyer, M. Leisegang et al., "Human antitumor $CD8^+$ T cells producing Th1 polycytokines show superior antigen sensitivity and tumor recognition," *Journal of Immunology*, vol. 189, no. 2, pp. 598–605, 2012.

[30] S. C. de Rosa, "Vaccine applications of flow cytometry," *Methods*, vol. 57, no. 3, pp. 383–391, 2012.

[31] T. M. Clay, A. C. Hobeika, P. J. Mosca, H. K. Lyerly, and M. A. Morse, "Assays for monitoring cellular immune responses to active immunotherapy of cancer," *Clinical Cancer Research*, vol. 7, no. 5, pp. 1127–1135, 2001.

[32] U. Keilholz, P. Martus, and C. Scheibenbogen, "Immune monitoring of T-cell responses in cancer vaccine development," *Clinical Cancer Research*, vol. 12, no. 7, part 2, pp. 2346s–2352s, 2006.

[33] N. Imai, H. Ikeda, I. Tawara, and H. Shiku, "Tumor progression inhibits the induction of multifunctionality in adoptively transferred tumor-specific $CD8^+$ T cells," *European Journal of Immunology*, vol. 39, no. 1, pp. 241–253, 2009.

[34] H. Horton, E. P. Thomas, J. A. Stucky et al., "Optimization and validation of an 8-color intracellular cytokine staining (ICS) assay to quantify antigen-specific T cells induced by vaccination," *Journal of Immunological Methods*, vol. 323, no. 1, pp. 39–54, 2007.

[35] M. R. Betts, J. M. Brenchley, D. A. Price et al., "Sensitive and viable identification of antigen-specific $CD8^+$ T cells by a flow cytometric assay for degranulation," *Journal of Immunological Methods*, vol. 281, no. 1-2, pp. 65–78, 2003.

[36] V. Rubio, T. B. Stuge, N. Singh et al., "Ex vivo identification, isolation and analysis of tumor-cytolytic T cells," *Nature Medicine*, vol. 9, no. 11, pp. 1377–1382, 2003.

[37] J. D. Altman, P. A. H. Moss, P. J. R. Goulder et al., "Phenotypic analysis of antigen-specific T lymphocytes," *Science*, vol. 274, no. 5284, pp. 94–96, 1996.

[38] C. Yee and P. Greenberg, "Modulating T-cell immunity to tumours: new strategies for monitoring T-cell responses," *Nature Reviews Cancer*, vol. 2, no. 6, pp. 409–419, 2002.

[39] P. Klenerman, V. Cerundolo, and P. R. Dunbar, "Tracking T cells with tetramers: new tales from new tools," *Nature Reviews Immunology*, vol. 2, no. 4, pp. 263–272, 2002.

[40] M. J. Pittet, D. E. Speiser, D. Valmori et al., "Ex vivo analysis of tumor antigen specific $CD8^+$ T cell responses using MHC/peptide tetramers in cancer patients," *International Immunopharmacology*, vol. 1, no. 7, pp. 1235–1247, 2001.

[41] P. Guillaume, D. Dojcinovic, and I. F. Luescher, "Soluble MHC-peptide complexes: tools for the monitoring of T cell responses in clinical trials and basic research," *Cancer Immunity*, vol. 9, article 7, 2009.

[42] S. K. Singh, B. Tummers, T. N. Schumacher et al., "The development of standard samples with a defined number of antigen-specific T cells to harmonize T cell assays: a proof-of-principle study," *Cancer Immunology, Immunotherapy*, vol. 62, no. 3, pp. 489–501, 2013.

[43] B. A. Fox, D. J. Schendel, L. H. Butterfield et al., "Defining the critical hurdles in cancer immunotherapy," *Journal of Translational Medicine*, vol. 9, article 214, 2011.

[44] S. H. van der Burg, M. Kalos, C. Gouttefangeas et al., "Harmonization of immune biomarker assays for clinical studies," *Science translational medicine*, vol. 3, no. 108, Article ID 108ps44, 2011.

[45] E. A. O'Donnell, D. N. Ernst, and R. Hingorani, "Multiparameter flow cytometry: advances in high resolution analysis," *Immune Network*, vol. 13, no. 2, pp. 43–54, 2013.

[46] S. Janetzki, C. M. Britten, M. Kalos et al., ""MIATA"-minimal information about T cell assays," *Immunity*, vol. 31, no. 4, pp. 527–528, 2009.

[47] Z. Moodie, L. Price, S. Janetzki, and C. M. Britten, "Response determination criteria for ELISPOT: toward a standard that can be applied across laboratories," *Methods in Molecular Biology*, vol. 792, pp. 185–196, 2012.

[48] C. M. Britten, S. Janetzki, L. Ben-Porat et al., "Harmonization guidelines for HLA-peptide multimer assays derived from results of a large scale international proficiency panel of the cancer vaccine consortium," *Cancer Immunology, Immunotherapy*, vol. 58, no. 10, pp. 1701–1713, 2009.

[49] M. J. Welters, C. Gouttefangeas, T. H. Ramwadhdoebe et al., "Harmonization of the intracellular cytokine staining assay," *Cancer Immunology, Immunotherapy*, vol. 61, no. 7, pp. 967–978, 2012.

[50] H. T. Maecker and J. P. McCoy, "Corrigendum: a model for harmonizing flow cytometry in clinical trials," *Nature Immunology*, vol. 12, no. 271, pp. 975–978, 2011.

[51] H. T. Maecker, A. Rinfret, P. D'Souza et al., "Standardization of cytokine flow cytometry assays," *BMC Immunology*, vol. 6, article 13, 2005.

[52] L. Nomura, V. C. Maino, and H. T. Maecker, "Standardization and optimization of multiparameter intracellular cytokine staining," *Cytometry A*, vol. 73, no. 11, pp. 984–991, 2008.

[53] A. Pierzchalski, A. Mittag, and A. Tárnok, "Introduction A: recent advances in cytometry instrumentation, probes, and methods—review," *Methods in Cell Biology*, vol. 102, pp. 1–21, 2011.

[54] P. Baumgaertner, C. Jandus, J.-P. Rivals et al., "Vaccination-induced functional competence of circulating human tumor-specific CD8 T-cells," *International Journal of Cancer*, vol. 130, no. 11, pp. 2607–2617, 2012.

[55] Y. Lin, H. F. Gallardo, G. Y. Ku et al., "Optimization and validation of a robust human T-cell culture method for monitoring phenotypic and polyfunctional antigen-specific CD4 and CD8 T-cell responses," *Cytotherapy*, vol. 11, no. 7, pp. 912–922, 2009.

[56] L. Lamoreaux, M. Roederer, and R. Koup, "Intracellular cytokine optimization and standard operating procedure," *Nature Protocols*, vol. 1, no. 3, pp. 1507–1516, 2006.

[57] P. Batard, D. A. Peterson, E. Devêvre et al., "Dextramers: new generation of fluorescent MHC class I/peptide multimers for visualization of antigen-specific $CD8^+$ T cells," *Journal of Immunological Methods*, vol. 310, no. 1-2, pp. 136–148, 2006.

[58] M. Roederer, J. L. Nozzi, and M. C. Nason, "SPICE: exploration and analysis of post-cytometric complex multivariate datasets," *Cytometry A*, vol. 79, no. 2, pp. 167–174, 2011.

[59] M. G. Duvall, M. L. Precopio, D. A. Ambrozak et al., "Polyfunctional T cell responses are a hallmark of HIV-2 infection," *European Journal of Immunology*, vol. 38, no. 2, pp. 350–363, 2008.

[60] S. C. Bendall, G. P. Nolan, M. Roederersend, and P. K. Chattopadhyay, "A deep profiler's guide to cytometry," *Trends in Immunology*, vol. 33, no. 7, pp. 323–332, 2012.

[61] F. Hahne, N. LeMeur, R. R. Brinkman et al., "flowcore: a bioconductor package for high throughput flow cytometry," *BMC Bioinformatics*, vol. 10, article 106, 2009.

[62] M. Roederer, W. Moore, A. Treister, R. R. Hardy, and L. A. Herzenberg, "Probability binning comparison: a metric for quantitating multivariate distribution differences," *Cytometry*, vol. 45, no. 1, pp. 47–55, 2001.

[63] T. Kalina, J. Stuchlý, A. Janda et al., "Profiling of polychromatic flow cytometry data on B-cells reveals patients' clusters in common variable immunodeficiency," *Cytometry A*, vol. 75, no. 11, pp. 902–909, 2009.

[64] P. Qiu, "Inferring phenotypic properties from single-cell characteristics," *PLoS One*, vol. 7, no. 5, Article ID e37038, 2012.

[65] P. Qiu, E. F. Simonds, S. C. Bendall et al., "Extracting a cellular hierarchy from high-dimensional cytometry data with SPADE," *Nature Biotechnology*, vol. 29, no. 10, pp. 886–891, 2011.

[66] J. Frelinger, J. Ottinger, C. Gouttefangeas, and C. Chan, "Modeling flow cytometry data for cancer vaccine immune monitoring," *Cancer Immunology, Immunotherapy*, vol. 59, no. 9, pp. 1435–1441, 2010.

[67] S. Simon, R. Guthke, T. Kamradt, and O. Frey, "Multivariate analysis of flow cytometric data using decision trees," *Frontiers in Microbiology*, vol. 3, article 114, 2012.

[68] S. Janetzki, K. S. Panageas, L. Ben-Porat et al., "Results and harmonization guidelines from two large-scale international elispot proficiency panels conducted by the cancer vaccine consortium (CVC/SVI)," *Cancer Immunology, Immunotherapy*, vol. 57, no. 3, pp. 303–315, 2008.

[69] S. C. De Rosa, F. X. Lu, J. Yu et al., "Vaccination in humans generates broad T cell cytokine responses," *Journal of Immunology*, vol. 173, no. 9, pp. 5372–5380, 2004.

[70] L. H. Butterfield, A. K. Palucka, C. M. Britten et al., "Recommendations from the iSBTc-SITC/FDA/NCI workshop on immunotherapy biomarkers," *Clinical Cancer Research*, vol. 17, no. 10, pp. 3064–3076, 2011.

Hindawi Publishing Corporation
BioMed Research International
Volume 2013, Article ID 678476, 7 pages
http://dx.doi.org/10.1155/2013/678476

Research Article

Novel Spectrophotometric Method for the Quantitation of Urinary Xanthurenic Acid and Its Application in Identifying Individuals with Hyperhomocysteinemia Associated with Vitamin B_6 Deficiency

Chi-Fen Chen,[1] Tsan-Zon Liu,[2] Wu-Hsiang Lan,[1] Li-An Wu,[3] Chin-Hung Tsai,[4] Jeng-Fong Chiou,[5,6] and Li-Yu Tsai[7]

[1] *Clinical Laboratories, Yuan's General Hospital, Kaohsiung 802, Taiwan*
[2] *Translational Research Laboratory, Cancer Center, Taipei Medical University Hospital, Taipei 110, Taiwan*
[3] *Clinical Laboratories, Chang Gung Memorial Hospital, Kwei-Shan 333, Taiwan*
[4] *Department of Food Science, National Penghu University of Science and Technology, Magong, Penghu 880, Taiwan*
[5] *Department of Radiation Oncology, School of Medicine, Taipei Medical University, Taipei 110, Taiwan*
[6] *Cancer Center and Department of Radiation Oncology, Taipei Medical University and Hospital, Taipei 110, Taiwan*
[7] *Division of Clinical Biochemistry, Graduate Institute of Medical Biotechnology, Kaohsiung Medical University, Kaohsiung 807, Taiwan*

Correspondence should be addressed to
Jeng-Fong Chiou; sjfchiou@xuite.net and Li-Yu Tsai; tsailiyu2005@yahoo.com.tw

Received 20 June 2013; Accepted 16 August 2013

Academic Editor: Natasa Tosic

A novel spectrophotometric method for the quantification of urinary xanthurenic acid (XA) is described. The direct acid ferric reduction (DAFR) procedure was used to quantify XA after it was purified by a solid-phase extraction column. The linearity of proposed method extends from 2.5 to 100.0 mg/L. The method is precise, yielding day-to-day CVs for two pooled controls of 3.5% and 4.6%, respectively. Correlation studies with an established HPLC method and a fluorometric procedure showed correlation coefficients of 0.98 and 0.98, respectively. Interference from various urinary metabolites was insignificant. In a small-scale screening of elderly conducted at Penghu county in Taiwan ($n = 80$), we were able to identify a group of twenty individuals having hyperhomocysteinemia (>15 μmole/L). Three of them were found to be positive for XA as analyzed by the proposed method, which correlated excellently with the results of the activation coefficient method for RBC's AST/B_6 functional test. These data confirm the usefulness of the proposed method for identifying urinary XA as an indicator of vitamin B_6 deficiency-associated hyperhomocysteinemic condition.

1. Introduction

Homocysteine (Hcy) is a sulfur-containing amino acid which is an intermediary product of the transmethylation reaction of methionine. Once formed, Hcy can either be remethylated back to methionine by a folate- and vitamin B_{12}-dependent enzymatic reaction or can undergo the transsulfuration pathway to form cysteine (the rate-limiting precursor for gluthathione) via a two-step enzymatic process catalyzed by cystathionine β-synthase (CBS) and cystathionase, both requiring vitamin B_6 coenzyme [1–3]. Park and Linkswiler [4] reported that urinary Hcy excretion increased considerably with six male volunteers who consumed a diet depleted of vitamin B_6 whereas several studies on experimental animals suggested that a vitamin B_6 deficiency could result in Hcy accumulation [5–7]. Collectively, these reports implicate that measurement of Hcy is not a specific biomarker for deficiency of vitamin B_6. In contrast, kynureninase (EC 3.7.1.3), a pyridoxal 5′-phosphate coenzyme-requiring enzyme is essential for the catalytic action of converting 3-hydroxykynurenin,

an intermediary product of tryptophan metabolism, to 3-hydroxyanthranilate [8]. Either subclinical deficiencies of vitamin B_6 or a genetic defeat on kynureninase can lead to the accumulation of xanthurenic acid (XA) in plasma and urine [5–7]. Collectively, despite vitamin B_6 deficiency can lead to a combined accumulation of XA and Hcy in urine, the former is considered to be a more sensitive and specific indicator than Hcy for the evaluation of vitamin B_6 deficiency because Hcy can be diverted to other pathways even in cases of vitamin B_6 deficiency.

Vitamin B_6 deficiency was first suggested earlier by scientists who demonstrated widespread vascular lesion in pyridoxine deficient monkeys with little or no lipid disposition, and their serum cholesterol were hardly elevated [9]. Furthermore, Ubbink et al. [10] reported that patients with cystathionine β-synthase (EC 4.2.1.22) deficiency, the first vitamin B_6-dependent enzyme catalyzing the transsulfuration pathway of homocysteine catabolism, exhibited widespread vascular disorders. In addition, patients with rheumatoid arthritis had been reported to possess reduced circulating level of vitamin B_6 and their plasma pyridoxal 5′-phosphate levels correlated with both the net Hcy increase in response to a methionine load test and 24 hr urinary XA excretion in response to a tryptophan load test [11]. Besides, Zhang et al. [12] implicated that pyridoxal 5′-phosphate, the principal active form of vitamin B_6, has a number of biological roles that potentially make it important in cancer. The rationale of this implication is that adequate vitamin B_6 levels are important for conversion of Hcy into cysteine and high intracellular levels of pyridoxal 5′-phosphate can lead to decreased steroid hormone-induced gene expression. In addition, these authors also presented evidence that higher plasma levels of folate and vitamin B_6 may reduce the risk of developing breast cancer. These data implies that vitamin B_6 deficiency itself may be a risk factor for cancer.

Measurement of urinary or plasma XA has been used clinically to study vitamin B_6 deficiency [8, 13, 14], including febrile disorder [15], theophylline-induced asthma [16], drug-induced diabetes [16], the effect of tryptophan and six of its metabolites on the nicotinic acid pathway [17], and the etiological role in a variety of chronic degenerative disease including a variety of cancers [18–22]. Among the methods developed for quantifying urinary XA [23–28], one tedious and lengthy assay involved the extraction of XA from urine with isobutanol, isolation by thin-layer chromatography, and eventually spectrophotometric determination [25]. The first fluorometric quantification of urinary XA was devised by Satoh and Price [23], based on the separation of XA by Dowex 50 (H^+), followed by measurement of its fluorescence in strong alkali, and kynurenic acid was simultaneously determined by fluorometry in strong H_2SO_4. This method was subsequently modified by Cohen et al. [24], who separated XA from other fluorescent substances in urine by a pH- and NaCl-dependent extraction with isobutanol and then determined the fluorescence of XA in alkaline solution so that potentially interfering compounds such as kynurenic acid could be obviated. However, all these methods involve multiple procedural steps which are rather tedious and time-consuming. In addition, several HPLC methods have also been devised for quantifying urinary XA [26, 28]. However, the expensive instruments required might not be readily available in a general clinical laboratory. For these reasons, we set out to develop this rapid and simple spectrophotometric method for measuring urinary XA that is free of interference and can be easily adoptable for routine use by clinical and micronutrient assessment laboratories. To further exemplify its clinical application, we performed a single-blind study on a group of urine specimens ($N = 20$) obtained from patients with hyperhomocysteinemia of unknown etiologies using proposed method to screen for XA. Based on this screening procedure, we were able to successfully identify three out of twenty patients with hyperhomocysteinemia that were actually originated from vitamin B_6 deficiency.

2. Material and Methods

2.1. Chemicals. Unless otherwise stated, reagents of the highest quality available were obtained commercially. XA (4,8-dihydroxyquinaldic acid), kynurenic acid (4-hydroxyquinoline-2-carboxylic acid), 2,4,6-tris-(pyridyl)-s-triazine (TPTZ), ferric chloride hexahydrate, vitamin C, uric acid, salicylate, acetaminophen, vanillylmandelic acid, and homovanillic acid were purchased from Sigma Chemical Co. (St. Louis, MO, USA). Solid-phase anionic-exchange resin (trimethylaminopropyl group bound to silica) was purchased from Analytichem (Harbor City, CA).

2.2. Reagents. (a) Acetate buffer, 0.3 mol/liter, pH 3.6, is prepared by dissolving 3.1 g of sodium acetate trihydrate in distilled water. Add 16.0 mL of glacial acetic acid. Dilute to 1 liter, check the pH, and adjust it to 3.6. (b) *TPTZ,* 8 mmol/liter, is prepared by dissolving 624 mg of TPTZ in 250 mL of HCl solution (36 mmol/liter, 0.75 mL conc. HCl and H_2O). (c) $FeCl_3 \cdot 6H_2O$ solution is prepared by dissolving 540 mg of ferric chloride hexahydrate in 100 mL HCl solution (0.02 mol/liter, 0.16 mL of conc. HCl, and H_2O).

2.3. Urine Purification. Routinely, 24 h urine specimens are collected in brown bottles with 6 N HCl as preservative and proceed for analyses without delay. The sample should be well mixed and an aliquot frozen if the sample cannot be analyzed within 48 hr after collection. Before analysis, the urine specimen (after thawing, if necessary) is filtered through Whatman No. 1 filter paper, and 5.0 mL of urine is applied to an anion-exchange solid-phase extraction column (100 mg/column). After the urine sample has passed through the extraction column, the adsorbed XA is eluted with 2.0 mL of 0.1 M HCl.

2.4. Spectrophotometry of XA. 0.5 mL of eluate from purified procedure mentioned previously is added and 0.5 mL of 1 N NaOH. 0.1 mL of this alkaline elute is then added to a solution containing 2.5 mL of acetate buffer, pH 3.6, 0.3 mL of TPTZ, and 0.1 mL of $FeCl_3$ solution. The tubes are well mixed and stand at room temperature for exactly 15 minutes. Immediately, the absorbance of each tube is read at 593 nm.

XA concentration of the unknown is estimated from the standard curve based on the absorbances of the standards.

2.5. Fluorometric Measurement of XA. The eluate containing XA from urine is dissolved into potassium phosphate buffer, pH 4.0. The fluorescence of XA is then determined at 460–470 nm (after excitation at 305 nm) with a Turner spectrofluorometer.

2.6. Correlation Studies. The results obtained by the proposed method were compared with those determined by an established HPLC method [27] and with a fluorometric method established in our laboratory [29].

2.7. Rapid Screening of Urinary XA in Elderly with Hyperhomocysteinemic Condition. We conducted a small-scale screening of the elderly (age 61 to 80 years) ($n = 80$) for hyperhomocysteinemia during a regular annual physical check up from Penghu County. The project was approved by the Institutional Review Board of Kaohsiung Medical University (KMUH-IRB-960036). Individuals who had hyperhomocysteinemic condition (>15 μmole/L) were asked by the physician to donate urine specimens with informed consent. These specimens were then analyzed by our proposed method for XA. For those urine samples positive for XA, a parallel determination of activation coefficients on RBC's aspartic acid aminotransferase (AST)/B-6 functional test was performed to confirm if XA-positive individuals were definitively deficient in vitamin B_6.

2.8. Statistics. Data are expressed as mean ± S.D. and analyzed using Student's t-test. P values lower than 0.05 were considered statistically significant.

3. Results

3.1. Absorption Spectra. Spectral scan for XA after reacting with Fe^{+3}-TPTZ complex in acidic buffer (pH 3.6) exhibit a maximum absorption peak at 593 nm. The absorption peak represents the formation of Fe^{+2}-TPTZ (intense blue color) (Figure 1).

3.2. Time Course Study. Reduction of Fe^{+3}-TPTZ complex by XA exhibits a time-dependent manner. The increment of absorption at 593 nm reaches a plateau approximately 30 min (Figure 2). For accuracy, the reaction time for the proposed method should be set at 30 min. If this procedural step is inconvenient, a short time of color development can be used (e.g., 15 min), but each tube should be timed for equal amount of incubation time, and the absorbance at 593 nm should be read immediately without delayed.

3.3. Linearity. Absorbances of calibrators at 593 nm were linearly related to XA concentrations from 2.5 to 100 mg/L (Figure 3). The limit of detection (LOD) is 10 μg/mL.

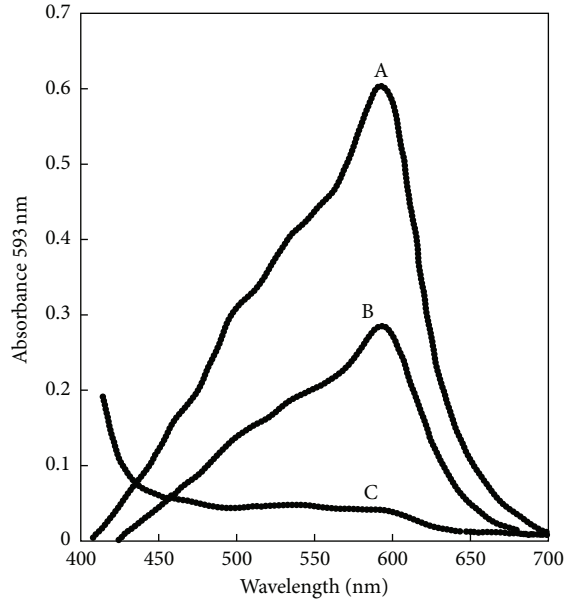

Figure 1: Spectral scan for xanthurenic acid after reacting with Fe^{3+}-TPTZ complex in acidic buffer (pH = 3.6) exhibiting a maximum absorption peak at 593 nm. The absorption peak represents the formation of Fe^{2+}-TPTZ (intense blue color). A = 8 μg XA in 0.1 mL MeOH versus reagent blank, B = 4 μg XA in 0.1 mL MeOH versus reagent blank, and C = reagent blank versus H_2O.

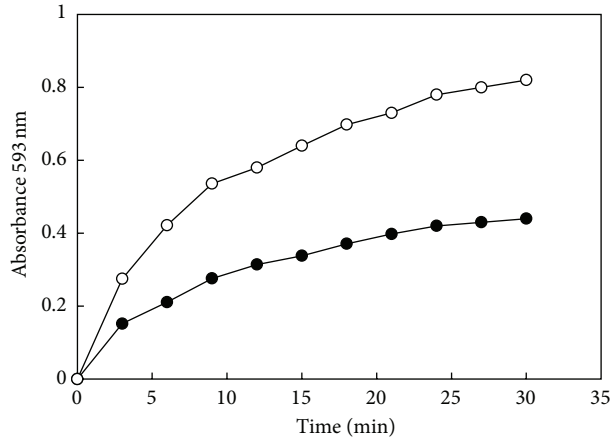

Figure 2: Reduction of Fe^{3+}-TPTZ complex by XA is a time-dependent process. The increment of absorption at 593 nm reaches a plateau at approximately 30 min. For accuracy, the reaction time for the proposed method should be set at 30 min. (•–•) = 4 μg XA in MeOH and (○–○) = 8 μg XA in MeOH.

3.4. Analytical Recovery. To determine the accuracy of the procedure, we performed a recovery study the percentage of recovery represents the measured value expressed as a percentage of the expected value. The mean percentage of recovery for 10 samples was 99.8 ± 2.1% (data not shown).

3.5. Precision. Reproducibility as reflected by day-to-day and within-run precision data were excellent (Table 1). Five repetitive determinations on two pooled XA-supplemented

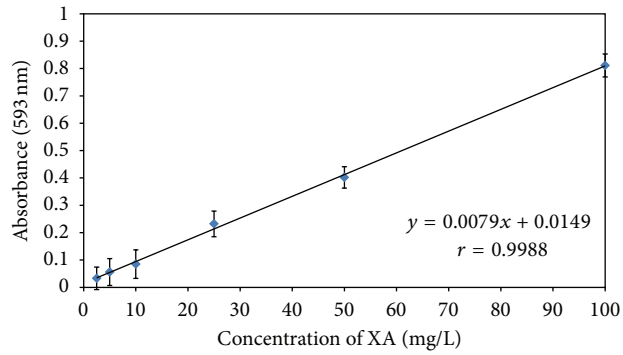

Figure 3: Linearity of XA determination as assayed by the proposed spectrophotometric method. Each point represents an average of triplicate determinations. The XA stock solution (100 mg/L) was prepared by dissolving 10 mg of XA into 1.0 mL of methanol and then made up to 100 mL with XA-free pooled urine. Various concentrations of standards were then made up by diluting with XA-free urine to the desired concentrations.

Table 1: Precision studies results.

	XA determined by the proposed method (mg/L)*	Indirect activation coefficient (AC) test for RBC/AST**
Within-run (n = 5)*		
Mean, mg/L	20.2	41.0
SD, mg/L	0.60	1.5
CV, %	3.0	3.7
Day-to-day (n = 25)**		
Mean, mg/L	20.2	41.0
SD, mg/L	0.7	1.9
CV, %	3.5	4.6

*Each level of pooled urine sample was determined simultaneously for 5 times at the same day.
**Each level of pooled urine sample was run 5 times per day for five consecutive days. The pooled data were then calculated for mean, SD and CV.

urine controls had a mean value of 20.2 and 41.0 mg/L, respectively (with CVs of <5.0%). The CVs for the same set of controls assayed on 5 consecutive days were 3.5% and 4.6%, respectively. Again, the day-to-day reproducibility was also excellent.

3.6. Correlation Studies. We compared results by the proposed method with those determined by an established HPLC method [27] for 30 samples. The correlation coefficient between the two methods was 0.98. (Figure 4(a)) Comparison of the proposed method with a fluorometric method [29] for 30 samples showed that the correlation coefficient between the two methods was also 0.98 (Figure 4(b)).

3.7. Interference Assay. The purification step with the solid-phase anion-exchange column presumably renders the assay free of interferences. However, to verify this assumption, we checked for possible interference from the following commonly encountered substances in urine: vitamin C, uric acid, salicylate, vanillylmandelic acid (VMA), and homovanillic (HVA). At concentrations of 0.5 g/L, all of these compounds gave no interference with the assay.

Table 2: A single blind study for 20 hyperhomocysteinemic urine specimens obtained through a small-scale screening of the elderly (n = 80) for assaying XA by our proposed method and their parallel comparison of assessing B_6 status by indirect activation coefficient test for RBC/AST.

Specimen code no.	XA determined* by the proposed method (mg/L)	Indirect activation coefficient (AC) test for RBC/AST**
1	ND	Normal
2	ND	Normal
3	ND	Normal
4	13.5	Abnormal (AC = 1.51)
5	ND	Normal
6	ND	Normal
7	14.2	Abnormal (AC = 1.43)
8	ND	Normal
9	ND	Normal
10	ND	Normal
11	ND	Normal
12	ND	Normal
13	25.3	Abnormal (AC = 1.80)
14	ND	Normal
15	ND	Normal
16	ND	Normal
17	ND	Normal
18	ND	Normal
19	ND	Normal
20	ND	Normal

*ND: nondetectable (<LOD).
**AC < 1.30 is designated as normal.

4. Discussion

The described method for the measurement of XA in urine was evaluated for its specificity, accuracy, and reproducibility for general use. First, the solid-phase extraction column (trimethylaminopropyl group bound to silica) concentrates not only the desired XA, but also leave behind urinary substances such as the tryptophan metabolites, kynurenin, and hydroxylkynurenine. This purification step for XA confers a unique specificity to the proposed method.

During the course of this developmental work, we considered incorporating a hydrolytic step to account for the possible presence of conjugated forms of XA. Rothstein and Greenberg [30] have previously reported that the urinary XA is conjugated as glucuronide in the rat and as the sulfate in the rabbit. In contrast, Wallace et al. [25] showed that the amount of XA in human urine remained steady after hydrolysis with acid or glucuronidase, indicating that very little conjugated XA was present. This observation was also

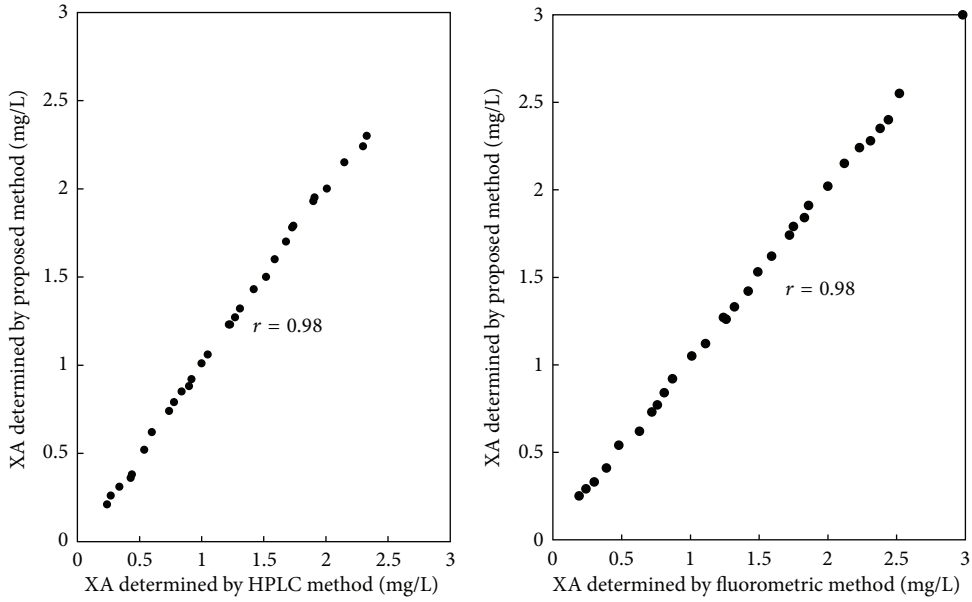

Figure 4: Correlation of results of XA concentrations obtained by the proposed method and those determined by an established HPLC method (a) or with an established fluorometric procedure (b).

previously confirmed by us [29]. Thus, we decided not to incorporate a hydrolysis step for urine in our proposed method.

The accuracy of the method, evaluated by measuring XA added to pooled urine in which no endogenous XA was detected that shows the mean percentage of recovery for 10 samples was 99.8 ± 2.1% (date not shown). Additionally, reproducibility as reflected by day-to-day and within-run precision data was also excellent (Table 1).

It has been well documented that one of the etiologic factors underlying chronic degenerative diseases such as cancer, diabetes, and Alzheimer's diseases may be oxidative stress to which the elderly population is specially prone. In addition, the elderly population may have deficiencies of several micronutrients including folate, pyridoxine, and cobalamin; if not treated in time, these deficiencies can lead to an accumulation of both XA and Hcy in the urine or plasma and present a serious health risk to these individuals. As an example, Wilson et al. [31] reported that about 10% of the US population consumes less than half of the RDA (1.6 mg/day) of vitamin B_6. As also pointed out by Ames [32], vitamin B_6 deficiency can cause a decrease in enzyme activity of serine hydroxylmethyltransferase which supplies the methylene group for methylene-THF [33]. If the methylene-THF pool is decreased in B_6 deficiency, an episode of uracil incorporation into DNA can be anticipated to cause chromosome breaks and the risk for cancer will be greatly increased. In a case-control study of diet and cancer, vitamin B_6 intake was inversely associated with prostate cancer [34]. Thus, we think that it is of importance to undertake a large-scale screening to identify individuals from an elderly population who maybe deficient in these micronutrients. Our proposed method is sample and rapid and can be modified to suit for semiautomated quantification of vitamin B_6 deficiency in a large scale screening purpose. More importantly, it can also be adopted as one of the tests for routine use in the clinical laboratory. Our small scale screening for elderly who were hyperhomocysteinemic followed by correctly identified individuals high in urinary XA which was indicative of vitamin B_6 deficiency can serve as a testimony of the applicability of our proposed method (Table 2). Further study is urgently needed to establish if there is a correlation between vitamin B_6 deficiency-induced hypercysteinemia and the risk of cancer. Our proposed noninvasive urinary XA test is well suited for the investigation of this kind.

5. Conclusion

This work describes a simple and rapid spectrophotometric method for quantifying urinary XA as an indicator of vitamin B_6 deficiency which allows one to differentiate hyperhomocysteinemic condition independent of folate/vitamin B12 involvement. We also exemplifiy its application by correctly identified these individuals whose hyperhomocysteinemia condition were solely derived from vitamin B_6 deficiency. This noninvasive spectrophotometric method for quantifying urinary XA may also be suitable for identifying individuals with vitamin B_6 deficiency and subsequently receiving vitamin B_6 supplementation to reduce the risk of cancer due to Hcy-evoked oxidative stress.

Conflict of Interests

The authors declare they have no conflict of interests.

Authors' Contribution

J.-F. Chiou and L.-Y. Tsai are cocorresponding authors.

Acknowledgments

The expert technical assistance of Ms. S. Y. Mau is greatly appreciated.

References

[1] J. D. Finkelstein, "Methionine metabolism in mammals," *Journal of Nutritional Biochemistry*, vol. 1, no. 5, pp. 228–237, 1990.

[2] S. C. Lu and J. M. Mato, "S-adenosylmethionine in cell growth, apoptosis and liver cancer," *Journal of Gastroenterology and Hepatology*, vol. 23, supplement 1, pp. S73–S77, 2008.

[3] O. Midttun, S. Hustad, and P. M. Ueland, "Quantitative profiling of biomarkers related to B-vitamin status, tryptophan metabolism and inflammation in human plasma by liquid chromatography/tandem mass spectrometry," *Rapid Communications in Mass Spectrometry*, vol. 23, no. 9, pp. 1371–1379, 2009.

[4] Y. K. Park and H. Linkswiler, "Effect of vitamin B6 depletion in adult man on the excretion of cystathionine and other methionine metabolites," *Journal of Nutrition*, vol. 100, no. 1, pp. 110–116, 1970.

[5] M. Slavik, K. J. Smith, and O. Blanc, "Decrease of serum pyridoxal phosphate levels and homocystinemia after administration of 6-azauridine triacetate and their prevention by administration of pyridoxine," *Biochemical Pharmacology*, vol. 31, no. 24, pp. 4089–4092, 1982.

[6] L. A. Smolin and N. J. Benevenga, "Accumulation of homocyst(e)ine in vitamin B-6 deficiency: a model for the study of cystathionine β-synthase deficiency," *Journal of Nutrition*, vol. 112, no. 7, pp. 1264–1272, 1982.

[7] L. A. Smolin, T. D. Crenshaw, D. Kurtycz, and N. J. Benevenga, "Homocyst(e)ine accumulation in pigs fed diets deficient in vitamin B-6: relationship to atherosclerosis," *Journal of Nutrition*, vol. 113, no. 10, pp. 2022–2033, 1983.

[8] F. Takeuchi, R. Tsubouchi, S. Izuta, and Y. Shibata, "Kynurenic metabolism and xanthurenic acid formation in vitamin B6-deficient rat after tryptophan injection," *Journal of Nutritional Science and Vitaminology*, vol. 35, no. 2, pp. 111–122, 1989.

[9] S. J. Chang, "Vitamin B6 antagonists alter the function and ultrastructure of mice endothelial cells," *Journal of Nutritional Science and Vitaminology*, vol. 46, no. 4, pp. 149–153, 2000.

[10] J. B. Ubbink, W. J. H. Vermaak, A. van der Merwe, and P. J. Becker, "Vitamin B-12, vitamin B-6, and folate nutritional status in men with hyperhomocysteinemia," *The American Journal of Clinical Nutrition*, vol. 57, no. 1, pp. 47–53, 1993.

[11] E. P. I. Chiang, J. Selhub, P. J. Bagley, G. Dallal, and R. Roubenoff, "Pyridoxine supplementation corrects vitamin B6 deficiency but does not improve inflammation in patients with rheumatoid arthritis," *Arthritis Research & Therapy*, vol. 7, no. 6, pp. R1404–R1411, 2005.

[12] S. M. Zhang, W. C. Willett, J. Selhub et al., "Plasma folate, vitamin B6, vitamin B12, homocysteine, and risk of breast cancer," *Journal of the National Cancer Institute*, vol. 95, no. 5, pp. 373–380, 2003.

[13] D. A. Bender, E. N. M. Njagi, and P. S. Danielian, "Tryptophan metabolism in vitamin B6-deficient mice," *The British Journal of Nutrition*, vol. 63, no. 1, pp. 27–36, 1990.

[14] J. E. Leklem, "Vitamin B-6: a status report," *Journal of Nutrition*, vol. 120, no. 11, pp. 1503–1507, 1990.

[15] R. C. Shaw and R. D. Feigin, "Excretion of kynurenic acid and xanthurenic acid during infection," *Pediatrics*, vol. 47, no. 1, pp. 47–56, 1971.

[16] J. B. Ubbink, R. Delport, P. J. Becker, and S. Bissbort, "Evidence of a theophylline-induced vitamin B6 deficiency caused by noncompetitive inhibition of pyridoxal kinase," *Journal of Laboratory and Clinical Medicine*, vol. 113, no. 1, pp. 15–22, 1989.

[17] S. Ikeda and Y. Kotake, "Urinary excretion of xanthurenic acid and zinc in diabetes: (3). Occurrence of xanthurenic acid-Zn^{2+} complex in urine of diabetic patients and of experimentally-diabetic rats," *Italian Journal of Biochemistry*, vol. 35, no. 4, pp. 232–241, 1986.

[18] J. V. Woodside, D. G. Fogarty, J. H. Lightbody et al., "Homocysteine and B-group vitamins in renal transplant patients," *Clinica Chimica Acta*, vol. 282, no. 1-2, pp. 157–166, 1999.

[19] E. P. I. Chiang, P. J. Bagley, R. Roubenoff, M. Nadeau, and J. Selhub, "Plasma pyridoxal 5′-phosphate concentration is correlated with functional vitamin B-6 indices in patients with rheumatoid arthritis and marginal vitamin B-6 status," *Journal of Nutrition*, vol. 133, no. 4, pp. 1056–1059, 2003.

[20] C. C. Lin and M. C. Yin, "B vitamins deficiency and decreased anti-oxidative state in patients with liver cancer," *European Journal of Nutrition*, vol. 46, no. 5, pp. 293–299, 2007.

[21] E. Schernhammer, B. Wolpin, N. Rifai et al., "Plasma folate, vitamin B6, vitamin B12, and homocysteine and pancreatic cancer risk in four large cohorts," *Cancer Research*, vol. 67, no. 11, pp. 5553–5560, 2007.

[22] E. Ma, M. Iwasaki, I. Junko et al., "Dietary intake of folate, vitamin B6, and vitamin B12, genetic polymorphism of related enzymes, and risk of breast cancer: a case-control study in Brazilian women," *BMC Cancer*, vol. 9, article 122, 2009.

[23] K. Satoh and J. M. Price, "Fluorometric determination of kynurenic acid and xanthurenic acid in human urine," *The Journal of Biological Chemistry*, vol. 230, no. 2, pp. 781–789, 1958.

[24] G. Cohen, R. A. Fishman, and A. L. Jenkins, "A fluorometric method for the determination of xanthurenic acid in urine," *Journal of Laboratory and Clinical Medicine*, vol. 67, no. 3, pp. 520–527, 1966.

[25] M. J. Wallace, H. W. Vaillant, and H. A. Salhanick, "Method for quantitative measurement of xanthurenic acid in urine," *Clinical Chemistry*, vol. 17, no. 6, pp. 505–511, 1971.

[26] S. A. Williams, J. A. Monti, L. R. Boots, and P. E. Cornwell, "Quantitation of xanthurenic acid in rabbit serum using high performance liquid chromatography," *The American Journal of Clinical Nutrition*, vol. 40, no. 1, pp. 159–167, 1984.

[27] J. B. Ubbink, A. M. Schnell, and C. H. Rapley, "Quantification of urinary xanthurenic acid excretion by anion-exchange solid-phase extraction and high-performance liquid chromatography," *Journal of Chromatography*, vol. 425, no. 1, pp. 182–186, 1988.

[28] E. Ohtsuki, M. Suzuki, M. Takayanagi, and T. Yashiro, "Colorimetric determination of urinary xanthurenic acid using an oxidative coupling reaction with N,N-diethyl-p-phenylenediamine," *Biological and Pharmaceutical Bulletin*, vol. 17, no. 1, pp. 139–141, 1994.

[29] M. Liu, G. R. Wang, T. Z. Liu, and K. J. Tsai, "Improved fluorometric quantification of urinary xanthurenic acid," *Clinical Chemistry*, vol. 42, no. 3, pp. 397–401, 1996.

[30] M. Rothstein and D. M. Greenberg, "Studies on the metabolism of xanthurenic acid-4-C14," *Archives of Biochemistry and Biophysics*, vol. 68, no. 1, pp. 206–214, 1957.

[31] J. W. Wilson, C. W. Enns, J. D. Goldman et al., "Data table: combined results from USDA's 1994 and 1995 continuing survey of food intakes by individuels and 1994 and 1995 diet and health knowledge survey," USDA/ARS Food Surveys Research Group, Beltsville Human Nutrition Research Center, Riverdale, Md, USA, 1997.

[32] B. N. Ames, "Micronutrient deficiencies cause DNA damage and cancer," *Food Science and Agricultural Chemistry*, vol. 1, pp. 1–15, 1999.

[33] S. P. Stabler, D. A. Sampson, L. P. Wang, and R. H. Allen, "Elevations of serum cystathionine and total homocysteine in pyridoxine- , folate-, and cobalamin-deficient rats," *Journal of Nutritional Biochemistry*, vol. 8, no. 5, pp. 279–289, 1997.

[34] T. J. Key, P. B. Silcocks, G. K. Davey, P. N. Appleby, and D. T. Bishop, "A case-control study of diet and prostate cancer," *The British Journal of Cancer*, vol. 76, no. 5, pp. 678–687, 1997.

Hindawi Publishing Corporation
BioMed Research International
Volume 2013, Article ID 192548, 5 pages
http://dx.doi.org/10.1155/2013/192548

Research Article

Expression of Bmi-1 in Pediatric Brain Tumors as a New Independent Prognostic Marker of Patient Survival

Shirin Farivar,[1,2] Reza Zati Keikha,[1] Reza Shiari,[3,4] and Farzaneh Jadali[3,4]

[1] *Department of Genetics, Faculty of Biological Science, Shahid Beheshti University (GC), Tehran 1983963113, Iran*
[2] *Laser and Plasma Research Institute, Shahid Beheshti University (GC), Tehran 1983963113, Iran*
[3] *Department of Pediatrics, Shahid Beheshti University of Medical Sciences, Mofid Children's Hospital, Tehran, Iran*
[4] *Pediatrics Infectious Research Center (PIRC), Shahid Beheshti University of Medical Sciences, Tehran, Iran*

Correspondence should be addressed to Shirin Farivar; s_farivar@sbu.ac.ir

Received 2 April 2013; Accepted 18 June 2013

Academic Editor: Natasa Tosic

Objectives. The B-cell-specific moloney leukemia virus insertion site 1 (the Bmi-1) gene is an important member in the family of polycomb group (PcG) genes that plays an oncogenic role in several types of cancer, but it's expression as a prognostic marker in pediatric brain tumors has not been indicated. *Materials and Methods*. The Bmi-1 gene expression, clinic pathological and prognostic significance in a series of pediatric brain tumors were examined by real-time PCR method in 56 pediatric brain tumors. *Results*. The Bmi-1 gene expression in various types of pediatric brain tumors compared to that in normal brain tissue was 4.85-fold. The relative expression varied from 8.64-fold in ependymomas to 2.89-fold in other types. Expression level in high-grade tumors compared to that in low-grade tumors was 2.5 times. In univariate survival analysis of the pediatric brain tumors, a significant association of high expression of the Bmi-1 with patient survival was demonstrated. In multivariate analysis, the Bmi-1 high expression provided significant independent prognostic factors. *Conclusion*. Increased expression of the Bmi-1 in pediatric brain tumors may be important in the acquisition of an aggressive phenotype. In addition, it can be used as a strong and independent molecular marker of prognosis in pediatric brain tumors.

1. Introduction

Brain tumors are the most common solid tumors and the second most frequent malignancy after leukemia in children [1]. So far, little is known about molecular mechanisms associated with these types of tumors. These tumors are the genotypically and phenotypically different from adult brain tumors [2, 3]. Five-year survival rate for children with brain tumors is estimated to be approximately 75% [4]. Gliomas comprises approximately 60% of cases among pediatric brain tumors, whereas the remaining 40% are heterogeneous and consist of medulloblastomas and other embryonal tumors (26%), craniopharyngiomas (4%), pineal tumors (1%), meningiomas (1%), and others [5]. Identification of molecular markers associated with pediatric brain tumors provides suitable conditions for treatment of these tumors. The B-cell-specific moloney leukemia virus insertion site 1 (Bmi-1) gene is an important member of the PRC1 complex. Members of PRC1 complex have been identified as transcriptional repressors [6–8]. The Bmi-1 mediates gene silencing by regulating chromatin structure, and it is essential for the maintenance and self-renewal of both haematopoietic and neural stem cells [9, 10]. This function of Bmi-1 depends on its ability to repress the INK4A locus. The INK4A locus as a target of Bmi-1 is a critical regulator of the p53 and Rb tumor suppressor pathways [11]. Thus, Bmi-1 would be the determining factor in the control of cell cycle. Overexpression of the Bmi-1 was found in high-grade B-cell non-Hodgkin Lymphomas (NHLs) [12], colorectal cancers [13], ovarian cancer, breast, cervical [14], skin cancer [15], neuroblastoma [16], and nonsmall cell lung cancer (NSCLC) [11]. Bmi-1 is known to be a useful prognostic marker in many cancers, including nasopharyngeal carcinoma [17], bladder cancer [18], gastric cancer [19], and others. The Bmi-1 expression as a prognostic marker in pediatric brain tumors has not been indicated. In this study, the Bmi-1 gene expression, clinicopathological, and prognostic significance in a series of pediatric brain tumors were examined.

2. Materials and Methods

2.1. Patients. A total of 56 pediatric brain tumors were obtained from archives of paraffin-embedded tissues between 2006 and 2012 at the Department of Pathology in Mofid Children's Hospital, Shahid Beheshti University of Medical Sciences. The selection of patients was based on distinctive pathologic diagnosis, availability of tissue, follow-up data, and not receiving radiation or chemotherapy. Pathological parameters and patient survival data were collected. These patients included 53.5% male and 46.5% female with mean age of 3.28 years. The pediatric brain tumor cases encompassed 20% medulloblastoma, 34% astrocytomas, 28% ependymomas, and 18% others (Primitive Neuro Ectodermal Tumors (PNET), gangliogliomas, and oligodendrogliomas). Clinicopathological characteristics of these patients were detailed in Table 1.

2.2. RNA Extraction and cDNA Synthesis. This protocol was used for extraction of total RNA from FFPE (formalin-fixed paraffin-embedded tissues) specimens [20]. Tissue sections were deparaffinized by 1.5 mL xylene at 37°C for 20 min and incubated in 1.5 mL 100% ethanol at 37°C for 30 min. 600 μL of RNA lysis buffer containing 10 mmol/L TrisHcl (pH8), 0.1 mmol/L EDTA (pH8), and 2% SDS (pH7.3) with 50 μL of 60 mg/mL proteinase K (Fermentas, Vilnius, and Lithuania) is added and incubated at 60°C for 16–20 h. Then total RNA was extracted by phenol chloroform method. The RNA concentration was measured using the Nano Drop 2000 (Thermo scientific, USA). Total RNA treated with DNase I (Invitrogen, Paisley, UK) to eliminate genomic DNA, for cDNA synthesis cDNA Accu Power Cycle Script RT PreMix (BioneerCo. Chungwon, South Korea), was used according to the manufacturer's instructions.

2.3. Real-Time PCR. Specific primers were designed for the Bmi-1 and Beta-actin as an internal control (Gen Bank accession numbers: NM-005180.8, NM-001101.3, Bmi-1 Forward: CTGCAGCTCGCTTCAAGATG. Bmi-1 Reverse: CACACACATCAGGTGGGGAT. Beta-actin Forward: ATGACTTAGTTGCGTTACACC. Beta-actin Reverse: TGCTGTCACCTTCACCGTTC) using oligo 7 software.

Real-time PCR reactions were performed using SYBR Green method with Accu Power Green Star qPCR Master Mix (BioneerCo. Chungwon, South Korea) on a Rotor-Gene 6000 (Corbett Research, Sydney, Australia). PCR was run as follows: 94°C for 10 min, amplification for 40 cycles with denaturation at 94°C for 10 seconds, annealing at 57°C for 10 seconds, and extension at 72°C for 15 seconds. All experiments were repeated in duplicate or triplicate. Relative expression results of real-time PCR were carried out by REST 2009 software (Relative Expression Software Tool, Corbett Research).

2.4. Statistical Analysis. Statistical analysis was implemented by using the SPSS statistical software package (standard version 18.0; SPSS, Chicago, USA). The association of the Bmi-1 gene expression with clinicopathological characteristics of pediatric brain tumor patients was assessed by T test and ANOVA test. The Kaplan Meier method was used for survival analysis, and a log-rank test was used to compare the differences among survival curves. The COX risk ratio model was used for multifactorial analysis on survival, where $P < 0.05$ had statistical significance.

Table 1: Correlation of the Bmi-1 gene expression to clinico-pathologic features of pediatric brain tumors.

	Cases	The Bmi-1 gene expression (fold change)	P value
All tumors	56	4.85	**0.009**
Sex			0.75
Male	30	4.50	
Female	26	5.35	
Embryonal/gliomas			**0.046**
Embryonal	16	3.59	
Gliomas	40	5.54	
Tumor grade			**0.03**
High grade	26	6.85	
Low grade	30	2.75	
Tumor type			0.061
Medulloblastoma	11	3.53	
Astrocytomas	19	5.11	
Ependymomas	16	8.64	
Other	10	2.89	

3. Results

3.1. Expression of the Bmi-1 in Pediatric Brain Tumors. The mean gene expression level of the Bmi-1 is used to segregate the patients into a low Bmi-1 gene expression (Bmi-1 expression < mean; $n = 32$) and a high Bmi-1gene expression (Bmi-1 expression > mean; $n = 24$). The Bmi-1 gene expression in various types of pediatric brain tumors compared to normal brain tissue was 4.85-fold ($P = 0.009$). The relative expression varied from 8.64-fold in ependymomas to 2.89-fold in other types. Expression level in high-grade tumors compared to low-grade tumors was 2.5 times (6.85 versus 2.75-fold change). The Bmi-1 gene expression in embryonal and gliomas tumors was 3.59- and 5.54-fold, respectively. The T test showed a significant difference between the Bmi-1 gene expression, embryonal/gliomas tumor, and high-grade/low-grade tumor ($P < 0.05$, Table 1).

3.2. Relationship between Clinicopathological Characteristics, Bmi-1 Gene Expression, and Pediatric Brain Tumor Patient Survival. In univariate survival analysis, the cumulative survival Kaplan-Meier curves were calculated according to the test. Differences in survival time were examined by Log-rank test. Kaplan-Meier curves showed a significant influence of the Bmi-1 gene expression ($P = 0.015$), high-grade/low-grade ($P = 0.011$) on patient survival. The mean survival time for patient with high expression levels of the Bmi-1 was 20.3 months compared to 39.6 months for patients with low

Table 2: Univariate survival analysis (Kaplan-Meier): survival times according to clinicopathological features and the Bmi-1 gene expression.

	Case	Mean survival time (months ± s.e.)	Chi-square	*P* value
Bmi-1 expression			5.87	**0.015**
High expression	24	20.31 ± 3.84		
Low expression	32	39.65 ± 5.90		
Sex			0.038	0.845
Male	30	35.28 ± 7.43		
Female	26	28.65 ± 4.25		
Embryonal/gliomas			1.88	0.17
Embryonal	16	36.23 ± 6.06		
Gliomas	40	23.53 ± 4.01		
Tumor grade			6.41	**0.011**
High grade	26	24.62 ± 5.52		
Low grade	30	34.44 ± 3.23		
Tumor type			1.43	0.21
Medulloblastoma	11	28.41 ± 4.47		
Astrocytomas	19	27.76 ± 5.44		
Ependymomas	16	19.46 ± 4.48		
Other	10	31.38 ± 7.77		

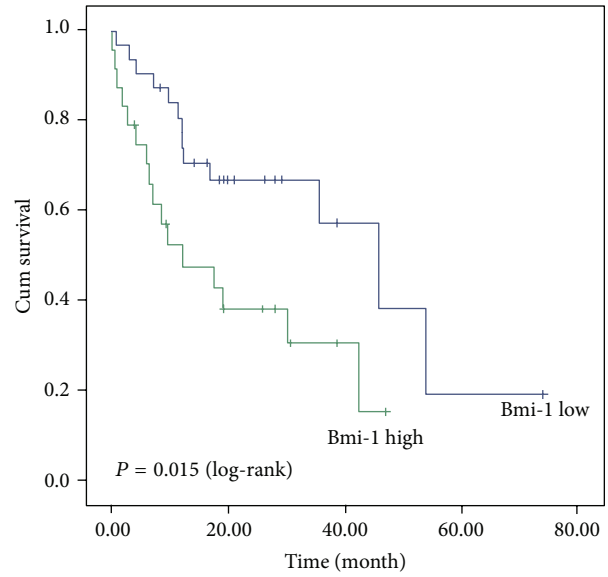

Figure 1: Univariate survival analysis of the Bmi-1 gene expression in all 56 pediatric brain tumors (32 patients with high expression and 24 patients with low expression). The Bmi-1 expression is a prognostic factor for survival ($P = 0.015$).

expression levels of the Bmi-1. The mean survival time was 24.6 months in high-grade tumors and 34.4 months in low-grade tumors. The time for M1, M2, M3, and M4 tumor stage was 37.6, 29.5, 24.9, and 20.1 months, respectively (Table 2). The comparison between survival curves of high expressions and low expression of the Bmi-1 is shown in Figure 1.

3.3. Independent Prognostic Factors of Pediatric Brain Tumors

3.3.1. Multivariate Cox Regression Analysis. The Bmi-1 expression and other clinicopathological parameters that were significant in univariate analysis (high grade/low grade) were examined in multivariate analysis. The results of this analysis showed that the Bmi-1 gene expression (B = 0.827, standard error = 0.403, Wald = 4.207, relative rate = 2.287, and $P < 0.05$) and high grade/low grade (B = 0.751, standard error = 0.393, Wald = 3.647, relative rate = 2.118, and $P < 0.05$) were independent prognostic factors of a patient with pediatric brain tumor.

4. Discussion

Pediatric brain tumors are the most common solid tumors of childhood which approximately 1,500 patients suffer from every year in the United States. These tumors are second in order after leukemia in overall cancer incidences and responsible for a high proportion of deaths [21–23]. Considering the high incidence and mortality of patients with pediatric brain tumors identifying a genetic molecular marker that is associated with patient survival is necessary. The gene, the Bmi-1, is an important member in the family of polycomb group genes that participates in the regulation of cell growth and proliferation as transcriptional repressor [6–8]. It is essential for self-renewal of both hematopoietic, neural stem cells and cancer stem cells [9, 10, 24, 25]. The Bmi-1 proto-oncogene has been upregulated in a large number of cancers such as breast cancer [14], skin cancer [15], lymphoma [12], leukemia [26], and other cancers and is known to be a useful prognostic marker in many cancers. As it is so widely expressed, the Bmi-1 expression cannot be used as a specific marker for pediatric brain tumors. This is the first study that evaluates the Bmi-1 gene expression by real-time PCR in various types of pediatric brain tumors in association with clinicopathological and prognostic significance. The results demonstrated that the expression level of the Bmi-1 was high in all types of the pediatric brain tumors, suggesting that the Bmi-1 gene expression is related to the incidence of pediatric brain tumors. A significant increasing expression of the Bmi-1 was observed from high-grade to low-grade tumors. These findings show that upregulated expression of the Bmi-1 in high-grade tumors may acquire phenotypic characteristics of malignant tumor cells. It also shows that at high expression levels, tumors biological behavior gets worse. We found that the expression of the Bmi-1 in gliomas tumors was significantly larger than embryonal tumors. It suggests that the Bmi-1 gene plays some roles in the progression of gliomas tumors. Therefore, clinically, the measurement of the Bmi-1 gene expression could be helpful in diagnosis of gliomas from embryonal tumors. Moreover, we found that the Bmi-1 gene expression and high- or low-grade tumors were predictor of survival as evidenced by Kaplan-Meier curves and long rank test. Multivariate Cox proportional hazards regression analysis demonstrated that high expression of the Bmi-1 in pediatric brain tumors was a predictor of short overall

survival, independent of high or low grade tumors. These findings show the important role of the Bmi-1 in pediatric brain tumors. Aberrant expression of the Bmi-1 in this tumors would change the composition of the PcG complex to proliferation cell cycle by transcription repressor of some genes such as p16Ink4A and p19Arf involved in tumor suppression, resulting in oncogenic effects, because the amounts of the Bmi-1 in the PcG complex determine its biochemical and biologic functions [27]. Moreover, overexpression of the Bmi-1 correlated with overexpression of PATCHED-1 (PTCH1), which is a reliable indicator of activation of the Shh pathway [27]. The abnormal activation of the Shh pathway is important in a subset of pediatric brain tumors [28]. Also it has been postulated that the Bmi-1 plays a role in self-renewal of cancer stem cells [24], so high expression of the Bmi-1 correlates with greater capacity of self-renewal and might represent the tumorigenesis and poor prognosis in pediatric brain tumors. We observed that data generated from FFPE material are comparable to data extracted from the fresh frozen samples; however, there was no significant association between the gene expression level and the time passed after formalin-fixed paraffin embedding.

5. Conclusion

In this study, to our knowledge, for the first time, we describe the Bmi-1 gene expression in various types of pediatric brain tumors. Our results demonstrated that increased expression of the Bmi-1 in pediatric brain tumors may be important in the acquisition of an aggressive phenotype. In addition, our study introduces the Bmi-1 expression as a strong and independent molecular marker of prognosis in pediatric brain tumors in addition to providing a specific target site for targeting therapy.

Acknowledgments

The authors are very grateful to Pediatric Infectious Research Center of Shahid Beheshti University of Medical Sciences and Mofid Children's Hospital for the excellent technical assistance.

References

[1] J. Li, T. D. Thompson, J. W. Miller, L. A. Pollack, and S. L. Stewart, "Cancer incidence among children and adolescents in the United States, 2001–2003," *Pediatrics*, vol. 121, no. 6, pp. e1470–e1477, 2008.

[2] D. Faury, A. Nantel, S. E. Dunn et al., "Molecular profiling identifies prognostic subgroups of pediatric glioblastoma and shows increased YB-1 expression in tumors," *Journal of Clinical Oncology*, vol. 25, no. 10, pp. 1196–1208, 2007.

[3] T. Sung, D. C. Miller, R. L. Hayes, M. Alonso, H. Yee, and E. W. Newcomb, "Preferential inactivation of the p53 tumor suppressor pathway and lack of EGFR amplification distinguish de novo high grade pediatric astrocytomas from de novo adult astrocytomas," *Brain Pathology*, vol. 10, no. 2, pp. 249–259, 2000.

[4] G. Perilongo, "Considerations on the role of chemotherapy and modern radiotherapy in the treatment of childhood low grade glioma," *Journal of Neuro-Oncology*, vol. 75, no. 3, pp. 301–307, 2005.

[5] P. Kaatsch, C. H. Rickert, J. Kühl, J. Schüz, and J. Michaelis, "Populationbased epidemiologic data on brain tumors in German children," *Cancer*, vol. 92, no. 12, pp. 3155–3164, 2001.

[6] J. A. Simon and R. E. Kingston, "Mechanisms of Polycomb gene silencing: knowns and unknowns," *Nature Reviews Molecular Cell Biology*, vol. 10, no. 10, pp. 697–708, 2009.

[7] A. Sparmann and M. Van Lohuizen, "Polycomb silencers control cell fate, development and cancer," *Nature Reviews Cancer*, vol. 6, no. 11, pp. 846–856, 2006.

[8] V. Orlando, "Polycomb, epigenomes, and control of cell identity," *Cell*, vol. 112, no. 5, pp. 599–606, 2003.

[9] A. V. Molofsky, R. Pardal, T. Iwashita, I.-K. Park, M. F. Clarke, and S. J. Morrison, "Bmi-1 dependence distinguishes neural stem cell self-renewal from progenitor proliferation," *Nature*, vol. 425, no. 6961, pp. 962–967, 2003.

[10] I.-K. Park, D. Qian, M. Kiel et al., "Bmi-1 is required for maintenance of adult self-renewing haematopoietic stem cells," *Nature*, vol. 423, no. 6937, pp. 302–305, 2003.

[11] S. Vonlanthen, J. Heighway, H. J. Altermatt et al., "The bmi-1 oncoprotein is differentially expressed in non-small cell lung cancer and correlates with INK4A-ARF locus expression," *British Journal of Cancer*, vol. 84, no. 10, pp. 1372–1376, 2001.

[12] F. J. Van Kemenade, F. M. Raaphorst, T. Blokzijl et al., "Coexpression of BMI-1 and EZH2 polycomb-group proteins is associated with cycling cells and degree of malignancy in B-cell non-Hodgkin lymphoma," *Blood*, vol. 97, no. 12, pp. 3896–3901, 2001.

[13] J. H. Kim, S. Y. Yoon, C.-N. Kim et al., "The Bmi-1 oncoprotein is overexpressed in human colorectal cancer and correlates with the reduced p16INK4a/p14ARF proteins," *Cancer Letters*, vol. 203, no. 2, pp. 217–224, 2004.

[14] A. Honig, C. Weidler, S. Häusler et al., "Overexpression of polycomb protein BMI-1 in human specimens of breast, ovarian, endometrial and cervical cancer," *Anticancer Research*, vol. 30, no. 5, pp. 1559–1564, 2010.

[15] S. Balasubramanian, K. Lee, G. Adhikary, R. Gopalakrishnan, E. A. Rorke, and R. L. Eckert, "The Bmi-1 polycomb group gene in skin cancer: regulation of function by (-)-epigallocatechin-3-gallate," *Nutrition Reviews*, vol. 66, no. 1, pp. S65–S68, 2008.

[16] H. Cui, B. Hu, T. Li et al., "Bmi-1 is essential for the tumorigenicity of neuroblastoma cells," *The American Journal of Pathology*, vol. 170, no. 4, pp. 1370–1378, 2007.

[17] L.-B. Song, M.-S. Zeng, W.-T. Liao et al., "Bmi-1 is a novel molecular marker of nasopharyngeal carcinoma progression and immortalizes primary human nasopharyngeal epithelial cells," *Cancer Research*, vol. 66, no. 12, pp. 6225–6232, 2006.

[18] Z. K. Qin, J. A. Yang, Y. L. Ye et al., "Expression of Bmi-1 is a prognostic marker in bladder cancer," *BMC Cancer*, vol. 9, no. 61, 2009.

[19] J.-H. Liu, L.-B. Song, X. Zhang et al., "Bmi-1 expression predicts prognosis for patients with gastric carcinoma," *Journal of Surgical Oncology*, vol. 97, no. 3, pp. 267–272, 2008.

[20] F. Zhang, Z.-M. Wang, H.-Y. Liu et al., "Application of RT-PCR in formalin-fixed and paraffin-embedded lung cancer tissues," *Acta Pharmacologica Sinica*, vol. 31, no. 1, pp. 111–117, 2010.

[21] D. Miltenburg, D. F. Louw, and G. R. Sutherland, "Epidemiology of childhood brain tumors," *Canadian Journal of Neurological Sciences*, vol. 23, no. 2, pp. 118–122, 1996.

[22] I. F. Pollack, "Brain tumors in children," *The New England Journal of Medicine*, vol. 331, no. 22, pp. 1500–1507, 1994.

[23] F. Sala, E. Colarusso, C. Mazza, A. Talacchi, and A. Bricolo, "Brain tumors in children under 3 years of age: recent experience (1987–1997) in 39 patients," *Pediatric Neurosurgery*, vol. 31, no. 1, pp. 16–26, 1999.

[24] M. Al-Hajj and M. F. Clarke, "Self-renewal and solid tumor stem cells," *Oncogene*, vol. 23, no. 43, pp. 7274–7282, 2004.

[25] S. K. Singh, I. D. Clarke, T. Hide, and P. B. Dirks, "Cancer stem cells in nervous system tumors," *Oncogene*, vol. 23, no. 43, pp. 7267–7273, 2004.

[26] M. Sawa, K. Yamamoto, T. Yokozawa et al., "BMI-1 is highly expressed in M0-subtype acute myeloid leukemia," *International Journal of Hematology*, vol. 82, no. 1, pp. 42–47, 2005.

[27] C. Leung, M. Lingbeek, O. Shakhova et al., "Bmi1 is essential for cerebellar development and is overexpressed in human medulloblastomas," *Nature*, vol. 428, no. 6980, pp. 337–341, 2004.

[28] J. T. Romer, H. Kimura, S. Magdaleno et al., "Suppression of the Shh pathway using a small molecule inhibitor eliminates medulloblastoma in $Ptc1^{+/-}p53^{-/-}$ mice," *Cancer Cell*, vol. 6, no. 3, pp. 229–240, 2004.

Hindawi Publishing Corporation
BioMed Research International
Volume 2013, Article ID 740195, 5 pages
http://dx.doi.org/10.1155/2013/740195

Clinical Study

Diffusion-Weighted Magnetic Resonance Application in Response Prediction before, during, and after Neoadjuvant Radiochemotherapy in Primary Rectal Cancer Carcinoma

Daniela Musio,[1] Francesca De Felice,[1] Anna Lisa Magnante,[1] Maria Ciolina,[2] Carlo Nicola De Cecco,[2] Marco Rengo,[2] Adriano Redler,[3] Andrea Laghi,[2] Nicola Raffetto,[1] and Vincenzo Tombolini[1,4]

[1] *Department of Radiotherapy, Policlinico Umberto I "Sapienza" University of Rome, Viale Regina Elena 326, 00161 Rome, Italy*
[2] *Department of Radiological Sciences, Oncology and Pathology, Policlinico Umberto I "Sapienza" University of Rome, Polo Pontino, Corso della Repubblica 79, 04100 Latina, Italy*
[3] *Department of Surgical Sciences, Policlinico Umberto I "Sapienza" University of Rome, Viale Regina Elena 326, 00161 Rome, Italy*
[4] *Spencer-Lorillard Foundation, Viale Regina Elena 291, 00161 Rome, Italy*

Correspondence should be addressed to Daniela Musio; daniela.musio@libero.it

Received 16 May 2013; Accepted 24 June 2013

Academic Editor: Aleksandra Nikolic

Introduction. Our interest was to monitor treatment response using ADC value to predict response of rectal tumour to preoperative radiochemotherapy. *Materials and Methods*. Twenty-two patients were treated with long course of radiochemotherapy, followed by surgery. Patients were examined by diffusion-weighted imaging MRI at three-time points (prior, during, and after radiochemotherapy) and were classified as responders and nonresponders. *Results*. A statistical significant correlation was found between preradiochemotherapy ADC values and during treatment ADC values, in responders ($F = 21.50$, P value < 0.05). An increase in ADC value during treatment was predictive of at least a partial response. *Discussion*. Response of tumour to neoadjuvant therapy cannot be easily evaluated, and such capability might be of great importance in clinical practice, because the number of irradiated and operated patients may be superior to the number of who will really benefit from this multimodal treatment. A reliable prediction of the final clinical TN stage would allow radiotherapist to adapt multidisciplinary approach to a less invasive management, sparing surgical procedure in responder patients or even allowing an early surgery in nonresponders, which would significantly reduce radiochemotherapy related toxicity. *Conclusion*. Early evaluation of response during neoadjuvant radiochemotherapy treatment shows great promise to predict tumour response.

1. Introduction

Local control rates have improved in rectal cancer [1]. Nowadays, preoperative radiochemotherapy (RT-CHT) is standard treatment for patients with locally advanced rectal cancer, due to less acute toxicity, greater tumour response, and higher rates of sphincter preservation when compared with adjuvant therapy [2]. Improvement in pathological complete response (pCR) and feasibility of R0 resections on operative specimen have encouraged researchers to investigate a nonsurgical approach for clinical stage 0 disease following radiochemotherapy [3]. But an appropriate identification of complete clinical response is mandatory. Therefore, the chance to predict the response to neoadjuvant therapy before surgery would allow individualizing treatment. Diffusion-weighted magnetic resonance (DW-MRI) as an imaging biomarker has the potentiality for early evaluation of the response to RT-CHT treatment in a large section of cancer types, including head and neck tumours, pancreatic tumours, cervical tumours, and rectal cancer [4].

DW-MRI explores the random Brownian motion of water molecules in intracellular and extracellular space and, measuring water motion, reflects the biological changes in the tumour microenvironment, before and after treatment [5].

The aim of this study was to establish whether the use of DW-MRI as an imaging modality for response assessment during and after RT-CHT, in patients with locally advanced rectal cancer, can predict treatment outcomes, with the goal of improving RT-CHT technique or modified surgical approach.

2. Materials and Methods

2.1. Patient Selection. This was a prospective study and it was approved by our Institutional Review Board. Patients were enrolled after singing an informed consent. All patients had histologically proven rectal adenocarcinoma, clinically staged on pelvic magnetic resonance imaging (MRI) or endorectal ultrasound as T3-4 and/or with positive regional lymph-node, without any evidence of distant metastases by other imaging modalities. Patients were excluded from the study in case of synchronous tumours, cardiovascular disease, history of neurological or psychiatric disorders, or previous pelvic radiotherapy, contraindication to MRI examination.

2.2. Treatment Plan. All patients were treated with a long course of RT-CHT. Radiation therapy was delivered with a 3D-conformational multiple field technique at a dose of 45 Gy (in 25 daily fractions of 1,8 Gy given in 5 weeks) to the whole pelvis, plus a 5,4–9 Gy (in 3–5 daily fractions of 1,8 Gy) to the tumour volume, with 6–15 MV energy photons. Chemotherapy consisted of 2-hour oxaliplatin infusion 50 mg/m^2 on the first day of each week of radiotherapy and five daily continuous infusion of 5-FU 200 mg/m^2/die. The choice of adding oxaliplatin to the standard schedule of 5-FU was dictated by our previous experience, in which the addition of oxaliplatin has resulted in a high rate of pathological complete response with acceptable toxicity [6].

Surgery was planned 7–9 weeks after the end of RT-CHT treatment. The type of surgery was chosen by the surgeon.

2.3. Magnetic Resonance Imaging. All patients were examined by MRI at three-time points: one week prior to RT-CHT (pre-RT-CHT MRI), at the beginning of the third week of RT-CHT (during RT-CHT MRI), and 6 weeks after the end of RT-CHT (post-RT-CHT MRI). All pre-, during, and post-RT-CHT MRI examinations were performed with a 3.0 T MR system (Discovery 750; GE Healthcare, Milwaukee, WI, USA) equipped with high-performance gradients (amplitude, 50 mT/m; slew rate 200 T/sec) using an 8-channel-phased array cardiac coil in the supine position. All patients underwent diffusion-weighted imaging (DWI) in addition to the conventional rectal MRI protocol. Axial DWI images were obtained using the single-shot echo-planar imaging technique. A spectral adiabatic inversion recovery fat saturation technique was used. Diffusion-encoding gradients were applied as a bipolar pair at 11 b-values of 0, 10, 20, 30, 50, 60, 100, 200, 600, 800, and 1000 sec/mm^2, along the three orthogonal directions of the motion-probing gradients. The acquisition was separated in two blocks: the first block included $b0$, $b10$, $b20$, $b30$, $b50$, $b60$, and $b100$ while the second block included $b200$, $b600$, $b800$, and $b1000$; each block was acquired in free-breathing. The total acquisition time for DWI was approximately 5 minutes.

2.4. Imaging Analysis. Pre-, during, and post-RT-CHT MR images were analyzed independently by two gastrointestinal radiologists assessing on a dedicated workstation with advanced imaging analysis software. Tumour dimension and DWI parameter (apparent diffusion coefficient, ADC) were evaluated. Quantitative analysis of DWI was performed using the MATLAB code (Release 7.10.0, The Mathworks Inc., Natick, MA, USA). To calculate ADC, a region of interest (ROI) was drawn on the rectal cancer on b800 images (mean size 165 mm^2; range, 100–230 mm^2). Then ROI was transferred to all b-values images using an automated process. Mean signal intensities (SI) were obtained for each ROI with careful exclusion of the necrotic or cystic portions inside the tumour.

The signal variation with increasing b-values was modeled by using the following biexponential function [7]: $S_b/S_0 = (1 - f)e^{-bD} + fe^{-b(D+D^*)}$, where S_b is the mean signal intensity with diffusion weighting b, S_0 is the mean signal intensity for b-value of 0 s/mm^2, f is the perfusion fraction, D, the diffusion coefficient (in mm^2/s), and D^* is the perfusion-related diffusion coefficient (in mm^2/s).

2.5. Data Analysis. Pretreatment stage (cT cN) was compared with pathologic stage (ypT ypN). A partial response to treatment was defined as downstaging, or reduction of at least one level in T or N staging between the baseline RM exam and histopathological staging. Pathological complete response (pCR) was defined as the absence of any residual tumour cells detected in the operative specimen (ypT0 ypN0). No response to treatment was defined as stable or progressive disease.

2.6. Statistical Analysis. The mean ADC values pre-, during, and post-RT-CHT were compared with Fisher's test (F-test) both in all patients and between responders versus nonresponders. Following one-way analysis of variance (ANOVA), we compare the mean ADC of one group with the mean ADC of another at each time, using Fisher's least significant Difference test (LSD-test). A P value < 0.05 was considered statistically significant in the F-test and P value < 0.005 in the LSD-test to improve test power.

3. Results

Between February 2011 and May 2012, 22 consecutive patients, 12 men (mean age: 63,2 years; range: 50–71 years) and 10 women (mean age: 63,2 years; range: 47–81 years), were enrolled in the study. All patients underwent programmed RT-CHT neoadjuvant treatment. After RT-CHT, 15 (68.2%) and 7 (31.8%) of the 22 patients were classified as responders and nonresponders, respectively. Twenty patients underwent surgery, and pathological evaluation was performed in all of them. Fifteen patients showed a downstaging on the surgical evaluation. Of these, 9 patients (60%) had a pCR.

Table 1: Mean ADC value of responders and nonresponders at each time point.

Group	Time point			F value	P value
	Pre-RT-CHT	During RT-CHT	Post-RT-CHT		
Responders	0.87 ± 0.23	1.13 ± 0.26	1.28 ± 0.32	21.50	<0.05
Nonresponders	0.75 ± 0.14	1.03 ± 0.10	1.18 ± 0.38	8.31	>0.05

Data at time point are means ± standard deviations.

Tumour ADC values of all 22 patients are reported in Table 1. The mean initial ADC value in patients with at least partial response was not significantly different than that in the nonresponders group. The evolution of the ADC values in the two groups was different. A statistical significant correlation was found between pre-RT-CHT ADC values and during treatment ADC values, in the responders ($F = 21.50$, P value < 0.05), so, this hypothesis was tested using least significant difference (LSD) method and result confirmed that the difference was significant ($T = 4.26$; P value < 0.005). No significant difference was observed among the during ADC and the posttreatment ADC values ($T = 2.18$; P value > 0.005), whereas, in the nonresponders group, F-test fails ($F = 8.31$, P value > 0.05).

4. Discussion

Multimodal treatment approach, combining radiotherapy, chemotherapy, and surgery, is the standard of care in locally advanced rectal cancer. RT-CHT gives the high chance of tumour downsizing and tumour downstaging, including pCR, as proven in randomised phase III trials, in which pCR rates range from 13 to 19.2% depending on preoperative RT-CHT regimens [8–10]. Moreover, several data demonstrated that a prolonged interval between neoadjuvant RT-CHT and surgery may still further improve pCR rates [11].

Pelvic magnetic resonance imaging (MRI) is the recommended diagnostic procedure for initial staging in rectal cancer [2], and it has recently been considered a noninvasive modality able to monitor treatment response, due to diffusion-weighted imaging (DWI) [12]. DW-MRI depends on the microscopic Brownian motion of water; the difference in water motion is quantified by the apparent diffusion coefficient (ADC), and it is inversely correlated to the tissue cellularity and the integrity of cell membranes. DW-MRI, therefore, provides microstructural information on tissue characterization and can estimate changes in cellularity of the tumour microenvironment, due to cellular death and vascular changes in response to treatment [5, 13]. So DW-MRI can help to discriminate posttreatment changes from residual active tumour. Usually, malignant tumour has lower ADC values, because of higher cellularity, tissue disorganization, and increased extracellular space tortuosity. After therapy, an increase in ADC values states a successful response to treatment, due to extracellular edema, and it is detectable before any change in tumour size [13, 14]. But water diffusion properties of tumour are not always so easy to interpret: in the same lesion can coexist different area with different cellular and vascular components, which, consequently, influence DWI properties [15]. So, the correlation ADC value-cellularity is not always preserved for adenocarcinomas and necrotic lesions, especially [13]. Lemaire et al. [16] evaluated induced rat mammary tumour response to chemotherapy using DW-MRI. Results showed that a high ADC value before treatment characterised tumours with high percentages of necrosis, predicting a worse chemosensitivity. Moreover, the ADC value varies dramatically during treatment, due to cell necrosis and lysis, and it makes difficult to understand the effects of treatment on DWI [15].

In rectal cancer DW-MRI has been used to predict tumour response to RT-CHT. Dzik-Jurasz et al. [17] compared baseline to posttreatment tumour ADC values in 14 patients with clinically advanced rectal adenocarcinoma. They noted poor response in pretreatment high tumour ADC, strengthening Lemaire's known relation between necrosis and worse response to treatment. Hein et al. [18] evaluated ADC in 16 patients with advanced rectal carcinoma submitted to neoadjuvant RT-CHT. After therapy, they reported a significantly lower ADC values in responders patients than in nonresponders. More recently Lambrecht et al. [19] came to similar correlation in 22 patients with adenocarcinoma of the rectum; they find that the initial ADC was significantly lower in patients with a pCR compared to patients with no pCR after RT-CHT.

Our interest was to monitor treatment response using ADC value to predict response of rectal tumour to RT-CHT. In this limited number of patients the initial ADC value shows no correlation with pCR. The initial ADC was not significantly different in responders versus nonresponders group. An ADC increase was observed in patients with at least a partial response to treatment. We have found that patients who respond to treatment show a significant rise in the ADC values after two weeks of therapy. An increase in the ADC value during treatment was predictive of at least a partial response. Our cohort group ($n = 22$) was, however, too small for a subgroup analysis. Study population increase would be necessary to provide predictive factors, such as ADC cut-off value.

Four studies already reported on the use of DW-MRI during and after preoperative RT-CHT for rectal cancer [20–23]. The main message was similar. Changes in ADC values during course of RT-CHT correlated to biological changes in the tumour tissue, predicting tumour downstaging.

Kremser et al. [20] studied changes of ADC in 8 patients with primary rectal carcinoma. ADC values were determined and compared weekly during RT-CHT. Results showed a significant increase in ADC value during 1st week of treatment in responded group. Hein et al. [22] analyzed diffusion data of 9 patients undergoing preoperative RT-CHT for rectal cancer

carcinoma. They demonstrated significant radiobiological changes during therapy by the detection of changes in water mobility.

Sun et al. [21] analysed, in a group of 37 patients with primary rectal carcinoma, whether changes in ADC values correlate with tumour histopathologic downstaging. ADC values were calculated at four-time point: before RT-CHT, at the end of the 1st week of therapy, at the end of the 2nd week of therapy, and before surgery. The study group was divided in downstaged patients and nondownstaged patients, based on pathological evaluation. At 1st week a significant ADC increase was recorded in the downstaged group. Barbaro et al. [23] evaluated prospectively a total of 62 patients with locally advanced nonmucinous rectal cancer. Patients underwent DW-MRI before, during (mean 12 days), and 6–8 weeks after RT-CHT. During treatment, tumour ADC was significantly greater in the responders group than in the nonresponders.

In clinical practice, according to Response Evaluation Criteria in Solid Tumors Group (RECIST), the objective tumour response to treatment is only characterized by the measurement of the lesion's longest diameter [24]. DW-MRI has been considered in the National Cancer Institute (NCI) consensus conference as integral part of oncologic imaging practice [13]. However, in case of clinical complete response (cCR) after preoperative RT-CHT, the standard treatment remains total mesorectal excision (TME) at the moment [2], because the benefit in using DW-MRI in the prediction of preoperative neoadjuvant therapy response in locally advanced rectal cancer is still debated [25].

Response of the tumour to neoadjuvant therapy cannot be easily evaluated, and such capability might be of great importance in clinical practice, because the number of irradiated and operated patients may be superior to the number of who will really benefit from this multimodal treatment. A reliable prediction of the final clinical T and N stages would allow the radiotherapist to adapt the multidisciplinary approach to a less invasive management, sparing the surgical procedure in responder patients or even allowing an early surgery in nonresponders, which would significantly reduce RT-CHT related toxicity. So an earlier and accurate prediction of the pathological tumour response during preoperative treatment could enable to guide modifications of treatment protocol. Further evidence is necessary to validate these observations.

5. Conclusions

DW-MRI provides important clinical information in management of patients with locally advanced rectal cancer. An early evaluation of response during neoadjuvant RT-CHT treatment shows great promise to predict tumour response. In our series, an increase in the ADC value during treatment was predictive of at least a partial response, with response being defined by pathological examination. DW-MRI should be tested in a large clinical study to demonstrate its accuracy to differentiate responders to nonresponders patients.

Conflict of Interests

The authors declare that they have no conflict of interests.

References

[1] F. Bonnetain, J. F. Bosset, J. P. Gerard et al., "What is the clinical benefit of preoperative chemoradiotherapy with 5FU/leucovorin for T3-4 rectal cancer in a pooled analysis of EORTC 22921 and FFCD 9203 trials: surrogacy in question?" *European Journal of Cancer*, vol. 48, no. 12, pp. 1781–1790, 2012.

[2] H. J. Schmoll, E. Van Cutsem, A. Stein et al., "ESMO Consensus Guidelines for management of patients with colon and rectal cancer. A personalized approach to clinical decision making," *Annals of Oncology*, vol. 23, no. 10, pp. 2479–2516, 2012.

[3] A. Habr-Gama, R. O. Perez, W. Nadalin et al., "Operative versus nonoperative treatment for stage 0 distal rectal cancer following chemoradiation therapy: long-term results," *Annals of Surgery*, vol. 240, no. 4, pp. 711–718, 2004.

[4] H. C. Thoeny and B. D. Ross, "Predicting and monitoring cancer treatment response with diffusion-weighted MRI," *Journal of Magnetic Resonance Imaging*, vol. 32, no. 1, pp. 2–16, 2010.

[5] D. M. Koh and D. J. Collins, "Diffusion-weighted MRI in the body: applications and challenges in oncology," *American Journal of Roentgenology*, vol. 188, no. 6, pp. 1622–1635, 2007.

[6] D. Musio, F. De Felice, N. Bulzonetti et al., "Neoadjuvant-intensified treatment for rectal cancer: time to change?" *World Journal of Gastroenterology*, vol. 19, no. 20, Article ID 237169, pp. 3052–3061, 2013.

[7] D. Le Bihan, E. Breton, D. Lallemand, M.-L. Aubin, J. Vignaud, and M. Laval-Jeantet, "Separation of diffusion and perfusion in intravoxel incoherent motion MR imaging," *Radiology*, vol. 168, no. 2, pp. 497–505, 1988.

[8] C. Aschele, L. Cionini, S. Lonardi et al., "Primary tumor response to preoperative chemoradiation with or without oxaliplatin in locally advanced rectal cancer: pathologic results of the STAR-01 randomized phase III trial," *Journal of Clinical Oncology*, vol. 29, no. 20, pp. 2773–2780, 2011.

[9] J.-P. Gérard, D. Azria, S. Gourgou-Bourgade et al., "Comparison of two neoadjuvant chemoradiotherapy regimens for locally advanced rectal cancer: results of the phase III trial accord 12/0405-Prodige 2," *Journal of Clinical Oncology*, vol. 28, no. 10, pp. 1638–1644, 2010.

[10] R. Rödel, T. Liersch, H. Becker et al., "Preoperative chemoradiotherapy and postoperative chemotherapy with fluorouracil and oxaliplatin versus fluorouracil alone in locally advanced rectal cancer: initial results of the German CAO/ARO/AIO-04 randomised phase 3 trial," *The Lancet Oncology*, vol. 13, no. 7, pp. 679–687, 2012.

[11] H. G. Moore, A. E. Gittleman, B. D. Minsky et al., "Rate of pathologic complete response with increased interval between preoperative combined modality therapy and rectal cancer resection," *Diseases of the Colon and Rectum*, vol. 47, no. 3, pp. 279–286, 2004.

[12] Y. C. Kim, J. S. Lim, K. C. Keum et al., "Comparison of diffusion-weighted MRI and MR volumetry in the evaluation of early treatment outcomes after preoperative chemoradiotherapy for locally advanced rectal cancer," *Journal of Magnetic Resonance Imaging*, vol. 34, no. 3, pp. 570–576, 2011.

[13] A. R. Padhani, G. Liu, D. Mu-Koh et al., "Diffusion-weighted magnetic resonance imaging as a cancer biomarker: consensus and recommendations," *Neoplasia*, vol. 11, no. 2, pp. 102–125, 2009.

[14] M. Zhao, J. G. Pipe, J. Bonnett, and J. L. Evelhoch, "Early detection of treatment response by diffusion-weighted ^{1}H-NMR

spectroscopy in a murine tumour in vivo," *British Journal of Cancer*, vol. 73, no. 1, pp. 61–64, 1996.

[15] D. Boone, S. A. Taylor, and S. Halligan, "Diffusion Weighted MRI: overview and implications for rectal cancer management," *Colorectal Disease*, vol. 15, no. 6, pp. 655–661, 2013.

[16] L. Lemaire, F. A. Howe, L. M. Rodrigues, and J. R. Griffiths, "Assessment of induced rat mammary tumour response to chemotherapy using the apparent diffusion coefficient of tissue water as determined by diffusion-weighted 1H-NMR spectroscopy in vivo," *Magnetic Resonance Materials in Physics, Biology and Medicine*, vol. 8, no. 1, pp. 20–26, 1999.

[17] A. Dzik-Jurasz, C. Domenig, M. George et al., "Diffusion MRI for prediction of response of rectal cancer to chemoradiation," *The Lancet*, vol. 360, no. 9329, pp. 307–308, 2002.

[18] P. A. Hein, C. Kremser, W. Judmaier et al., "Diffusion-weighted MRI—a new parameter for advanced rectal carcinoma?" *RoFo Fortschritte auf dem Gebiet der Rontgenstrahlen und der Bildgebenden Verfahren*, vol. 175, no. 3, pp. 381–386, 2003.

[19] M. Lambrecht, C. Deroose, S. Roels et al., "The use of FDG-PET/CT and diffusion-weighted magnetic resonance imaging for response prediction before, during and after preoperative chemoradiotherapy for rectal cancer," *Acta Oncologica*, vol. 49, no. 7, pp. 956–963, 2010.

[20] C. Kremser, W. Judmaier, P. Hein, J. Griebel, P. Lukas, and A. de Vries, "Preliminary results on the influence of chemoradiation on apparent diffusion coefficients of primary rectal carcinoma measured by magnetic resonance imaging," *Strahlentherapie und Onkologie*, vol. 179, no. 9, pp. 641–649, 2003.

[21] Y.-S. Sun, X.-P. Zhang, L. Tang et al., "Locally advanced rectal carcinoma treated with preoperative chemotherapy and radiation therapy: preliminary analysis of diffusion-weighted MR imaging for early detection of tumor histopathologic downstaging," *Radiology*, vol. 254, no. 1, pp. 170–178, 2010.

[22] P. A. Hein, C. Kremser, W. Judmaier et al., "Diffusion-weighted magnetic resonance imaging for monitoring diffusion changes in rectal carcinoma during combined, preoperative chemoradiation: preliminary results of a prospective study," *European Journal of Radiology*, vol. 45, no. 3, pp. 214–222, 2003.

[23] B. Barbaro, R. Vitale, V. Valentini et al., "Diffusion-weighted magnetic resonance imaging in monitoring rectal cancer response to neoadjuvant chemoradiotherapy," *International Journal of Radiation Oncology, Biology, Physics*, vol. 83, no. 2, pp. 594–599, 2011.

[24] P. Therasse, S. G. Arbuck, E. A. Eisenhauer et al., "New guidelines to evaluate the response to treatment in solid tumors," *Journal of the National Cancer Institute*, vol. 92, no. 3, pp. 205–216, 2000.

[25] L. M. Wu, J. Zhu, J. Hu et al., "Is there a benefit in using magnetic resonance imaging in the prediction of preoperative neoadjuvant therapy response in locally advanced rectal cancer?" *International Journal of Colorectal Disease*. In press.

Hindawi Publishing Corporation
BioMed Research International
Volume 2013, Article ID 389672, 7 pages
http://dx.doi.org/10.1155/2013/389672

Research Article

Positron Emission Tomography as a Surrogate Marker for Evaluation of Treatment Response in Patients with Desmoid Tumors under Therapy with Imatinib

Bernd Kasper,[1] Antonia Dimitrakopoulou-Strauss,[2] Lothar R. Pilz,[3] Ludwig G. Strauss,[2] Christos Sachpekidis,[2] and Peter Hohenberger[1]

[1] *Sarcoma Unit, ITM—Interdisciplinary Tumor Center Mannheim, Mannheim University Medical Center, University of Heidelberg, Theodor-Kutzer-Ufer 1–3, 68167 Mannheim, Germany*
[2] *Clinical Cooperation Unit Nuclear Medicine, German Cancer Research Center, Im Neuenheimer Feld 280, 69120 Heidelberg, Germany*
[3] *Medical Faculty Mannheim, University of Heidelberg, Theodor-Kutzer-Ufer 1–3, 68167 Mannheim, Germany*

Correspondence should be addressed to Bernd Kasper; mail@berndkasper.de

Received 11 March 2013; Accepted 7 May 2013

Academic Editor: Aleksandra Nikolic

We used 2-deoxy-2-[^{18}F] fluoro-D-glucose (FDG) positron emission tomography (PET) to evaluate patients with desmoid tumors undergoing therapy with imatinib. The study included 22 patients with progressive disease (PD) of a biopsy proven desmoid tumor treated orally with imatinib 800 mg daily. Patients were examined using PET prior to onset of therapy and during treatment. Restaging was performed in parallel using computed tomography (CT) and/or magnetic resonance imaging (MRI). Outcome of 22 evaluable patients was as follows: five patients with partial response (PR); twelve patients with stable disease (SD) accounting for 77% with non-progressive disease; five patients showed PD. A 30% decrease of the mean average standardized uptake value (SUV) of sequential PET examinations could be demonstrated; no patient demonstrated a substantial increase in SUV. Patients with PR/SD were matched to a group of nonprogressive disease and tested versus PD. The initial average SUV and SUV_{max} seem to be candidates for a response prediction with an approximate P-value of *0.06553* and *0.07785*, respectively. This is the first larger series of desmoid patients monitored using PET showing that early SUV changes may help to discriminate responders from nonresponders and, thus, to decide whether imatinib therapy should be continued.

1. Introduction

According to the World Health Organisation, desmoid tumors are defined as "clonal fibroblastic proliferations that arise in the deep soft tissues and are characterized by infiltrative growth and a tendency toward local recurrence but an inability to metastasize." They may affect all sites including extremities, trunk, and abdomen with an incidence less than 3% of soft tissue sarcomas [1, 2]. They occur between the age of 15 and 60 years, but particularly during early adolescence and with a peak age of about 30 years. There is a special relationship between desmoids and familial adenomatous polyposis (FAP, Gardner syndrome) with an incidence from 3.5% to 32% [3, 4]. Surgical resection remains the therapeutic mainstay in first-line treatment for locally circumscribed desmoid tumors. However, R0 resection is not always possible, and adjuvant radiotherapy is, therefore, common. Due to their locally aggressive growth, desmoids have a high relapse rate after surgery and/or radiotherapy; they can often take a multiply relapsing, multifocal course and, therefore, not be amenable to curative surgical treatment. In this situation, pharmacotherapy is used to prevent disease progression comprising antihormonal therapy, nonsteroidal anti-inflammatory drugs, or chemotherapy with highly variable results [5, 6]. The primary aim is to preserve the patient's quality of life which is threatened by loss of function and pain

caused by the proliferative disease. It has not yet been possible to establish an optimal therapeutic strategy or treatment algorithm for this disease.

Imatinib is a selective inhibitor of the tyrosine kinases ABL and KIT and platelet-derived growth factor receptors α and β (PDGFRA and PDGFRB) being effective in patients with Philadelphia chromosome-positive chronic myelogenous leukemia and metastatic gastrointestinal stromal tumors (GIST) [7, 8]. Initial data on the use of imatinib in desmoid tumors observed a response in two patients [9]. In desmoids, it is uncertain whether the response is due to the inhibition of known imatinib targets, and no genomic mutations have been observed showing that the response to imatinib is attributable to c-kit expression [10]. Heinrich et al. (2006) treated 19 patients with desmoid tumors with 800 mg imatinib daily; three PR and four SD were observed. Genomic analyses revealed no mutations of KIT, PDGFRA, or PDGFRB [11]. The French Sarcoma Group published a phase II study with 40 patients demonstrating one complete response and three PR at three months. The nonprogression rates at 3, 6, and 12 months were 91%, 80%, and 67%, respectively. The 2-year progression-free (PFS) and overall survival (OS) rates were 55% and 95%, respectively [25]. Chugh et al. observed similar response and nonprogression rates in 51 patients [12].

It is still questionable whether a change in tumor size is a meaningful tool for the evaluation of patients' outcome when treated with tyrosine kinase inhibitors. Standard radiographic response according to RECIST has not correlated consistently with histological response, disease-free survival, or OS. Other methods identifying patients who likely benefit from chemotherapy or other agents are needed. Therefore, ^{18}F-FDG PET has found increasing use in oncology as it can visualize soft tissue tumors and detect local and distant disease recurrence in malignancies [13]. The SUV of ^{18}F-FDG correlates with the metabolic rate of FDG accumulation in tumor cells [14]. Hence, the SUV could function as an easily measurable surrogate marker of tumor viability during treatment. In a group of 46 patients with localized, intermediate/high grade extremity soft tissue sarcomas, it could be demonstrated that SUV changes during neoadjuvant chemotherapy can be used to predict therapy outcome [15]. Thus, it has been suggested that ^{18}F-FDG PET can act as a noninvasive method to predict patients who are less likely to benefit from doxorubicin-based chemotherapy [16].

However, no data have been published for the use of PET in desmoid tumor patients under treatment with imatinib, except of a pilot study from our group [17]. The purpose of the present study was to analyze and discuss semiquantitative ^{18}F-FDG PET measurements in a collective of patients with desmoid tumors treated with imatinib.

2. Patients and Methods

2.1. Patients. The study included 22 patients with desmoid tumors with a mean age of 46.6 ± 16.4 years and a median age of 42.5 years ranging from 22 to 75 years. Patients' characteristics including gender, age, tumor site, and previous treatments are summarized in Table 1. All patients were referred to our outpatient service with the diagnosis of a desmoid tumor confirmed by histology obtained from surgical specimens. Tumor specimens were classified according to the Fédération Nationale des Centres de Lutte Contre le Cancer (FNCLCC) system [18]. The indication for patients' inclusion in the study was RECIST PD, not amenable to surgical resection with R0 intent or accompanied by an unacceptable function loss or deficit. Main exclusion criteria were prior therapy with imatinib, severe hepatic dysfunction, and prior malignancies. Patients were treated at the Mannheim University Medical Center, University of Heidelberg since May 2006. The research was carried out according to the principles set out in the Declaration of Helsinki in 1964 and all subsequent revisions.

Table 1: Patients' characteristics (n = 22).

Gender	
Female	16
Male	6
Age	
Median (years)	42.5 (range: 22–75)
Histology	
Desmoid tumor	22
Tumor site at initial diagnosis	
Abdomen/trunk	17
Extremities	5
Previous treatment	
None	8
Surgery alone	7
Surgery plus radiotherapy	7
Systemic treatment	2

2.2. Imatinib. Imatinib mesylate was supplied as 400 mg capsules that were taken orally (Novartis Pharma GmbH, Nurnberg, Germany). All patients with advanced and/or non resectable disease started imatinib therapy in a daily dose of 400 mg; treatment dose was escalated within two weeks to 800 mg daily (2 × 400 mg).

2.3. Imaging Studies. Patients were examined using ^{18}F-FDG PET prior to onset of therapy with imatinib and during imatinib treatment. The treatment/imaging algorithm was as follows. (a) An initial PET examination was performed at baseline before start of imatinib treatment. (b) A second PET examination was done for therapy monitoring after one to three months; if SUV decreased or was stable, imatinib treatment was continued. (c) Another follow-up PET was performed in some cases for further treatment monitoring. Conventional imaging of the same target lesion using CT and/or MRI was performed in parallel to determine response according to RECIST. This data served as reference to evaluate the response determined with ^{18}F-FDG PET. Dynamic PET studies were performed after intravenous injection of 300–370 MBq FDG for 60 min. A dedicated PET system (ECAT

EXACT HR plus, Siemens, Erlangen, Germany) or a PET-CT system (Biograph mCT, S128) was used for patient studies as described before [19]. PET-CT studies were performed using a low-dose CT (30 mA) with current modulation without any contrast material. The CT data were used for attenuation correction and for the image fusion. The last images (55–60 minutes after injection) were used for semiquantitative analysis. PET cross-sections were reconstructed with an image matrix of 256 × 256 (for ECAT EXACT HR plus) or 400 × 400 (for Biograph mCT) using an iterative reconstruction program. Images were scatter- and attenuation-corrected. Volumes of interest (VOI) were placed over the lesion. To acquire information about the tumor viability, the hypermetabolic areas of the tumors were evaluated and hypometabolic areas that correlate to necrotic tissue were excluded. The SUV in the tumor was calculated according to the following equation: SUV = tissue concentration (MBq/g)/[injected dose (MBq)/body weight (g)]. The SUV reflected the average SUV value provided by the quantification software in VOI. This value is more robust than the maximum SUV (SUV_{max}), because it is less influenced by the parameters used for the image reconstruction as well as by potential artefacts. A major limitation of the use of SUV_{max} is that it is highly dependent on the statistical quality of the images and the size of the maximal pixel and is, therefore, less robust than the use of the average SUV within VOI [20]. The analysis of the PET images was performed by two nuclear medicine physicians using a dedicated software package.

2.4. Statistical Analysis. Standard descriptive statistical analysis for the data was performed. PFS was defined as the time interval from the date of imatinib therapy induction until tumor progression, end of therapy, or data acquisition. Parameters for PFS and SUV were given as mean and median with range. Skewness for SUV1 and $SUV1_{max}$ was higher than for the other variables. For calculated ratios and differences of the variables, the facts are so far different, since the differences show a greater skewness and the ratios are near normal distributed meaning that the Wilcoxon rank sum test will be suitable for the differences but not the *t*-test. For descriptive statistical analysis, StatXact-9 of Cytel Studio, Version 9.0.0, Cytel Inc., Cambridge, MA, USA, and for the tests the SAS software 9.2 (TS2M3) by the SAS Institute Inc., Cary, NC, USA, were used.

3. Results

3.1. Clinical Response Based on RECIST Criteria. Imatinib was taken orally in a dose of 800 mg daily. The therapy interval with imatinib was in the mean 19.7 months with a median of 12.5 months (range: 1–74) until time of data acquisition. In spite of CTCAE grade I/II fatigue and edema, no major (grade III/IV) toxicities occurred. First CT and/or MRI scan was performed in all patients prior to onset of therapy with imatinib. Restaging was performed using CT and/or MRI every three months after start of imatinib treatment. The remission status was evaluated according to RECIST based on the tumor shrinkage in the CT and/or MRI scan. Clinical outcome according to RECIST was as follows: five patients with PR (23%), 12 patients with SD (55%), and five patients with PD (23%). The mean PFS from the date of therapy induction until end of therapy or data collection for all patients was 20.6 months with a median of 14 months ranging from 1 to 74 months. The six-month PFS rate was 68%, and all patients are alive at the time of data acquisition.

3.2. Clinical Response Based on PET Imaging. In all patients, two sequential PET examinations have been performed within a median time interval of 53.5 days; in 13 patients, more than two PET examinations were done during imatinib treatment within a median time interval of 199.5 days from the baseline PET. The median average SUV prior to onset of targeted therapy with imatinib was 2.9 (range: 2.0–11.6) in comparison to 2.1 (range: 1.5–3.4) during treatment. The median SUV_{max} was 5.1 (range: 2.8–16.8) prior to therapy with imatinib in comparison to 4.1 (range: 2.3–6.1) following treatment. Hence, a decrease of 28% of the median average SUV and a decrease of 20% of the median SUV_{max} for sequential PET examinations could be demonstrated for the evaluated patients; no patient demonstrated a substantial increase in SUV. However, the main question was whether the PET results can predict response evaluation by conventional RECIST criteria and, thus, act as a surrogate marker. Therefore, the initial SUV and SUV_{max} (SUV1 and $SUV1_{max}$) were used as a basis for multiple testing in the three categories PR, SD, and PD in comparing these with the data of the second or third PET examination if available. Multiple testing was performed with the multiple Wilcoxon rank sum test and the multiple *t*-test; however, none of the tests were significant. In a second approach, patients with PR and SD were matched to a group of nonprogressive disease and tested versus patients showing PD. Using the Wilcoxon rank sum test, SUV1 and $SUV1_{max}$ seem to be candidates for a response prediction with an approximate *P* value of *0.06553* and *0.07785*, respectively, (Figure 1). In the literature, for soft tissue sarcomas in general, a cut-off value of 40% SUV reduction from baseline has been chosen to differentiate responders [21]. In our collective, four patients demonstrated an at least 40% SUV decrease, three of them showing SD and one PR *(compare* Table 2*),* whereas the other patients showed stabilization or an SUV decrease of less than 40%.

3.3. Patient Example. A 31-year-old female with a retroperitoneal desmoid tumor (case 3, Table 2; Figure 2) diagnosed in 2006 was treated with imatinib 800 mg daily. The FDG PET prior therapy with imatinib showed an average SUV of 4.2 and an SUV_{max} of 8.1. After one month of imatinib treatment, the FDG PET demonstrated a decrease of the average SUV to 3.3 (−22%) and of the SUV_{max} to 6.1 (−25%). Follow-up PET examinations in 2011 and 2012 did not show any pathological FDG uptake. The corresponding conventional MRI documented PR according to RECIST.

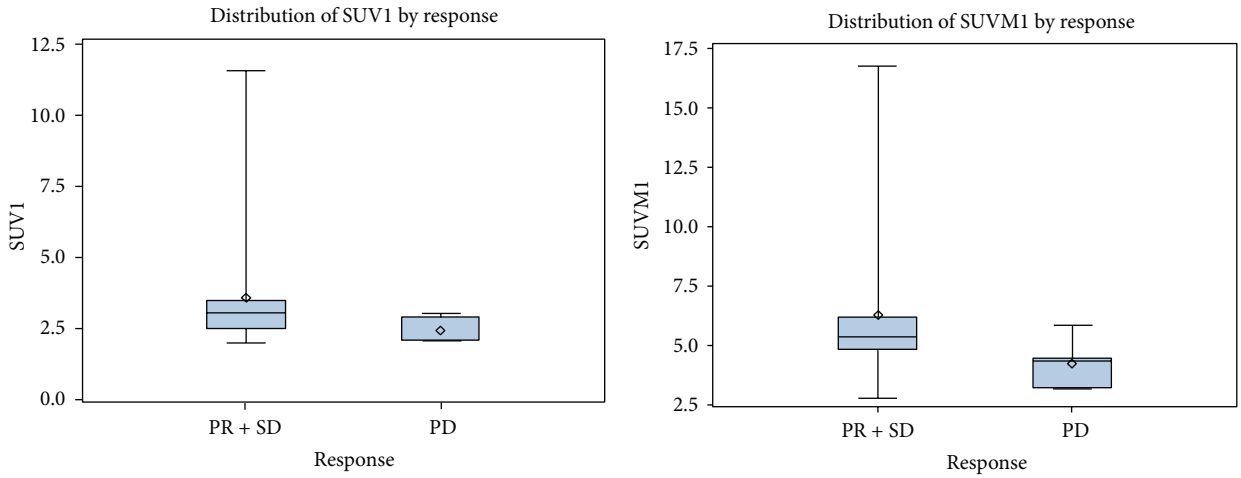

Figure 1: The box plots show the distribution of the average SUV1 and $SUV1_{max}$ values by conventional response evaluation according to RECIST criteria for the group of nonprogressive patients (PR + SD) versus patients with PD with an approximate P value of *0.06553* and *0.07785*, respectively.

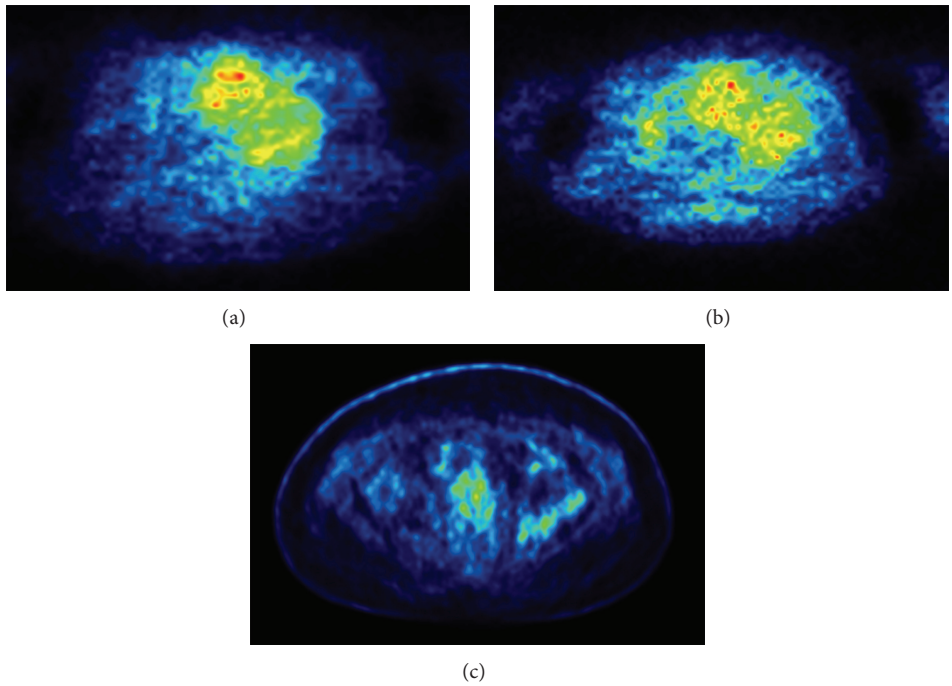

Figure 2: A 31-year-old female with a retroperitoneal desmoid tumor (case 3, Table 2; Figure 2) diagnosed in 2006 was treated with imatinib 800 mg daily. The FDG PET prior therapy with imatinib showed an average SUV of 4.2 and an SUV_{max} of 8.1 (a). After one month of imatinib treatment, the FDG PET demonstrated a decrease of the average SUV to 3.3 (−22%) and of the SUV_{max} to 6.1 (−25%) (b). Follow-up PET examinations in 2011 and 2012 (c) did not show any pathological FDG uptake. The corresponding conventional MRI documented PR according to RECIST.

4. Discussion

There are different implications for the use of PET in soft tissue tumors. It has been studied to predict the malignant potential and grading, to stage the malignant disease, to monitor tumor response and predict clinical benefit from chemotherapy [22]. However, most of the studies comprised only small numbers of patients using different imaging protocols and evaluation procedures making comparison extremely difficult. Changes in tumor size to chemotherapeutic treatment have been the parameter to predict the therapeutic benefit for the patients. However, changes in

Table 2: PET results for desmoid patients ($n = 22$) treated with imatinib.

Patient no.	Age (years)	Tumor localization	Imatinib treatment duration (months)	Average SUV (initial)	Average SUV (follow-up)	SUV change (%)	Response according to RECIST	PFS (months)
1	64	Chest	6	2.902	2.538	−13	PD	6
2	70	Pelvis	5	3.171	3.364	6	SD	5
3	31	Retroperitoneal	74	4.233	3.294	−22	PR	74+
4	42	Mesenterium	4	3.023	2.793	−8	PD	4
5	**22**	**Chest**	**15**	**3.320**	**1.711**	**−48**	**SD**	**15**
6	35	Supraclavicular	6	2.115	1.851	−12	SD	6
7	27	Upper limb	58	3.112	2.428	−22	SD	58+
8	70	Buttock	60	2.785	2.632	−6	SD	60+
9	38	Pelvis	49	2.376	1.735	−27	SD	49+
10	68	Shoulder	12	2.098	1.458	−31	PD	12
11	43	Upper limb	8	2.100	1.600	−24	PD	8
12	48	Pelvis	9	2.900	2.800	−3	SD	9+
13	**40**	**Pelvis**	**26**	**3.500**	**2.100**	**−40**	**PR**	**26+**
14	47	Upper limb	28	2.300	1.800	−22	PR	28+
15	**54**	**Chest**	**1**	**5.229**	**3.100**	**−41**	**SD**	**22**
16	30	Pelvis	18	3.074	2.400	−22	SD	18+
17	**24**	**Mesenterium**	**17**	**11.573**	**1.981**	**−83**	**SD**	**16+**
18	48	Chest	3	2.059	1.975	−4	PD	3
19	41	Buttock	15	2.000	2.100	5	PR	15+
20	70	Parascapular	13	2.900	2.114	−27	PR	13+
21	39	Fossa ischiorectalis	5	2.492	2.100	−16	SD	5+
22	75	Mesenterium	1	4.037	n.e.	n.e.	SD	1+

SUV: standardized uptake value; RECIST: Response Evaluation Criteria in Solid Tumors; PFS: progression-free survival; PR: partial response; PD: progressive disease; SD: stable disease; n.e.: not evaluable; +: patient is still progression-free at the time of data collection and continues treatment with imatinib.

tumor size measured with CT and/or MRI did not correlate consistently with sarcoma patients' outcomes. For GIST, this finding has already been well documented: a study of ^{18}F-FDG PET in imatinib treated GIST showed that patients with normalization of the SUV within the first month of treatment have a significantly longer time to disease progression and better OS than those patients with increased ^{18}F-FDG accumulation [23]. ^{18}F-FDG PET appears to be more useful than CT/MRI imaging in GIST to predict therapy response. Moreover, there is even doubt if RECIST criteria adequately describe the remission status to chemotherapy or other targeted agents. Therefore, a new classification of response criteria, "(PERCIST) Positron Emission tomography Response Criteria In Solid Tumors," has been introduced taking into consideration both changes in tumor volume as well as changes in metabolism [24].

To our knowledge, the present paper describes the first larger series of desmoid tumor patients under therapy with imatinib monitored with sequential PET imaging despite a pilot study presented from our group [17]. In our patient population, a significant SUV decrease (≥ 40%) of sequential PET examinations could be demonstrated in four patients (18%), whereas the other patients showed stabilization or an SUV decrease of less than 40%. There was no patient in this series demonstrating a substantial SUV increase. Considering the fact that patients had to demonstrate RECIST PD to enter the study, the high proportion of 77% of patients with nonprogressive disease means a significant benefit. RECIST criteria seem inadequate to describe responses seen in patients with desmoid tumors. Complete or even PR are documented in the literature in around 10% of patients treated with imatinib [11, 12, 25]; in our series with 23% the response rate was relatively high. Most of the patients show disease stabilization or even shrinkage of the tumor. However, considering the fact that patients were inoperable or demonstrated PD at the time entering the study, control of symptoms and disease stabilization mean a substantial clinical benefit for most of the patients initially suffering from pain or functional loss. Therefore, benefit can be defined for most of the patients as a progression arrest.

The characteristics of imatinib treatment in desmoid tumor patients seem to be confirmed by PET: imatinib has a remarkable ability to slow the growth and stabilize the tumor. Of course, compared to high-grade soft tissue sarcomas, baseline SUV values are relatively low in desmoid tumors (initial median average SUV of 2.9). Therefore, documented SUV changes under treatment with imatinib were relatively small. We could show that PET monitoring of desmoid patients under treatment with imatinib may be used to determine whether patients benefit from imatinib

therapy or not in the lack of an adequate CT and/or MRI imaging [26]. In particular the initial average SUV1 and $SUV1_{max}$ data seem to be candidates for a response prediction and may act as surrogate markers. Figure 1 shows that the higher initial average SUV1 and $SUV1_{max}$ data are obviously associated with a higher probability of treatment response in the PR/SD versus PD proportion of patients. Therefore, we have shown that early SUV changes may be detected helping to discriminate responders from nonresponders and, thus, to decide whether imatinib therapy should be continued or not. For example, therapy with imatinib would be continued if an SUV decrease or stabilization is documented. However, if there is a substantial SUV increase, continuation of imatinib treatment is questionable having also an impact on treatment costs.

In summary, PET will certainly play an increasingly important prognostic and predictive role in the management of "semimalignant" and malignant soft tissue tumors [27–29]. It could be used to characterize the aggressiveness of the tumor in order to make clinical decisions whether treatment is useful for the patients or not. Our present data suggest that the ability of imatinib treatment to slow down the growth of desmoid tumors—resulting in a 77% progression arrest rate—is reflected by SUV stabilization or a SUV decrease of up to 83%. Furthermore, PET imaging may be used as a surrogate marker in order to predict response to therapy early in the course of treatment for cytotoxic chemotherapy and other targeted agents like sorafenib [30]. However, more data have to be evaluated to demonstrate statistically significant results.

Conflict of Interests

The authors declare the following conflict of interests: BK, honoraria from Novartis; PH, consultant for Novartis.

References

[1] J. S. Biermann, "Desmoid tumors," *Current Treatment Options in Oncology*, vol. 1, no. 3, pp. 262–266, 2000.

[2] O. Micke and M. H. Seegenschmiedt, "Radiation therapy for aggressive fibromatosis (desmoid tumors): results of a national patterns of care study," *International Journal of Radiation Oncology Biology Physics*, vol. 61, no. 3, pp. 882–891, 2005.

[3] L. Bertario, A. Russo, P. Sala et al., "Multiple approach to the exploration of genotype-phenotype correlations in familial adenomatous polyposis," *Journal of Clinical Oncology*, vol. 21, no. 9, pp. 1698–1707, 2003.

[4] S. K. Clark and R. K. S. Phillips, "Desmoids in familial adenomatous polyposis," *The British Journal of Surgery*, vol. 83, no. 11, pp. 1494–1504, 1996.

[5] J. Janinis, M. Patriki, L. Vini, G. Aravantinos, and J. S. Whelan, "The pharmacological treatment of aggressive fibromatosis: a systematic review," *Annals of Oncology*, vol. 14, no. 2, pp. 181–190, 2003.

[6] G. Pignatti, G. Barbanti-Bròdano, D. Ferrari et al., "Extraabdominal desmoid tumor: a study of 83 cases," *Clinical Orthopaedics and Related Research*, no. 375, pp. 207–213, 2000.

[7] B. J. Druker, S. Tamura, E. Buchdunger et al., "Effects of a selective inhibitor of the Ab1 tyrosine kinase on the growth of Bcr-Ab1 positive cells," *Nature Medicine*, vol. 2, no. 5, pp. 561–566, 1996.

[8] G. D. Demetri, M. von Mehren, C. D. Blanke et al., "Efficacy and safety of imatinib mesylate in advanced gastrointestinal stromal tumors," *The New England Journal of Medicine*, vol. 347, no. 7, pp. 472–480, 2002.

[9] J. Mace, J. S. Biermann, V. Sondak et al., "Response of extraabdominal desmoid tumors to therapy with imatinib mesylate," *Cancer*, vol. 95, no. 11, pp. 2373–2379, 2002.

[10] A. Leithner, M. Gapp, R. Radl et al., "Immunohistochemical analysis of desmoid tumours," *Journal of Clinical Pathology*, vol. 58, no. 11, pp. 1152–1156, 2005.

[11] M. C. Heinrich, G. A. McArthur, G. D. Demetri et al., "Clinical and molecular studies of the effect of imatinib on advanced aggressive fibromatosis (desmoid tumor)," *Journal of Clinical Oncology*, vol. 24, no. 7, pp. 1195–1203, 2006.

[12] R. Chugh, R. G. Maki, D. G. Thomas et al., "A SARC phase II multicenter trial of imatinib mesylate (IM) in patients with aggressive fibromatosis," *Journal of Clinical Oncology*, vol. 24, no. 18, abstract 9515, 2006.

[13] M. Schulte, D. Brecht-Krauss, B. Heymer et al., "Fluorodeoxyglucose positron emission tomography of soft tissue tumours: is a non-invasive determination of biological activity possible?" *European Journal of Nuclear Medicine*, vol. 26, no. 6, pp. 599–605, 1999.

[14] J. F. Eary and D. A. Mankoff, "Tumor metabolic rates in sarcoma using FDG PET," *Journal of Nuclear Medicine*, vol. 39, no. 2, pp. 250–254, 1998.

[15] S. M. Schuetze, B. P. Rubin, C. Vernon et al., "Use of positron emission tomography in localized extremity soft tissue sarcoma treated with neoadjuvant chemotherapy," *Cancer*, vol. 103, no. 2, pp. 339–348, 2005.

[16] S. M. Schuetze, "Utility of positron emission tomography in sarcomas," *Current Opinion in Oncology*, vol. 18, no. 4, pp. 369–373, 2006.

[17] B. Kasper, A. Dimitrakopoulou-Strauss, L. G. Strauss, and P. Hohenberger, "Positron emission tomography in patients with aggressive fibromatosis/desmoid tumours undergoing therapy with imatinib," *European Journal of Nuclear Medicine and Molecular Imaging*, vol. 37, no. 10, pp. 1876–1882, 2010.

[18] M. Trojani, G. Contesso, J. M. Coindre et al., "Soft-tissue sarcomas of adults: study of pathological prognostic variables and definition of a histopathological grading system," *International Journal of Cancer*, vol. 33, no. 1, pp. 37–42, 1984.

[19] M. H. M. Schwarzbach, U. Hinz, A. Dimitrakopoulou-Strauss et al., "Prognostic significance of preoperative [18-F] fluorodeoxyglucose (FDG) positron emission tomography (PET) imaging in patients with resectable soft tissue sarcomas," *Annals of Surgery*, vol. 241, no. 2, pp. 286–294, 2005.

[20] R. Boellaard, N. C. Krak, O. S. Hoekstra, and A. A. Lammertsma, "Effects of noise, image resolution, and ROI definition on the accuracy of standard uptake values: a simulation study," *Journal of Nuclear Medicine*, vol. 45, no. 9, pp. 1519–1527, 2004.

[21] E. Y. Cheng, J. W. Froelich, J. C. Manivel, J. Weigel, and K. M. Skubitz, "Correlation of FDG-PET with histologic response after neoadjuvant chemotherapy for soft tissue sarcomas," *Proceedings of the American Society of Clinical Oncology*, vol. 25, no. 18, abstract 10583, 2009.

[22] B. Kasper, S. Dietrich, A. Dimitrakopoulou-Strauss et al., "Early prediction of therapy outcome in patients with high-risk soft tissue sarcoma using positron emission tomography," *Onkologie*, vol. 31, no. 3, pp. 107–112, 2008.

[23] P. L. Jager, J. A. Gietema, and W. T. A. van der Graaf, "Imatinib mesylate for the treatment of gastrointestinal stromal tumours: best monitored with FDG PET," *Nuclear Medicine Communications*, vol. 25, no. 5, pp. 433–438, 2004.

[24] R. L. Wahl, H. Jacene, Y. Kasamon, and M. A. Lodge, "From RECIST to PERCIST: evolving considerations for PET response criteria in solid tumors," *Journal of Nuclear Medicine*, vol. 50, supplement 1, pp. 122S–150S, 2009.

[25] N. Penel, A. Le Cesne, B. N. Bui et al., "Imatinib for progressive and recurrent aggressive fibromatosis (desmoid tumors): an FNCLCC/French Sarcoma Group phase II trial with a long-term follow-up," *Annals of Oncology*, vol. 22, no. 2, pp. 452–457, 2011.

[26] C. Ramos-Font, A. S. Chinchilla, A. C. R. Aguirre, A. R. Fernández, A. M. Benítez, and J. M. L. Elvira, "Desmoid tumor of the chest wall characterized with 18F-fluorodeoxyglucose PET/CT scan. Correlation with magnetic resonancy and bone scintigraphy. Review of the literature," *Revista Espanola de Medicina Nuclear*, vol. 28, no. 2, pp. 70–73, 2009.

[27] A. Dimitrakopoulou-Strauss, L. G. Strauss, G. Egerer et al., "Prediction of chemotherapy outcome in patients with metastatic soft tissue sarcomas based on dynamic FDG PET (dPET) and a multiparameter analysis," *European Journal of Nuclear Medicine and Molecular Imaging*, vol. 37, no. 8, pp. 1481–1489, 2010.

[28] A. Dimitrakopoulou-Strauss, L. G. Strauss, G. Egerer et al., "Impact of dynamic 18F-FDG PET on the early prediction of therapy outcome in patients with high-risk soft-tissue sarcomas after neoadjuvant chemotherapy: a feasibility study," *Journal of Nuclear Medicine*, vol. 51, no. 4, pp. 551–558, 2010.

[29] A. Dimitrakopoulou-Strauss, P. Hohenberger, L. Pan, B. Kasper, S. Roumia, and L. G. Strauss, "Dynamic PET with FDG in patients with unresectable aggressive fibromatosis: regression-based parametric images and correlation to the FDG kinetics based on a two-tissue compartment model," *Clinical Nuclear Medicine*, vol. 37, no. 10, pp. 943–948, 2012.

[30] M. M. Gounder, R. A. Lefkowitz, M. L. Keohan et al., "Activity of sorafenib against desmoid tumor/deep fibromatosis," *Clinical Cancer Research*, vol. 17, no. 12, pp. 4082–4090, 2011.